Charles University
Faculty of Medicine in Pilsen

DISSERTATION

Pilsen *2024* **Annu Kala**

Charles University
Faculty of Medicine in Pilsen

Study programme: Physiology and Pathological Physiology

Effect of sepsis on dynamics of hippocampal oscillations and CA1 cells

Dissertation

Supervisor: Dr. Karel Jezek, Ph. D

Pilsen, *2024* **MSc. Annu Kala**

Declaration

I declare hereby that I made this dissertation thesis by myself and that I mentioned and cited properly all the sources and literature. At the same time, I declare that this thesis was not used to obtain another or the same title.

I agree with permanent deposition of an electronic version of my thesis in the system database of interuniversity project Thesis.cz for a permanent control of similarities of theses.

In Pilsen

Annu Kala

CHARLES UNIVERSITY

Faculty of Medicine in Pilsen

Extended abstract of doctoral dissertation

Effect of sepsis on dynamics of hippocampal oscillations and CA1 cells

Vliv sepse na dynamiku oscilací hipokampu a buněk CA1

Annu Kala

Pilsen *2024*

The Dissertation was written during full-time doctoral study.

Programme at the Department of Physiology, Faculty of Medicine in Pilsen, Charles University.

Student: Annu Kala, Biomedical Center

Chair of the Subject Area Board: full name with all titles and his/her /workplace

Supervisor: **Dr. Karel Jezek, Ph.D, Biomedical Center, Faculty of Medicine in Pilsen**

Opponents: **Dr. Daniel Klement, MD., PhD, Dr. David Levcik, PhD.**

The defence will take place before the Board for the Defense of the Subject Area Board

..... on ..... in ....

from .... hours

This work has been supported by grant FIND, START/MED/107

The dissertation is available for inspection at the Department for Science and Research of the Dean´s Office, Faculty of Medicine in Pilsen, Charles University, alej Svobody 76, Pilsen.

ACKNOWLEDGEMENTS

I would start by thanking my parents, Mrs. Nirmala Devi and Mr. Balwan Singh and brother Aman Kala, who have always been a constant source of support throughout my PhD journey. It wouldn't have been possible without their encouragement and love. I am extremely grateful to my partner Mr. Vivek Thusu, who rather emboldened me when I was unsure about making the switch from molecular biology to the world of electrophysiology. He has been very supportive and kind towards my decisions. I would like to extend my sincere thanks to my supervisor, Dr. Karel Jezek for always believing in me and providing me the independence to carry out my research work. I could not have asked for a better PI. A special thanks to my consultant, Dr. Susan Leemburg who played a pivotal role in shaping my interest in the field of neuroscience. She helped me broaden my horizons and made me believe that it was always possible to learn new things along the way. Next, I would like to thank my dear colleague Dr. Karel Blahna who was very patient and insightful while supervising me. I thank my friends Akanksha and Athira who kept me positive when the times got hard and for being the amazing cheerleaders. Thanks to Patricia, Siddharth and Athira for keeping the work environment home-like. I would like to thank our very talented technician cum artist Lenka Sykorova for making the beautiful drives for us and giving the artistic soul to the lab. Next, I would like to thank the entire KJ lab for such a stress-free, healthy and hence productive work environment. It was a small chosen family that worked together as a team. I would like to thank the animal caretakers for taking such good care of the animals. A final thanks to my in-laws Mr. Ravinder Thusu and Mrs. Neeru Thusu who became a part of my this journey towards the end and encouraged me to pursue my dreams.

This study was supported by-

FIND No. Z.02.1.01/0.0/0.0/16_019/0000787.

Fighting INfectious Diseases "& SVV260 394

START/MED/107

TABLE OF CONTENTS

LIST OF ABBREVIATIONS

SAE - *Sepsis Associated Encephalopathy*

LPS - *Lipopolysaccharide*

SIRs - *Systemic Inflammatory Response Syndrome*

SOFA - *Sequential Organ Failure Assessment*

TLR - *Toll-Like Receptor*

APCS - *Antigen Presenting Cells*

NETS - *Neutrophil Extracellular Traps*

AP- *Area Postrema*

NTS - *Nucleus Solitarius*

DMN - *Dorsal Motor Nucleus*

IC - *Insular Cortex*

CRH - *Corticotropin Releasing Hormone*

SABD - *Sepsis Associated Brain Dysfunction*

ROS - *Reactive Oxygen Species*

CNS - *Central Nervous System*

EEG - *Electroencephalography*

EMG - *Electromyography*

EOG - *Electrooculography*

NREM - *Non-Rapid Eye Movement Sleep*

REM - *Rapid Eye Movement Sleep*

SWS - *Slow Wave Sleep*

RAS - *Reticular Activating System*

VLPO - *Ventrolateral Pre-Optic Area*

CN - *Caudate Nucleus*

BF - *Basal Forebrain*

VTA - *Ventral Tegmental Area*

SCN - *Suprachiasmatic Nucleus*

CSF - *Cerebrospinal Fluid*

OSA - Obstructive Sleep Apnea

SD - *Sleep Deprivation*

SWRs - *Sharp Wave Ripples*

EC - *Entorhinal Cortex*

ABSTRACT (ENGLISH)

Sepsis associated encephalopathy (SAE) is a severe complication of sepsis leading to high mortality and long-term brain dysfunction. SAE often manifests as altered consciousness, delirium, coma, inattention and cognitive impairments. Sleep disturbances depicted as sleep-wake fragmentation occurring in the acute phase of sepsis have been directly linked to the poor outcomes in sepsis patients. Septic shock survivors typically develop post-sepsis syndrome characterised by extreme fatigue, sleep disturbances and cognitive impairments. Central nervous system specifically hippocampus is one of the first regions that gets affected as a result of SAE. Despite the role of sleep in maintaining a functional immune system and its importance in memory consolidation, an in-depth understanding of sleep-wake patterns remains poorly understood. In the present work, we aimed at understanding the fine dynamics of the hippocampal oscillations in an lipopolysaccharide (LPS) model of sepsis (10mg/kg) under urethane anaesthesia. Urethane exerts minimum effects on respiratory and cardiovascular system making it a suitable system to study fine kinetics of brain oscillations without any external sensory modalities. Next, we aimed at confirming our findings on sleep architecture and spectral properties in unanaesthetised animals under a standardised dose of 5mg/kg LPS. Furthermore, we aimed at understanding hippocampal CA1 cellular response to sepsis. We found that LPS led to extensive state fragmentation in both, urethane injected and unanaesthetised model of sepsis. In urethane model of sepsis, we used a 2D state space approach to study the dynamics of REM-like and NREM-like states with respect to each other. LPS resulted in increased spectral similarity and velocity driven by low (1-9 Hz) and high frequency (15-45 Hz) component respectively. The parametrization of periodic and aperiodic components of REM and NREM spectra showed that the spectral changes during sepsis were more prominently driven by the oscillatory component. We found similar state fragmentation in unanaesthetised rats accompanied by REM suppression. Spectrum analysis showed LPS-associated dampened power for up to at least 25 Hz frequency during sleep sessions. Furthermore, hippocampal CA1 interneuron and pyramidal activity decreased after 1 and 4 hrs of LPS injection, respectively. Incidence of sharp wave ripples increased post LPS.

Decreased inter-state distance accompanied by increased with-in state velocity may represent a key feature in altering the oscillatory landscape of brain state attractors causing

sleep-wake fragmentation. This may further result in failure to attain deep restorative NREM sleep associated with poor sleep quality in sepsis survivors and animal models of SAE. Dampened hippocampal cellular response and increased synchrony events after LPS injection may signify altered hippocampal network processing which may play a key role in cognitive impairment in septic shock survivors.

ABSTRACT (CZECH)

Sepsí asociovaná encefalopatie (SAE) je závažnou komplikací sepse, která vede k vysoké mortalitě a dlouhodobé mozkové dysfunkci. SAE se často projevuje jako změna vědomí, delirium, kóma, nepozornost a kognitivní poruchy. Poruchy spánku zobrazené jako fragmentace spánku a bdění vyskytující se v akutní fázi sepse byly přímo spojeny se špatnými výsledky u pacientů se sepsí. U osob, které přežily septický šok, se typicky rozvíjí postseptický syndrom charakterizovaný extrémní únavou, poruchami spánku a kognitivními poruchami. Centrální nervový systém, konkrétně hipokampus, je jednou z prvních oblastí, které jsou v důsledku SAE postiženy. Navzdory úloze spánku při udržování funkčního imunitního systému a jeho významu pro konsolidaci paměti zůstává důkladné pochopení vzorců spánku a bdění nedostatečně prozkoumáno. V této práci jsme se zaměřili na pochopení jemné dynamiky oscilací hipokampu na modelu sepse s LPS (10 mg/kg) v uretanové anestezii. Uretan má minimální účinky na dýchací a kardiovaskulární systém, což z něj činí vhodný systém pro studium jemné kinetiky mozkových oscilací bez vnějších senzorických modalit. Dále jsme se zaměřili na potvrzení našich zjištění o architektuře spánku a spektrálních vlastnostech u neanestetizovaných zvířat pod standardizovanou dávkou 5 mg/kg LPS. Dále jsme se zaměřili na pochopení buněčné odpovědi hipokampu CA1 na sepsi. Zjistili jsme, že LPS vede k rozsáhlé fragmentaci stavu jak u modelu sepse s uretanovou injekcí, tak u modelu bez anestezie. V uretanovém modelu sepse jsme použili přístup 2D stavového prostoru ke studiu dynamiky stavů podobných REM a NREM ve vzájemném vztahu. LPS vedl ke zvýšení spektrální podobnosti a rychlosti řízené nízkofrekvenční (1-9 Hz)respektive vysokofrekvenční (15-45 Hz) složkou. Parametrizace periodických a aperiodických složek spekter REM a NREM ukázala, že spektrální změny během sepse jsou výrazněji poháněny oscilační složkou. Podobnou fragmentaci stavů jsme zjistili i u potkanů bez anestezie doprovázenou potlačením REM. Analýza spektra ukázala, že během spánkových seancí došlo k tlumení výkonu spojeného s LPS až do frekvence 25 Hz. Kromě toho se po 1 hodině injekce LPS snížila aktivita hipokampálních CA1 interneuronů a po 4 hodinách pyramid. Výskyt ostrých vlnových pulzací se po LPS zvýšil.

Snížení mezistavové vzdálenosti doprovázené zvýšením rychlosti se stavem uvnitř může představovat klíčový rys při změně oscilační krajiny mozkových stavových atraktorů způsobující fragmentaci spánku a bdění. To může mít dále za následek nedosažení

hlubokého regeneračního spánku NREM spojeného se špatnou kvalitou spánku u osob, které přežily sepsi, a zvířecích modelů SAE. Tlumená buněčná odpověď hipokampu a zvýšený počet synchronních událostí po injekci LPS mohou znamenat změněné zpracování hipokampální sítě, které může hrát klíčovou roli v kognitivní poruše u osob, které přežily septický šok.

1.1 SEPSIS

Sepsis is a life-threatening condition and a primary cause of mortality in critically ill patients, caused by dysregulated host response against any infection (Lever and Mackenzie 2007). Sepsis affects around 47-50 million individuals worldwide accounting for about 2% of all hospitalizations leading to 25% mortality (Arwyn-Jones and Brent 2019; M. Huang, Cai, and Su 2019). It is responsible for about 6 million deaths worldwide including 1 million neonates per year (Wilcox et al., 2022). According to the latest report on global epidemiology and burden of sepsis, WHO declared sepsis as a medical emergency. Patients with weakened immune system, children, pregnant women, and adults above 60 are at a higher risk of developing sepsis (Khanina et al., 2020). Bacterial infections are the most common causes of sepsis but viral, fungal, and parasitic agents can also participate in its ethiology (Ramachandran 2014). Most common sepsis-causing bacteria include Streptococcus pyogenes (S. pyogenes), Pseudomonas aeruginosa (P. aureginosa), Staphylococcus aureus (S. aureus), Klebsiella pneumoniae, and Escherichia coli (E. coli) (Minasyan 2019). Pneumonia and peritoneal infections are the leading sources of sepsis resulting in high morbidity and mortality (Novosad 2016). Urinary tract infection and skin infections can also progress into sepsis (Porat, Bhutta, and Kesler 2023). During sepsis, overactivation of immune system leads to the initiation of sequential cascade of proinflammatory pathways resulting in cytokine storm (Megha et al., 2021). This is followed by endothelium activation which may cause vasculature collapse at organ level leading to multiple organ dysfunction (Megha et al., 2021).

Systemic inflammatory response syndrome (SIRS) scoring scale has been used to diagnose sepsis since 1992. It considers two or more symptoms which include temperature change, heart rate and white blood cell count (Gaddis and Gaddis n.d.). These parameters may not always be accurate for sepsis diagnosis - for example, immunosuppressed patients might not show an increase in temperature in response to an infection and likewise critically ill patients having hyperthermia do not necessarily have an infections (Laupland et al., 2012). Given the complexity of signs in critically ill patients with multiple comorbidities, a revised definition of sepsis was introduced (Marik and Taeb 2017). The recommendations have been made for replacing SIRS with Sequential Organ Failure Assessment (SOFA) score to quantify sepsis severity (Marik and Taeb 2017). According to the new guidelines, sepsis is

defined as a condition of hyperactivated immune system in response to an infection accompanied by organ dysfunction. Sepsis assessment involves using quick SOFA score which includes 1 point each for the criteria 1) >38°C temperature, 2) heart rate >90 beats per minute, 3) respiratory rate > 22 breaths per minute. A score of >2 signifies higher risk of developing sepsis and are further diagnosed for organ failure (Singer et al., 2016).

Septic shock is a severe case of sepsis with 4 times higher risk of mortality wherein the patients show persistent hypotension even after vasopressor administration and higher blood lactate non-responsive to lactate guided resuscitation (Hernandez et al., 2012). ´Severe sepsis´ terminology has been abolished in the revised definitions as sepsis itself causes more than 10% mortality and hence is considered severe (Singer et al., 2016). An elaborated version of these definitions is described in the table below.

SIRS	• >38°C temperature • Heart rate >90 beats per minute. • Respiratory rate, > 22 breaths per minute. • Elevated white blood cell count
Sepsis	• SIRS (2 or more symptoms) • qSOFA>2 • Delirium/altered mental status • Systolic blood pressure < 100mmHg • Respiration rate > 22 bpm
Septic shock	• Sepsis • Persistent hypotension in the presence of vasopressors

	• Blood lactate >2 mmol/L after resuscitation

***TABLE 1**: Definitions of sepsis and their severities.*

1.2 ANIMAL MODELS OF SEPSIS

Since the pathophysiology of sepsis is highly complex, potential therapeutic targets need to be tested which is not always feasible in human patients (Jarczak, Kluge, and Nierhaus 2021). Therefore, suitable animal models of sepsis are required to understand the complex pathogenesis and to test the potential treatment strategies. There exists a debate about animal models being able to capture the complexity and progression of human sepsis and hence choosing a suitable model is a matter of research question given the limitations associated with each model system. There are 3 major types of animal models, 1) Model of endotoxemia, 2) Bacterial injections and 3) Host barrier dysfunction (Buras, Holzmann, and Sitkovsky 2005)

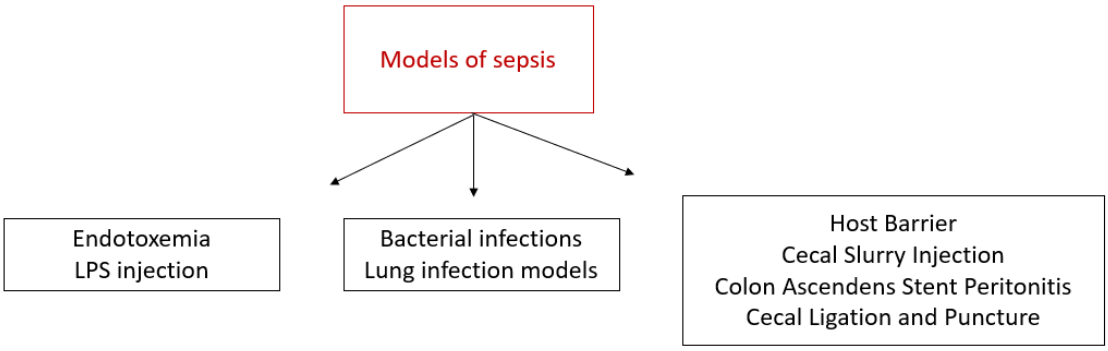

***Figure 1:** Major types of animal models of sepsis.*

1.2.1 ENDOTOXEMIA

LPS model of sepsis is an example of endotoxemia (Buras, Holzmann, and Sitkovsky 2005). LPS is a component of outer wall of gram-negative bacteria which is capable of eliciting a heightened immune response by binding to Toll-like receptor 4 on antigen-presenting cells

(APCs) (Park and Lee 2013). In this case, a high dose of LPS is administered in animals usually intraperitonially. It causes extensive cytokine storm as is the case in human sepsis but the resolution is relatively quicker than in humans (Lewis, Seymour, and Rosengart 2016). It also does not take into account the response towards gram positive bacteria and polymicrobial agent (Poli-de-Figueiredo et al., 2008). However, these models are highly standardised making them a reliable source to study pathology of sepsis (Lewis, Seymour, and Rosengart 2016).

1.2.2 BACTERIAL INFECTIONS

In this model, a higher dose of bacterium (E. coli, Staphylococcus or Pseudomonas) is injected either intravenously (i.v) or intraperitonially (i.p) (Cai et al., 2023). Usually, higher doses are preferred as lower doses are effectively cleared by the system failing to result in sepsis. This model has similar limitations to that of LPS model as it is injected as a bolus and does not capture the evolution of human septic state (Lewis, Seymour, and Rosengart 2016). To combat this limitation, vascular catheters can be used to infuse bacterium over a course of time to achieve steady state of infection present in human sepsis (Poli-de-Figueiredo et al., 2008). This model of sepsis is highly dependent on antibiotic therapy and fluid resuscitation if the survival of the animals is crucial for chronic studies (Poli-de-Figueiredo et al., 2008).

1.2.3 FIBRIN CLOT IMPLANTATION

As an alternative, in order to improvise the bacterial model of sepsis in terms of standard dose delivery, fibrin clots containing specific doses of bacteria are implanted in the abdominal cavity. Rate of infection can be then controlled by titrating the doses with respect to the desired severity (Ghanta, Kwon, and Perrella 2021).

1.2.4 CECAL LIGATION AND PUNCTURE MODEL

This model of sepsis involves laparotomy wherein cecum is ligated and punctured using a needle which causes polymicrobial peritonitis, bacteraemia and eventually septic shock (Wen 2013). This model is able to capture the prognosis of sepsis better than the endotoxemia or bacterial model. It causes bacteraemia and also the activation of pro and anti-inflammatory pathways simultaneously enabling it to be used as a gold standard in the field (Seemann, Zohles, and Lupp 2017). Resuscitation plays a major role in this model as in

the absence of optimal fluids, animals do not enter the hyperdynamic circulation leading to higher mortality (Wen 2013). The severity of infection depends on the length of cecum ligation and also on the size of puncture which makes it difficult to standardize the protocol (Toscano, Ganea, and Gamero 2011).

1.2.5 CECAL SLURRY MODEL

CLP model lacks standardisation in terms of bacterial load. In order to optimise the severity of infection, cecal slurry model was developed wherein a specific amount of faecal mass from a donor rodent is injected in the recipient animal (Lewis, Seymour, and Rosengart 2016). This model does capture the evolution of sepsis but the kinetics still vary from CLP method which could be attributed to the additional tissue trauma associated with CLP (Poli-de-Figueiredo et al., 2008). Another advantage of cecal slurry model is the ability to use it in neonates to understand neonatal sepsis as CLP is not possible due to smaller organ size (Rincon et al., 2021).

1.3 PATHOPHYSIOLOGY OF SEPSIS

Multiple organ failure is considered to be an important hallmark of sepsis which is characterised by dysfunction of two or more organs as a result of hyper-activated immune response (G.-D. Sun et al., 2021). Mechanism of sepsis-mediated organ failure comprises of two phases- initial phase which involves the production of proinflammatory cytokines like TNFα, IL-1β and IL-6 from monocytes/leukocytes (Sygitowicz and Sitkiewicz 2020). This leads to upregulation of vascular cell adhesion molecule 1 and endothelial-leukocyte adhesion molecule 1 on endothelial cells, increasing the adhesivity of T cells and monocytes (Goligorsky and Sun 2020). During initial inflammatory state, neutrophils get activated leading to production of reactive oxygen species (ROS)(Stanzani, Duchen, and Singer 2019). Collectively, these events may cause extensive activation and damage to endothelium. Integrity of endothelium plays a crucial role in maintaining the proper vasculature and functioning of organ systems (Dolmatova et al., 2020). Inflammation-mediated proinflammatory cytokines lead to increased membrane permeability, apoptosis and swelling (Chousterman, Swirski, and Weber 2017). The second phase of infection involves the alterations in the interstitial space of the organs. The activated leukocytes near endothelium migrate to the interstitial space in the organs leading to excessive production

of cytokines and ROS causing damage to parenchyma. The cytokines produced as a result can eventually migrate to other organs and initiate a cascade of inflammatory response (Sygitowicz and Sitkiewicz 2020).

Gut is an immunologically active organ with immune cell-rich intestinal mucosa capable of synthesising pro-inflammatory cytokines as a result of sepsis (Haussner et al., 2019). These cytokines along with toxic ROS production can cause disintegration of mucosal epithelium by downregulating the tight junction proteins like claudin and occluding (Yoseph et al., 2016). Mucosal disintegration leads to translocation of toxic substances to interstitial tissue leading to secondary cytokine storm. Lymph drainage and microcirculation can exacerbate the deleterious effects of sepsis by causing the influx of cytokines and inflammatory mediators to the blood (Turner 2009).

Another key organ that gets affected as a result of sepsis is lung, developing into acute respiratory distress syndrome in patients (Hu, Hao, and Tang 2020). Initial cytokines and ROS-mediated epithelium dysfunction cause disruption in fluid transport and alveolar flooding (Rios, Iscar, and Cardinal-Fernández 2017). Hepatic injuries and liver dysfunction also account for a greater proportion of sepsis-mediated MODs (D. Wang, Yin, and Yao 2014). NK cells, NKT and Kupffer cells are the major contributing cell types triggering inflammatory response in liver (Highton et al., 2021; D. Wang, Yin, and Yao 2014). Kupffer cells lining the lumen of sinusoids upon activation can trigger the production of pro-inflammatory cytokines directly into the blood stream(D. Wang, Yin, and Yao 2014). The general consequence of cytokine storm is an impairment of mitochondrial functions across large variety of organ tissues. It is a main cause of multi organ failure and a resistance to resuscitation attempts. Kidneys are the most affected organ as cells of the proximal convoluted tubule express one of the highest mitochondrial densities. Other vital organs-heart and brain, are also affected as a result of sepsis (Caraballo and Jaimes 2019).

Excessive endothelium activation and disruption in response to inflammatory mediators can alter the microcirculation, disturbed coagulation and haemodynamic collapse (Dolmatova et al., 2020). During septic shock, the autonomic regulatory mechanisms to counter the hypotension as a result of heightened immune response are impaired (Ferrer et al., 2014). Overactivation of sympathetic nervous system and under-activation of parasympathetic

nervous system are the key outcomes in septic shock patients (Carrara et al., 2021). These patients show excessive amount of catecholamines (nor-epinephrine and epinephrine) which are correlated with high morbidity and mortality (Boldt et al., 1995). Imprudent production of catecholamines causes overwhelming adrenergic stress (Dünser and Hasibeder 2009). Beta-adrenergic receptors in heart make it highly vulnerable to these changes leading to detrimental effects like tachycardia, myocardial ischemia, impairment in diastolic functioning and apoptosis (Dünser and Hasibeder 2009). Cytokines and iNOS production are known to downregulate beta adrenergic receptors in heart diminishing the sympathetic functioning of cardiovascular system (Suzuki et al., 2017). Studies in animal models have demonstrated the impairment in baroreceptor mechanisms failing to restore hypotension (Carrara et al., 2018).

1.3.1 TOLL-LIKE RECEPTOR SIGNALLING

During optimal conditions, bacterial infections are cleared by the system efficiently. Pathogen associated molecular patterns (PAMPs) present on the bacteria are recognised by PAMP receptors (for e.g., toll-like receptors (TLRs)) present on the APCs which constitute the first line of defence against an infection (Lu, Yeh, and Ohashi 2008). Binding of PPRs to PAMPS leads to the initiation of pro-inflammatory cascade resulting in the production of cytokines (Pålsson-McDermott and O'Neill 2004). The pro-inflammatory and anti-inflammatory processes are highly regulated during standard conditions. However, in case of sepsis, binding of TLRs to PAMPs causes a dysregulated host response wherein both pro-inflammatory and anti-inflammatory pathways get activated (CHAUDHRY et al., 2013). Binding of TLRs to PPRs causes transduction of NFκB to the nucleus leading to the expression of pro-inflammatory cytokines, like interleukin- 12 (IL-12), IL-18, tumour necrosis factor alpha (TNFα) and interferons (IFNs). These in turn activate IL-6, INF-γ and the complement cascades which inhibit adaptive immune system by negative feedback (Lu, Yeh, and Ohashi 2008). During severe infections, due to high bacterial load, large number of neutrophils (mature and immature) are released to the site of infection (Liu et al., 2017). Binding of PAMPs to TLRs on immature neutrophils can lead to inefficient phagocytosis and an eventual increase in neutrophil extracellular traps (NETS) which are capable of immobilizing pathogens (Denning et al., 2019). Overproduction of NETS due to bacterial load

is associated with hypercoagulation during sepsis(Cox et al., 2020). A schematic overview of TLR signalling is described below.

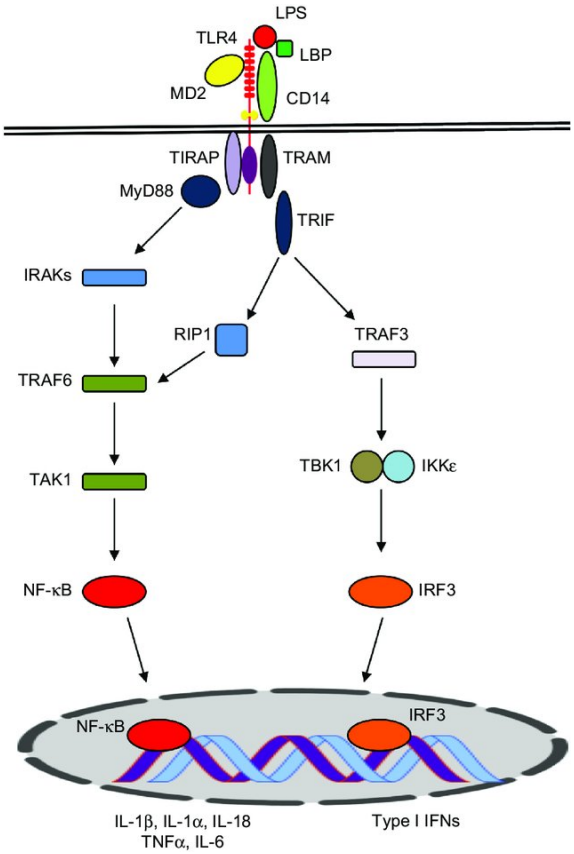

Figure 2: *Schematic overview of TLR4 signalling pathway. LPS binding to TLR4 complex may activate MyD88 (Myeloid differentiation primary response 88) dependent or independent pathways. MyD88 dependent pathways rely on recruitment of IRAKs (Interleukin -1 receptor associated kinase) and TRAF6 (TNF- receptor associated factor 6) resulting in the activation of TAK1 (Transforming growth factor-beta-activated kinase 1) which phosphorylates IKKβ(Iκβ Kinase) releasing the NFκB (Nuclear factor kappa-light-chain-enhancer of activated B cells) to be translocated to the nucleus leading to the transcription of pro-inflammatory cytokines like IL-1β, IL-1α, IL18, TNFα etc. MyD88 independent pathway recruits TRIF (TIR-domain containing adaptor inducing interferon – β) and TRAF3 which activate IRF3 (Interferon regulatory factor 3) via TBK1 (TANK-binding kinase 1). IRF3 leads to the transcription of interferons and IFN (Interferon) inducible genes (Diamond et al., 2015).*

1.3.2 SYSTEMIC INFLAMMATION AND BRAIN

The recognition of systemic inflammation by brain is a vital step in development of a suitable response against infections (Sankowski, Mader, and Valdés-Ferrer 2015). Systemic inflammation leading to secretion of pro-inflammatory cytokines like TNF-α, IL-1 β or IL-6

can activate brain either by humoral or neural pathway (Bourhy, Mazeraud, Bozza, et al., 2022). Humoral pathway may signal the brain via circumventricular organs lacking blood brain barrier (BBB), through inflammation-mediated disrupted BBB passages or by active transport of cytokines via receptor mediated endocytosis which are better described below (Dantzer et al., 2008). The neural pathway on the other hand signals the brain through receptors present on the afferent nerve endings of vagus nerve (Akrout, Sharshar, and Annane 2009; McCANN et al., 2000).

Cross talk between brain and immune system- cholinergic anti-inflammatory pathway

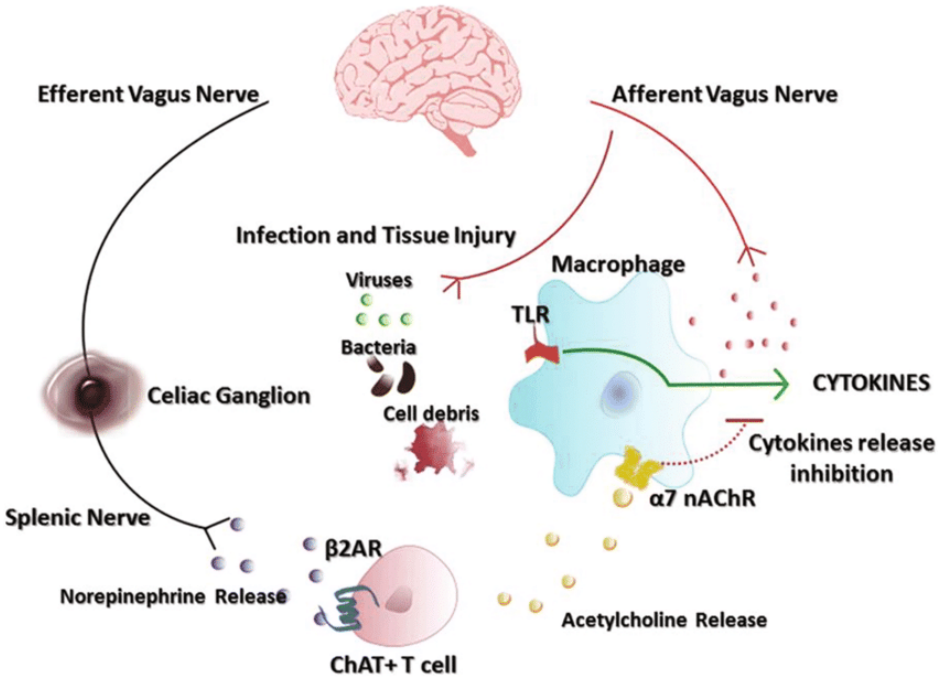

Figure 3: *Cholinergic anti-inflammatory pathway (CAP): Systemic inflammation leading to the production of pro-inflammatory cytokines stimulate the afferent arm of vagus nerve which signals the nucleus tractus solitarius resulting in the production of noradrenaline. The activated ascending terminal of vagus nerve containing splenic projections leads to the production of acetylcholine. This in turn acts on macrophages and inhibits inflammatory response (Benfante et al.,, 2021).*

The vagal afferent nerve endings terminate in dorsal vagal complex comprising of area postrema (AP), nucleus tractus solitarius (NTS) and dorsal motor nucleus (DMN) of medulla oblongata (McCANN et al., 2000). The major site of information reception in vagal afferent nerves is NTS, taking a role in coordinating the endocrine and autonomic system (Carrara et

al., 2021). The vagal sensory input is further relayed to forebrain areas like amygdala, hypothalamic nuclei and insular cortex (IC). Paraventricular nucleus of hypothalamus facilitates the release of corticotropin releasing hormone (CRH) which modulates the anti-inflammatory responses during inflammation. NTS projects to rostral ventrolateral medulla (RVM) which further project to locus coeruleus (LC), a major noradrenergic source to higher brain regions. LC and RVM then project to the spinal cord via sympathetic pathways (Berthoud and Neuhuber 2000). During inflammation, stimulation of vagal nerve results in the activation of hypothalamic pituitary axis (HPA) and sympathetic nervous system leading to production of glucocorticoids and catecholamines, respectively (Bonaz, Sinniger, and Pellissier 2017). Glucocorticoids exert their effect by supressing the NFκB factor consequently decreasing the production of pro-inflammatory cytokines. Adrenergic receptor containing splenic T lymphocytes synthesize acetylcholine which then acts on the α7 subunit of the nicotinic receptors AChR (α7 nAChR) (Benfante et al., 2021). Activation of these receptors initiates a cascade of pathway leading to the inhibition of TNFα, IL-1β, IL-8, IL-8 high-mobility group box 1 (HMGB1) consequently supressing inflammatory response (H. Wang et al., 2004). Various studies have confirmed the role of vagus nerve in modulating the immune response by stimulation and inhibition studies in experimental animals. This has been considered as one of the main therapeutic targets during systemic inflammatory conditions (Kelly et al., 2022).

1.3.3 SEPSIS-ASSOCIATED BRAIN DYSFUNCTION (SABD)

Main pathological consequences of acute systemic inflammation on brain include cerebral damage, blood brain barrier disruption, hypoperfusion, prolonged microglial activation, neuroinflammation, amyloid beta accumulation and tau pathology (Sekino, Selim, and Shehadah 2022).

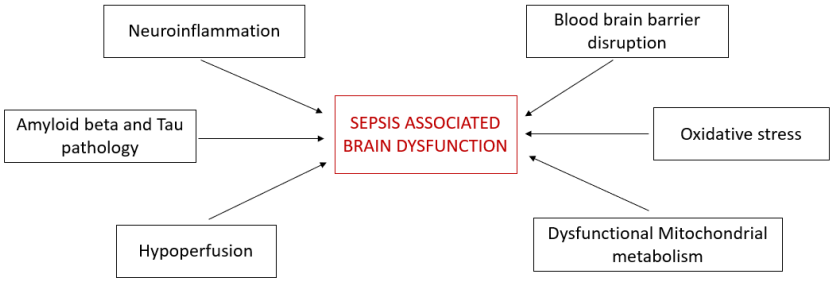

***Figure 4**: Schematic showing major factors leading to SABD.*

1.4.1 NEUROINFLAMMATION

Cytokines produced during systemic inflammation can enter brain through areas lacking blood brain barrier like circumventricular organs and endothelium of choroid plexus (Laflamme et al., 2003). Cerebral endothelial cells have IL-1β and TNF-α receptors, binding of which to the systemically produced pro-inflammatory cytokines initiates a cascade of inflammatory pathway in the brain activating microglia. Continual activation of microglia is associated with enhanced neuroinflammation and production of reactive oxygen species (ROS) (X. Yan et al., 2022).

1.4.2 BBB DYSFUNCTION

BBB in the vessels of central nervous system plays a very important role in maintaining the homeostasis of central nervous system (CNS). Endothelial cells present on the walls of vessels form tight junctions thereby providing physical barrier which isolates and hence protects the brain from the dynamic fluctuations of ions or pathogens in peripheral system (Daneman and Prat 2015). Due to proinflammatory cytokine production during systemic inflammation, endothelial cells get activated causing the initiation of TNFα pathway which eventually leads to the downregulation of tight junction proteins like ZO-1 and claudin-5 leading to a leaky BBB (Erikson et al., 2020). A study in a rat model of sepsis (10mg/kg) has shown dysfunctional BBB for at least up to 1 week of LPS injection in hippocampus, cerebral cortex and perirhinal cortex and for up to 6 weeks in cerebral cortex demonstrating the BBB dysfunction can be used as a long term neuroinflammatory marker of sepsis (Towner et al., 2018).

1.4.3 MITOCHONDRIAL DYSFUNCTION

Mitochondria in physiological conditions play a vital role in regulating metabolism and oxygen consumptions in the body (Osellame et al.,, 2012). Mitochondrial dysfunction in terms of inhibition of enzymatic complexes and oxygen consumptions has been evidenced in sepsis patients (Garrabou et al., 2012). Organ failure in sepsis has now been linked to mitochondrial depletion as it leads to reliance of system to derive energy anaerobically resulting in cytopathic hypoxia (D. R. Schwartz, Malhtora, and Fink 1999). One of the factors contributing to sepsis associated brain dysfunction is the mitochondrial-induced change in immunological profiling of microglia. Injection of exogenous functional mitochondria intracerebroventricularly led to the M2 polarity of microglia and reversal of cognitive deficits in a CLP model of sepsis in mice (Yan et al.,, 2020, Manfredini et al.,, 2019).

1.5 EFFECT OF ACUTE SEPSIS ON BRAIN

Patients in the acute phase often suffer from altered mental status, inattention and confusion collectively termed as delirium (Tsuruta and Oda 2016). Diagnosis of SABD relies on neurological assessment, including EEG and in some cases, MRI scanning (Bozza et al., 2010; Pantzaris et al., 2021). Polysomnography evaluations in the sepsis patients in ICU show an abnormal EEG activity with predominance of epileptic and periodic discharges (Oddo et al., 2009). Twenty percent of critically ill patients develop convulsive or non-convulsive seizures which may be caused by the neuroinflammation mediated excitotoxicity (Alessandri, Badenes, and Bilotta 2021; Oddo et al., 2009). Studies in human sepsis patients have shown the correlation of occurrence of periodic discharge activity, increased delta power and decreased EEG reactivity with ICU mortality emphasising on the importance of EEG as a biomarker of SAE (Azabou et al., 2015; Pantzaris et al., 2021). Lack of EEG reactivity remains to be an important factor related to outcomes in septic shock patients for up to 1 year which shows the influence of these parameters even in chronic phases (Gilmore et al., 2015). Polysomnography recordings in acute phase have shown sleep-wake disturbances (often called as ´sleep fragmentation´) which are known to be associated with poor outcomes in septic shock patients (Telias and Wilcox 2019). Despite being an important indicator of progression of SAE, mechanism of changes of oscillatory activity in CNS in the acute phase of sepsis is poorly understood. ICU environments are known to play a key role in aggravating sleep related disturbances in critically ill patients (Jung et al., 2020). Sleep

fragmentation and changes in EEG activity, namely decreased delta power in NREM and increased occurrence of epileptic discharge activity have been confirmed in animal models of sepsis as well (Baracchi et al., 2011; Sewal et al., 2017). At cellular level, excessive neuroinflammation and production of complement anaphylatoxin C5a during sepsis may lead to neuronal DNA damage in hippocampus, hypothalamus and amygdala (Akrout, Sharshar, and Annane 2009). Considering the direct effect on hippocampal memory system, sepsis-associated neuronal damage in hippocampus is apparent within a few hours after its induction in endotoxemia model, signifying hippocampal circuitry is one of the most vulnerable parts of the CNS (Orihuela et al., 2006). Pro-inflammatory cytokines are known to be elevated in hippocampus, among others resulting in an inhibition of long term potentiation, a main mechanism of synaptic plasticity and learning (Annane 2009). Behavioural and memory outcomes in the acute phase of sepsis have been also demonstrated experimentally. In a caecal slurry model of sepsis, neuroinflammation-mediated changes led to impairment in avoidance and spatial memory tasks after 24 hrs post inoculation (P. C. Alexandre et al., 2013). In line with this, an endotoxemia model of sepsis showed deterioration in spatial and working memory in T-maze after 24 hrs of sepsis induction (Gamal et al., 2015).

1.6 SUSTAINED CONSEQUENCES OF SEPSIS IN SURVIVORS

One-sixth of sepsis survivors suffer from post-sepsis syndrome which includes detrimental consequences on cardiovascular, respiratory, and cognitive abilities of the patients leading to frequent re-hospitalizations (Goodwin and Ford 2018). As has been described above, sepsis leads to various forms of insults to brain which eventually results into SABD. These changes are not confined to the acute phase but rather manifest into post sepsis syndrome in survivors (van der Slikke et al., 2020). Post-sepsis syndrome is associated with a wide group of symptoms that includes memory impairment, delirium, cognitive fatigue, depression and sleep disturbances (van der Slikke et al., 2020). Prevalence of developing cognitive impairments in septic shock survivors is 3 times higher and leads to the deterioration of quality of life and significant duty demands for their caregivers (Li, Ji, and Yang 2022). There is abundance of evidence showing the impact of sepsis on various forms of memory including long-term and short-term memory, and also on different memory types spanning from non-declarative to declarative memories (Bourhy, Mazeraud, Costa, et

al., 2022; Seidel et al., 2020). These clinical observations are supported by experimental studies. Consequences of high dose of LPS on behavioural and neuroanatomical alterations have shown to be prevalent for up to 3 months in rats (Semmler et al., 2007). Besides the neuronal destruction by excitotoxicity and neuroinflammation, accumulation of amyloid plaques in a long-term span was identified as one of the important mechanisms of sepsis-mediated cognitive impairment in sepsis models (Basak et al., 2021). It has been shown that sepsis leads to exacerbation of the amyloid via activation of astrocytes and upregulation of complement gene C4b (Basak et al., 2021). Previous studies pointed to an increased amyloid plaque load and hyperphosphorylation of tau protein in hippocampus for up to at least 1 week post LPS injection. The animals showed cognitive deficits in episodic-like memory and spatial memory (Kirk et al., 2019). The mechanism of amyloid production during sepsis was explained via the elevation of receptor for advanced glycation end products (RAGE) (Gasparotto et al., 2018).

Polysomnography in sepsis patients during intensive care units (ICU) stays show severely fragmented sleep-wake patterns and hence a highly altered sleep architecture (Telias and Wilcox 2019). Sleep quality has a major impact on survival and outcomes in these patients.

Septic shock survivors often experience poor sleep quality in the form of frequent awakenings leading to day time fatigue and other serious complications (C. Y. Huang et al., 2019; Song, Park, and Oh 2021). Given the essential role of sleep in brain physiology and its common impairments in acute and chronic stages of sepsis, I would start by describing the fundamentals of sleep physiology and the technical terminologies of sleep recordings below. The detailed association of sleep and sepsis is described in section 1.8.

1.7 SLEEP

Sleep is a reversible state of reduced consciousness, vital in almost all forms of living organisms pointing towards its evolutionary relevance (D. A. Lee et al., 2019). Humans spend about one third of their lives sleeping. The functions of sleep remain to be fully elucidated but its deprivation is known to have deleterious effects (Everson, Bergmann, and Rechtschaffen 1989). Importance of sleep for survival dates back to the experiments performed in rats by Rechtschaffen (Everson, Bergmann, and Rechtschaffen 1989). The animals were sleep deprived for about 32 days which eventually led to death due to infection and tissue lesion (Everson, Bergmann, and Rechtschaffen 1989). Sleep assessment is performed using polysomnographic recordings both in clinical and research settings (Campbell 2009). Classical polysomnography involves recording brain activity using electroencephalography (EEG), muscle atonia using electromyography (EMG) and eye movements using electrooculography (EOG). Combination of identified activity patterns is the used to define different sleep states (J. Zhang et al., 2019). Broadly, sleep activity is categorized into two states, non-rapid eye movement sleep (NREM) and rapid eye movement sleep (REM). In laboratory rodents NREM is predominated by slow wave activity and high delta power (0.1-4Hz) whereas REM has a relatively high frequency theta activity (5-10Hz) accompanied by muscle atonia and rapid eye movements (H. Huang et al., 2021). In rodents, sleep classification is majorly limited to NREM and REM states but NREM state in humans is further classified in four substates, N1 through N4. Each cycle of NREM-REM lasts for about 75-90 minutes and REM comprises of about 15-20% of sleep time predominating

in the last one third of sleep (Memar and Faradji 2018). NREM-state 1 is the transition state from wakefulness to sleep which lasts for about 1-7 minutes and is easily interrupted by external stimuli. Stage 2 is characterised by low voltage, mixed frequency waves called K-complexes and spindles which are known to be involved in memory consolidation (Gais et al., 2002). It lasts for about 10-25 minutes, gets longer with each successive sleep cycle and also requires slightly stronger stimuli for awakening compared to stage 1. Stage 3 and 4 are characterised by high voltage slow wave activity and are called slow wave sleep (SWS) (Carley and Farabi 2016). Stage 3 lasts for a few minutes and comprises of 3-8% of total sleep time, while stage 4 is the deepest of all states which lasts for about 20-40 minutes per cycle comprising 10-15% of total sleep time (Patel et al., 2023). Arousal threshold for stage 4 is the highest. REM state, characterised by high theta frequency follows NREM state (Memar and Faradji 2018). First episode of REM may last for about 1 to 5 minutes but increases progressively with further cycles. This sleep state is accompanied by complete muscle atonia and vivid dreams (Brooks and Peever 2008).

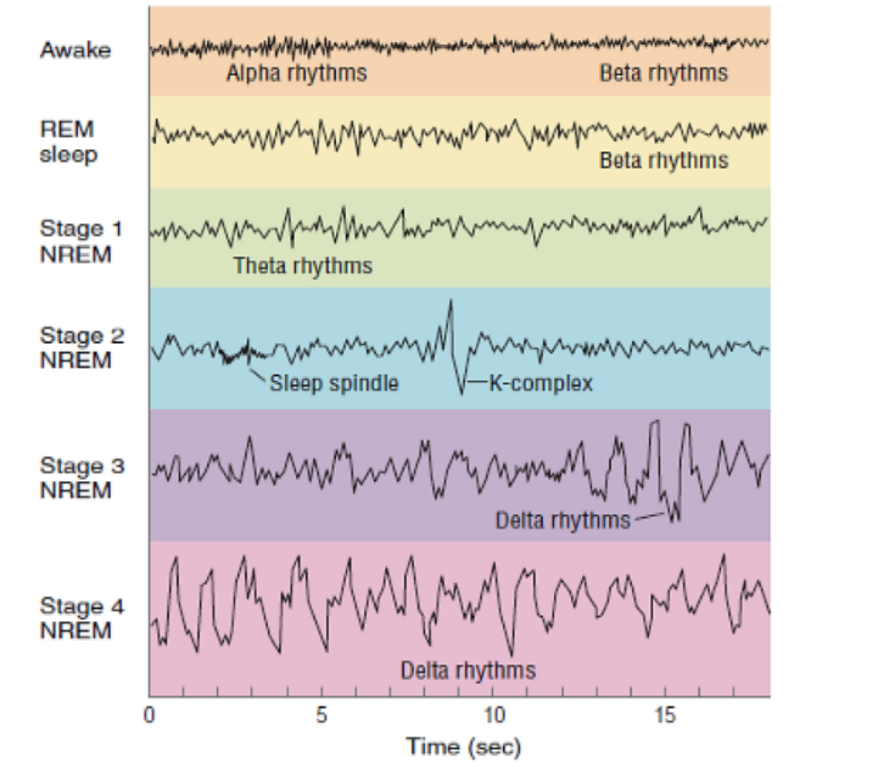

Figure 5: *Types of brain oscillations in human brain are classified in canonical frequency bands. Alpha frequency encompassing 8-13 Hz is associated with resting period with eyes closed during wakefulness. Beta rhythms (13-32 Hz) are prominent during conscious wakefulness and concentration. Stage 1 of NREM comprises of theta rhythms (4-8Hz)*

associated with drowsiness and unconsciousness with time. Sleep spindles ranging in the frequency band of 9-16 Hz occur in stage 2 of NREM occurring in short bursts of 0.5-2 s and are known to be the hallmark of NREM stage. Delta rhythms (0.1-2Hz), the highest voltage waveforms prevail during stage 3 and 4 and are indicative of sleep intensity/propensity (Khan and Aadil 2012).

1.7.1 PHYSIOLOGY OF WAKEFULNESS AND SLEEP

Maintenance of vigilance states is a highly regulated process and requires coordination of wakefulness (reticular activating system, (RAS)) and sleep-inducing pathways (ventrolateral preoptic area (VLPO))(Carley and Farabi 2016). Experimental evidence of midbrain transection in cats leading to permanent coma is indicative of importance of brainstem in wakefulness (Brown et al., 2012). Another set of experiments stimulating areas from medulla to thalamus in cats resulted in the desynchronised EEG activity which was abolished by electrolytic lesion in midbrain tegmentum, again indicating the importance of midbrain tegmentum in maintaining wakefulness (Lindsley, Bowden, and Magoun 1949). Cell specific ablations to unravel the neurons responsible for wakefulness did not give promising results as inhibiting a subgroup of neurons only led to mild decrease in arousal pointing towards a network of neurons working in concert to maintain wakefulness (Buchanan and Richerson 2010). There exists an interconnected network of nuclei from the brainstem projecting to cortex leading to wakefulness. There are four major group of neurons that constitute RAS, the excitatory nor-epinephrine system consisting of neurons in LC which gets its input from brainstem and prefrontal cortex and projects extensivity to cortical areas maintaining wakefulness (Grady, Boes, and Geerling 2022). Lesions in LC lead to reduced wakefulness and complimentary experiments on stimulation lead to awakening from sleep in rodents (Tsubokawa and Katayama 1985). Dopaminergic system of substantia nigra projecting to caudate nucleus (CN) and putamen is involved in muscle tone regulation(Double and Crocker 1995). Another adjacent group of dopaminergic neurons of ventral tegmentum (VT) of the midbrain project outputs to two different pathways, mesolimbic pathway projecting to amygdala, basal forebrain (BF) and hippocampus involved in memory and emotion, and another is the mesocortical pathway projecting to prefrontal cortex involved in attention and planning (Double and Crocker 1995; Hauser, Eldar, and Dolan 2017; Kim, Ghazizadeh, and Hikosaka 2014). Serotonergic system comprising of nuclei from dorsal raphe projecting to thalamus, hypothalamus, BF, cerebral cortex and LC lead to wakefulness but further work

is required to confirm the findings as serotonin has effects on mood, reward and patience (Monti 2011). The cholinergic mesolimbic pathway from VT to nucleus accumbens, also known as motivational and reward circuitry, plays a role in wakefulness. Optogenetic and chemogenic stimulation of VTA in mice leads to initiation and maintenance of wakefulness (Eban-Rothschild et al., 2016).

Cholinergic neurons of BF projecting extensively to cortex are important in wakefulness (Chen et al., 2016). Lesions in BF are known to cause coma and slowing of EEG, while stimulation leads to active wakefulness (S. Kaur et al., 2008). The firing of cholinergic neurons is associated with cortical rhythms in sleep-wake cycles (Boucetta et al., 2014). GABAergic BF neurons promote wakefulness by reducing the inhibitory activity of interneurons eventually increasing the cortical firing (Anaclet et al., 2015). Histaminergic TBN of hypothalamus has been demonstrated to be important in sustaining wakefulness, as H1 knockout mice showed its deterioration (Therapeutics 2002).

1.7.2 HYPOCRETIN-OREXIN NEURONS

Hypocretin producing neurons present in hypothalamus are important regulators of sleep-wake cycles (de Lecea 2012). These cell populations project to cholinergic and dopaminergic populations of RAS including LC, BF, brainstem, VTA signifying their importance in sleep-wake regulation (Inutsuka and Yamanaka 2013). Stimulation of orexin system leads to increased probability of sleep-wake transitions resulting in wakefulness (C. Alexandre, Andermann, and Scammell 2013). Loss of orexin neurons is associated with narcoleptic phenotype with prominent state fragmentation due to inability to maintain wakefulness (De la Herrán-Arita, Guerra-Crespo, and Drucker-Colín 2011).

1.7.3 VENTROLATERAL PRE-OPTIC NUCLEUS (VLPO)

Sleep promoting neural networks often act as inhibitors of the wakefulness-promoting neural circuits (Scammell, Arrigoni, and Lipton 2017). Hypothalamus and BF are two major sleep regulatory regions associated with GABA-ergic projections to wake-promoting circuits resulting in inhibition of pyramidal cells (Vanini, Lydic, and Baghdoyan 2012). These GABA-ergic cell populations are most active during NREM sleep and silent during wakefulness and REM (Zhao et al., 2022). During sleep deprivation (SD), firing activity in cortex increases subsequently corresponding to the sleep need (Vyazovskiy et al., 2009). This sleep center

specifically exists in rostral hypothalamus in the VLPO, lesions of which leads to sleep reduction and fragmentation (Lu et al.,, 2000). Previous studies have shown projections from VLPO to tuberomammillary nucleus to be GABAergic and galanin-containing neurons which are hypothesized to inhibit the pyramidal populations in these regions (Sherin et al., 1998). It has been shown that galanin-containing VLPO neurons project to other circuits of ascending arousal system (adrenergic LC, cholinergic BF, serotonergic raphe nuclei, hypothalamic orexin system) along with reciprocal projections from these regions (Melander, Hökfelt, and Rökaeus 1986).

1.7.4 SLEEP REGULATORY PROCESSES

In complex organisms, sleep regulation is explained by two process model proposed by Alexander Borbély (Borbély 2022). Process C, also called circadian rhythm which is defined by internal pacemaker regulating the hormonal balance and body temperature across a 24-hr cycle and process H known as homeostatic process which maintains these parameters nearly constant (Stiller and Postolache 2005). Process C focuses on fluctuations and timings of sleep onset and other parameters while process H is majorly associated with keeping the sleep related parameters constant to maintain sleep homeostasis (Achermann 2004). There is experimental evidence showing that these two are not independent and influence each other to a greater extent (Vibha and Shukla 2014). The idea of rheostat combines the two terms and is defined by change in parameters across a 24-hour cycle within homeostatic ranges (Perelis, Ramsey, and Bass 2015). Process S is associated with the sleep pressure/propensity which builds up during the day and reaches its peak values at night and decreases exponentially during the course of sleep (Borbély 2022). Process C determines the threshold for process S. Process S is represented by the power of delta in SWA which is the highest at the onset of sleep and decreases exponentially (Waterhouse, Fukuda, and Morita 2012).

1.7.5 PROCESS C REGULATED BY SUPRACHIASMATIC NUCLEUS

Earth's rotation around its central axis is associated with various environmental alterations including temperature, light intensity etc. Species have evolved a way to deal with such alterations in the form of circadian pacemaker called suprachiasmatic nucleus in the anterior hypothalamus regulated by photic and non-photic signals (Easton et al., 2004). In

response to light cues, photic signals travel from retinal ganglionic cells via retinothalamic tract to SCN (Kalsbeek et al., 2006). Non photic inputs are mainly associated with serotonergic inputs from midbrain raphe to regulate phase shifts (Reghunandanan and Reghunandanan 2006). Each cell in SCN behaves as an autonomous circadian oscillator, synchronisation of which leads to an effective pace making potential (Welsh, Takahashi, and Kay 2010). Electrophysiological profiling of SCN neurons forms a sinusoidal waveform pattern which shows the highest activity of cells during wakefulness compared to sleep period (Ramkisoensing and Meijer 2015).

1.7.6 SLEEP AND GLYMPHATIC SYSTEM

CNS is associated with high metabolic rate but also lacks classical lymphatic system (Jessen et al., 2015). Waste removal in CNS is an essential step for maintaining the homeostasis of tissue fluid which is facilitated by a network of astrocytic perivascular channels (J. Kaur et al., 2021; Louveau et al., 2017). This network of flow consists of CSF flowing through periarterial space eventually mixing with the interstitial fluid (IF) carrying all the waste products to perivenous space (Plog and Nedergaard 2018). The system of fluid transfer between CSF and IF facilitating the elimination of waste is termed as glymphatic system (Jessen et al., 2015). The ground breaking discovery by Iliff et al.,, showed that injecting tracer molecules in subarachnoid space travelled through a series of channels which used pressure instead of simple diffusion leading to an efficient clearance of waste products from the brain (Iliff et al., 2012). It was speculated that the functioning of glymphatic system might play a key role in the accumulation of amyloid beta in Alzheimer's disease. This hypothesis was tested by injecting amyloid beta in the brains of wildtype mice and genetically modified mice with disrupted glymphatic system (Iliff et al., 2012; Jessen et al., 2015). The inability of genetically modified mice for glymphatic system to clear amyloid plaques compared to the healthy mice signified the important role of glymphatic system in AD pathogenesis (Iliff et al., 2012). Glymphatic system is most effective during sleep when the interstitial space is increased enabling the flow and exchange of fluids much more efficient (O. C. Reddy and van der Werf 2020). Poor sleep quality and quantity in AD has been implicated in alteration of glymphatic system (Reeves et al., 2020). Sleep fragmentation in general is associated with deterioration in glymphatic system by modulating the activity of aquaporin-4 (AQP4) present on the astrocytic end feet (Vasciaveo

et al., 2023). Under septic shock conditions, blood brain barrier is disrupted leading to altered composition of CSF requiring the clearance of waste more efficiently by the glymphatic system. However, the altered morphology of astrocytes as a result of neuroinflammation slows down the glymphatic functioning (Hinkerohe et al., 2010; Jha et al., 2018). Sleep disturbances associated with sepsis and inflammation may be associated with further deterioration of glymphatic system as it may affect the flow and secretion of CSF (Ren et al., 2021).

1.7.7 SLEEP ABNORMALITIES

Any disturbances in the sleep-wake regulatory mechanisms can lead to sleep disorders which may have subsequent detrimental effects on physical, mental and cardiovascular systems(Dijk and Landolt 2019). Usually, sleep disturbances are related to the patient's personal history which often includes improper sleep habits, alcohol consumption, neurological or psychiatric illnesses (Kong, Choi, and Seo 2019). Clinically, sleep disorders are characterised based on disturbances in sleep-wake transitions, time spent in a particular vigilance state or disturbances at the level of muscle atonia (Chokroverty 2010).

1.7.7.1 OBSTRUCTIVE SLEEP APNEA (OSA)

OSA is a condition of partial or total pharyngeal collapse resulting in decreased oxygen saturation and fragmented sleep episodes which are often non-restorative (Sankri-Tarbichi 2012). The narrowing of air passage is directly linked to obesity wherein factors like neck circumference along with decrease in muscle tone leads to pharyngeal collapse (Schwab et al., 1995). It is more prominent in males than females (Lin, Davidson, and Ancoli-Israel 2008). Common symptoms include, snoring, breathing cessation while sleeping, day-time sleepiness and fatigue. Day time sleepiness can be quantified using Epworth Sleepiness Scale which can score the severity of sleepiness (Johns 1991). Brain imaging in OSA have shown cellular atrophy and damage in CNS (Steward et al., 2022). Hippocampal Inflammation is one of the major factors associated with OSA outcomes which have been partially restored using CPAP treatment (O'Donoghue et al., 2012).

1.7.7.2 NARCOLEPSY

Narcolepsy is characterised by excessive day time sleepiness and difficulty in attention for longer hours and day-to day tasks (Chavda et al., 2022). The diagnosis can take 5-15 years

from the onset of symptoms (Frauscher et al., 2013). The neuronal cause of narcolepsy is associated with dysfunctional hypothalamic neuropeptides called orexins (hypocretin 1 and 2)(Siegel and Boehmer 2006). People with narcolepsy have disrupted sleep at night and during the day, are unable to maintain the state of wakefulness for optimal periods which are often termed as sleep attacks (Roth et al., 2013). Narcolepsy in some cases can be accompanied by cataplexy which involves loss of muscle tone at any given time in the day. Under optimal conditions, transitions occur from NREM sleep to REM sleep but in narcolepsy, direct transitions from wakefulness to REM are possible making the patients much more vulnerable to perform basic day-to day tasks (Dauvilliers, Arnulf, and Mignot 2007). CNS stimulants like modafinil or sodium oxybate are helpful in promoting wakefulness and alertness in narcoleptic patients (Wise et al., 2007).

1.7.7.3 INSOMNIA

Insomnia is a condition of inability to fall asleep or increased sleep latencies, difficulty in maintaining uninterrupted continuous sleep, early awakenings leading to poor sleep quality or insufficient time of sleep (Bonnet and Arand 1997). It can present independently or as a comorbidity of pain or depression (Finan and Smith 2013). Assessing neural behavioural performances in these patients is associated with poor attention and memory deficits (Basta et al., 2007). Constant fatigue is a major symptom of this condition consequently leading to poor quality of life (Harvey 2001). Pathophysiology of insomnia is not well defined but it is often correlated with hyperarousal syndrome with enhanced metabolic activity during wakefulness as well as sleep (Nofzinger et al., 2004). Electrophysiological recordings show an increased high frequency oscillation in insomniac brains compared to controls (Riemann et al., 2010). Benzodiazepines agonists are used to treat insomnia as they bind to GABA receptor complex leading to the inactivation of RAS, thereby promoting sleep (Fu et al., 2023).

1.8 EFFECT OF SEPSIS ON SLEEP

Sleep and sepsis-mediated inflammation are related bidirectionally. Sleep plays a major role in proper functioning of immune system (Ibarra-Coronado et al., 2015). In the early 20s, sleep-inducing muramyl peptide was discovered to be accumulated during the wakefulness which was cleared during sleep. These peptides are known to activate sleep modulatory substances like TNF α and IL-1β which play a role in homeostatic regulation of slow wave

sleep (Shoham et al., 1987). Sleep-related disturbances are associated with increased levels of cytokines eventually leading to metabolic and cardiovascular disorders (Amin et al., 2020). Despite the well described bidirectional relationship between immune system and sleep processes, the impact of sepsis on sleep is poorly understood. Polysomnography in sepsis patients during ICU stays show severely fragmented sleep-wake patterns. The sleep architecture is highly altered which is reflected in predominance of stage 1 and 2 of NREM but a significant decrease in stage 3 and REM state (Freedman et al., 2001). Total sleep time may not get affected but there is extensive sleep fragmentation associated with acute sepsis thus leading to qualitative SD but not necessarily quantitative. (Freedman et al., 2001; Mistraletti et al., 2008). EEG recordings in sepsis patients also show a predominant occurrence of epileptic discharges, seizure like activity and triphasic waves pointing towards the potential of EEG as biomarker of sepsis (Pantzaris et al., 2021; Young et al., 1992). The aetiology of sleep disruptions during ICU stays can, to some degree, result from various external factors like noisy ICU environments involving alarms, ventilators, constant lights, beeping, phone etc. (Weinhouse and Schwab 2006). Previous studies have quantified the level of noise under ICU conditions speculating it to be one of the most important external stimuli playing a major role in sleep-wake disturbances (Gabor et al., 2003). However, a number of studies have shown no significant correlation between the noise levels and sleep-wake patterns emphasising the importance of intrinsic factors being responsible for such fragmentation (Freedman et al., 2001; Roth, Kramer, and Trinder 1972). During acute sepsis, melatonin secretion is known to be disrupted and being an important regulator of sleep-wake patterns by resetting circadian alterations, melatonin therapies are used in an attempt to normalise these vigilance states (Bourne and Mills 2006). There is profound evidence of sleep disturbances in animal models of sepsis. In a CLP model of sepsis, Berrachi et al.,, showed NREM discontinuity, REM suppression for 24 hrs and decreased delta power in NREM showing diminished sleep quality (Baracchi et al., 2011). Similar outcomes of sleep architecture and quality were shown in an endotoxemia model of sepsis (Ingiosi and Opp 2016). Effect of low dose LPS resulting in immune challenge has shown similar outcomes in sleep-wake patterns but spectral characteristics showed enhanced delta power in NREM. These state specific differences however could be attributed to rather unusually defined range of NREM delta used in the study (0.5-7Hz) or the dose of LPS (Lancel et al., 1995).

Despite quality of sleep is an important factor determining the outcomes in septic shock patients, there is still a wide caveat in detailed understanding of sleep pattern changes.

There is abundance of evidence showing the impact of sepsis on various types of memories including long-term and short-term memories, fear memories, learning tasks and also procedural memories (Barichello et al., 2019; Comim et al., 2011; Semmler et al., 2007, 2007). Before describing a detailed impact of sepsis on cognition in animal and human studies, I will first discuss the types of memories and the proposed theories of memory consolidation and processing.

1.9 MEMORY

Our personality to large degree is originating from direct and indirect experiences we gain and remember. Without memories an essential part of adaptive processes, the life of individual would not be sustainable in a longer time course. Memories are the core basis of our personal lives wherein we adapt to certain situations based on previously acquired information modulating our responses for the best possible outcomes. Consolidation hypothesis of memory proposed by Müller and Pilzecker more than a century ago sheds light on the time dynamics of memory formation (McGaugh 1999). The studies performed in humans suggested that newly formed memories are fragile and consolidated in a time dependent manner (McGaugh 2000). At the cellular level, the discovery of long-term potentiation describes the storage of memory traces in the form of strengths of synaptic connections (Lømo 2003). After the initial memory encoding, the neural representations are known to follow two types of consolidation processes named synaptic consolidation and systems consolidation (Mascetti et al., 2013). Synaptic consolidation is associated with the remodelling of synaptic structure within the given memory engram enhancing its stability. System consolidation on the other hand, is a much slower process involving the initially stabilised memories to be redistributed to other brain networks (Tononi and Cirelli 2014).

Brain has a massive capacity to store information and to retrieve it when required. Memories can be broadly classified into three major categories, sensory memories, lasting for about 1-3 seconds, short term memories lasting for about few minutes to hours and long-term memories which can last until years or a lifetime (Jenkins and Dallenbach 1924). Sensory memories can be further classified into iconic (visual, Sperling et al.,, 1960), echoic

auditory, (Eriksen and Johnson 1964), and haptic (touch) memories. Short term memories are the ones wherein a small amount of information is retained for a short period of time (Goelet et al., 1986; B. Schwartz 1989). Long term memories can be categorised into two classes, explicit and implicit memories(Barco, Bailey, and Kandel 2006). Explicit memories are further classified into episodic and semantic memories(Cortina and Liotti 2007). Explicit memories are consciously evoked memories and episodic ones include the memories which are subjective to one's life and reflect personal experiences (Robbins 2009). Autobiography is a good example of episodic memory wherein one describes their personal life experiences associated with a sense of ownership. Brain regions important in storing such type of memories include hippocampus, perirhinal cortex, entorhinal cortex and para hippocampal cortex (Thompson and Kim 1996) Semantic ones are associated with facts and concepts which may or may not be associated with place and time (Duff et al., 2020). This type of memory usually includes general knowledge and concepts learned at a particular point in life and can be utilized in logical reasoning or problem solving (Duff et al., 2020).

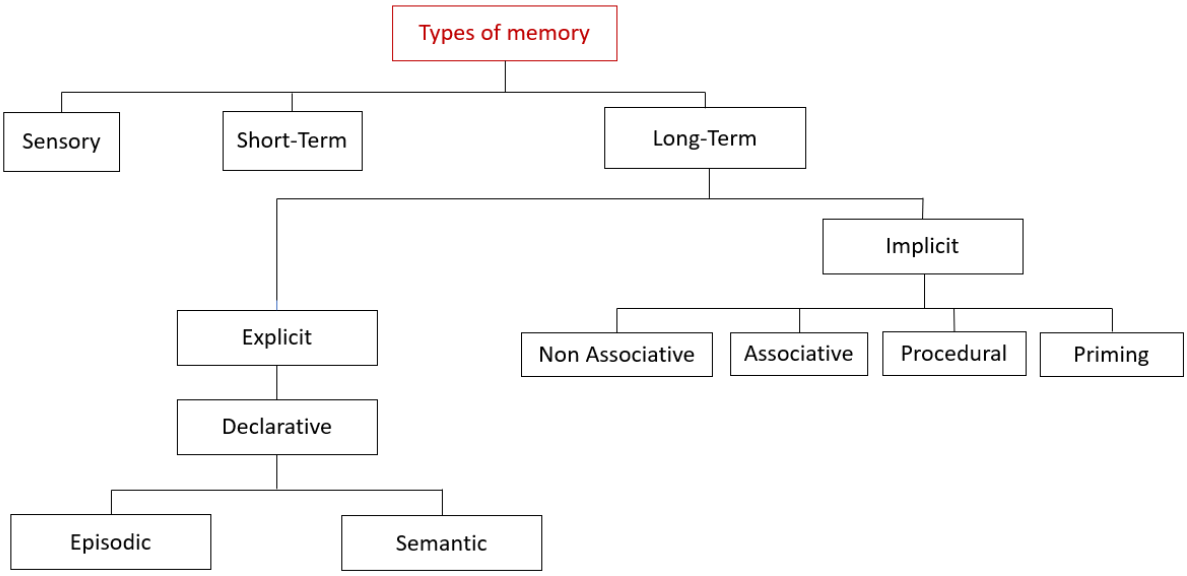

Figure 6: *Schematic showing different types of memories.*

Implicit memories are the ones which do not require consciousness but are evoked subconsciously and include procedural, associative, non-associative and priming types of memories (Schacter, Chiu, and Ochsner 1993). Priming is a cued recall of a task which influences the response to a subsequent task without the conscious or explicit recollection (Schott et al., 2005). Associative memory involves the association of two unrelated stimuli

for e.g., a person wearing a particular perfume, association of that fragrance can elicit the recall of that person (Pritz et al., 2023). Non-associative memory is the one wherein stimuli are unpaired and can be recollected independently (Thorwart and Livesey 2016). Procedural memory involves learning of tasks requiring motor skills which once learnt, do not require active conscious, for e.g., riding a bicycle, swimming, driving a car, skiing etc. Major brain areas associated with implicit memories include basal ganglia, cerebellum, and motor cortex (Mochizuki-Kawai 2008).

Memory function comprises of three stages, memory encoding, memory consolidation and retrieval. Memory encoding is the process of learning a new piece of information and at this stage, it is fragile and more vulnerable to a wide range of modulatory inputs (Winocur and Moscovitch 2011). Encoding is facilitated by multiple brain areas depending on the type of information. For e.g., declarative memories are encoded using hippocampus whereas cerebellum and basal ganglia are important in procedural memory formation (Eichenbaum 2001; Mochizuki-Kawai 2008). Memory consolidation is the process of stabilisation of this fragile or labile piece of information into a stable one and integrate it into the pre-existing networks. Consolidation process happens during wakefulness and offline-sleep (Achermann 2004; Tononi and Cirelli 2014). Studies have shown significant consolidation during both NREM and REM states. The idea of consolidation during sleep is strengthened by the argument of having reduced inputs from the external stimuli which could interrupt the process of consolidation. Third stage of memory processing involves memory retrieval which is the process of recall of acquired memories (Mascetti et al., 2013).

1.10 THEORIES DEMONSTRATING THE ROLE OF SLEEP IN MEMORY PROCESSING

Importance of sleep in memory processing and consolidation dates back to the experiments performed in 1885 by Hermann Ebbinghaus who showed a correlation between sleep and memory outcomes in humans (Ebbinghaus (1885) 2013).These finding were replicated by Jenkins and Dallenbach supporting the importance of sleep in memory (Jenkins and Dallenbach 1924).

To be stored for long time duration, the short term memories after their acquisition/encoding undergo process of consolidation in the pre-existing networks. Awake state is optimized for information acquisition and retrieval whereas sleep is known to be

optimal for consolidation which protects the information from decay or external stimuli (Ebbinghaus (1885) 2013). Earlier, sleep's role was known to be limited in this aspect as opposed to today's idea of sleep being an active player in the memory consolidation (Klinzing, Niethard, and Born 2019). Previously, REM sleep's role in consolidation was actively studied but now the focus has been shifted more towards the role of NREM in memory consolidation (Pereira and Lewis 2020; Siegel 2001). Described below are the theories to support the role of sleep in memory consolidation.

1.10.1 SYSTEM CONSOLIDATION THEORY

According to this theory, after the initial encoding of information in the hippocampus, cell sequences are replayed during the SWS. This process is known to strengthen the memory trace (Bendor and Wilson 2012). Molecular evidence of synaptic strengthening is shown for instance by enhanced spine density between neurons post learning tasks (Runge, Cardoso, and de Chevigny 2020). According to this theory, memories are dependent on hippocampus only in the initial phase post acquisition and eventually are transferred to the extra hippocampal regions like neocortex (Squire et al., 2015). Experimental evidence of replay of memory sequences has been confirmed in human studies as well by intracranial recordings showing cognitive-motifs similarity in sleep sessions following a learning task (Jiang et al., 2017). Retrieval of episodic memory elicited the similar replay in cortex in humans showing the relevance of this parameter in human brain (Vaz et al., 2020). Temporally graded retrograde amnesia(RA) supports the system consolidation theory wherein more recent memories are severely affected due to hippocampal damage in contrast to remote ones (McGaugh 2000). Once the initial consolidation of fragile memories is complete, they are independent of hippocampus and hence remain unaffected (Winocur and Moscovitch 2011).

1.10.2 MULTIPLE TRACE THEORY

Hippocampal damage does not always lead to RA which led to the emergence multiple trace theory by Lynn Nadel and colleagues wherein they emphasize the importance of hippocampus in retrieval of episodic memory irrespective of age of memory (Nadel et al., 2000). Semantic memories however can become independent of hippocampus over time and retrieval is facilitated by cortical representations which explains the intactness of

semantic memories in retrograde amnesia (Nadel et al., 2000). The binary categorization of hippocampi's role in retrieval is too simplistic for the complex memory processes which resulted in yet another theory known as Competitive Trace Theory (CTT)(Yassa and Reagh 2013).

1.10.3 COMPETITIVE TRACE THEORY

Competitive Trace Theory focuses on the transformation of memory in the form of recontextualization of traces. Each retrieval leads to competition between the overlapping traces when episodic memories get 'semanticized' (Hirano and Noguchi 1998). According to this view, memory consolidation favours conceptualisation over contextualisation enhancing the semantic representation of a memory (Yassa and Reagh 2013). During reactivation of a memory, it is encoded by hippocampus leading to partially overlapping traces which will compete with the pre-existing traces in the neocortex. Overlapping features of the memory will be strengthened in the neocortex and non-overlapping ones become conceptualized or decontextualized (Reagh and Yassa 2014). Amnesiac patients fail to recollect new/recent memories because of the failure of hippocampal-dependent consolidation. The remote memories however can still be recalled as a result of decontextualization of memory traces over time (Yassa and Reagh 2013).

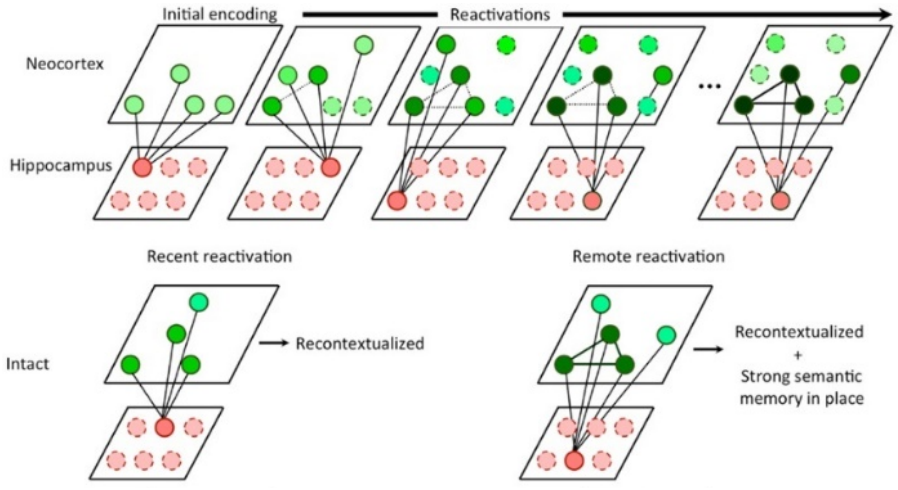

Figure 7: *Hippocampal competitive trace theory: When a memory gets reactivated, a partially overlapping trace is encoded by hippocampus which competes with similar memory traces in the neocortex. Overlapping features in the neocortex are strengthened as a result*

of subsequent reactivations but the non-overlapping traces get decontextualised (Yassa and Reagh 2013).

1.10.4 SYNAPTIC HOMEOSTATIC THEORY

During wakefulness, there are continuous stimuli accompanied by overload of information encoding which can posit energetic and informational constraints on the active brain (Tononi and Cirelli 2014). This can further be associated with decreased signal to noise ratio in terms of synaptic connections and can also saturate these interactions (Karni et al., 1994; Karni and Sagi 1993). Sleep is a state of disconnection from the external environment when synaptic strength between neurons is decreased along with an increase in specificity eventually increasing the signal to noise ratio and optimizing the relevant synaptic connections (Weiss and Donlea 2022). In conclusion, it is hypothesized that sleep serves as a defence mechanism erasing some of recent plasticity induced changes and helps in reducing the burden of neurons thereby increasing selectivity (Tononi and Cirelli 2014).

1.11 OUTCOMES OF SLEEP DISRUPTION ON MEMORY

A myriad of modalities manifest sleep disruption and can be majorly categorised into sleep deprivation, sleep restriction or sleep fragmentation which could be associated with differential outcomes (Medic, Wille, and Hemels 2017) . Among others, SD results in malfunction in attention and working memory which are known to be two important key factors in memory formation and processing (Short and Banks 2014). Impact of SD on attention and working memory tasks has been elucidated by various fMRI studies. (Habeck et al., 2004; Lythe et al., 2012). Neural mechanisms of SD-mediated malfunction of working memory has been demonstrated by decrease in functional connectivity between default mode network, frontoparietal network and dorsal attention network (Dai et al., 2020). SD has a negative impact on neurovascular coupling decreasing the cerebral blood flow during active task thereby disrupting the homeostatic mechanisms (Csipo et al., 2021). Molecular mechanism to understand SD-induced cognitive deficits show reduction of dendritic tree counts in hippocampal CA1 leading to reduced connectivity via overactivation of actin severing protein called cofilin in mice (Havekes et al., 2016). Sleep fragmentation, another form of sleep disruption is defined as the inability to maintain uninterrupted sleep episodes

of appropriate length, an usual outcome of either sleep related disorders like sleep apnea, periodic limb movement etc, or medical conditions involving chronic pain (Short and Banks 2014). Effect of experimental manipulation on sleep-wake patterns using external stimuli has been shown to negatively impact cognition and hence sleep continuity and efficacy are important factors for optimal cognitive functioning (Newbury et al., 2021). Such effects are very well documented and recognised in rodent models and human studies. Deleterious effects of sleep fragmentation on cognitive fatigue have been studied by Benkirane et al., (Benkirane et al., 2022). Animals trained in a hippocampus-dependent contextual fear-conditioning task which was followed by sleep fragmentation showed normal short-term memory but impaired long-term memory (M. L. Lee et al., 2016). This may be associated with impaired memory consolidation. Deterioration of spatial task as a result of post-acquisition sleep fragmentation has also been demonstrated in animal models signifying that consolidation is more susceptible to fragmentation than encoding/acquisition (Ward et al., 2009). Human studies have shown weakened reactivations and eventually poor memory outcomes as a result of disrupted sleep patterns. Duration of undisturbed SWS has been positively correlated with memory benefits emphasising the importance of uninterrupted sleep in memory consolidation (Whitmore, Bassard, and Paller 2022). In order to demonstrate the positive effects of sleep quality and reactivations, a very interesting study performed targeted memory reactivations (TMR) during sleep at different stimulus intensities. They found positive memory outcomes associated with low intensity stimulus which had no impact on sleep continuity (Whitmore et al., 2022). It has been shown that in human patients, sleep disturbances occur way earlier than cognitive disabilities and CSF markers, pointing towards the importance of sleep quality as a potential early biomarker of the disease (Liguori et al., 2020). Widely accepted view of memory reactivation during sleep as an important mechanism of memory processing and storage has been strengthened by above mentioned studies.

1.12 ROLE OF HIPPOCAMPUS IN MEMORY

Hippocampus, a seahorse shaped structure embedded in the deep temporal lobe, plays an important role in memory encoding, consolidation, and spatial navigation (Anand and Dhikav 2012). Studies performed on a patient called ‘HM’ initially uncovered the role of hippocampus in cognitive neuroscience. At the age of 7, he met with an accident and

started developing seizures which became unbearable at the age of 27 even after taking anti-convulsants (Corkin 1984; Squire 2009). William Scoville, who was at the time a neurosurgeon decided to perform bilateral resection of temporal lobe which led to control in seizures at the cost of severe memory loss (Milner, Corkin, and Teuber 1968). He forgot the episodes minutes after they occurred and suffered from retrograde amnesia (Scoville and Milner 1957). He continued to be studied for almost five decades by Brenda Milner (doctoral student of Donald Hebb)(Squire 2009) and others. He became one of the most famous patients in the history of neuroscience contributing to the emergence of modern era of memory research. These findings emphasised the importance of temporal lobe in memory formation and consolidation. Of note, it supported the idea that memory is a distinct cerebral function and can be separated from perceptual and intellectual components (Milner, Corkin, and Teuber 1968).

Structurally, it consists of hippocampal proper (Cornu Ammonis fields), dentate gyrus and subiculum (Cherubini and Miles 2015). CA fields are further divided into three types, CA1, CA2 and CA3 (Fogwe, Reddy, and Mesfin 2023). CA1 is the largest subfield which is delimited by CA2 and presubiculum medially and laterally, respectively. CA2 is bounded laterally by CA1 and medially by CA3 (M. Witter 2012). 90% of cells in CA fields are excitatory glutamatergic pyramidal and 10% are interneurons (Amaral, Scharfman, and Lavenex 2007). Molecular layers of CA subfields consist of alveus, stratum oriens, stratum pyramidale, stratum radiatum, and stratum lacunosum-moleculare(Maccaferri 2005). Ventricular surface of hippocampus consists of thin white myelinated matter which makes up the alveus (Deller et al., 1996). Stratum oriens is the next layer comprising of axons of pyramidal cells, commissure fibres and recurrent axon collateral (Fogwe, Reddy, and Mesfin 2023). Stratum pyramidale comprises of excitatory pyramidal neurons arranged in about 10-30 layers forming an apex and base (Slomianka et al., 2011). The arrangement is such that the base is oriented towards the alveus and apex towards the outermost molecular layer (Fogwe, Reddy, and Mesfin 2023). The basal dendrites diverge into stratus oriens and receive inputs from commissure fibres of identical contralateral parts while the apical ones branch into the deeper layers receiving inputs from commissure fibres of non-identical contralateral parts. EC and mossy fibres of dentate gyrus send outputs to apical dendrites of pyramidal layer (Jonas and Lisman 2014). Stratum radiatum is composed of stellate cells and apical

dendrites of pyramidal cells (Nelson and Chris 2006). The layer closest to hippocampal fissure is the Stratum lacunosum-moleculare which relays the information between CA1 and entorhinal cortex (Maccaferri 2011). It also contains inhibitory interneurons which project to retrosplenial cortex (Jinno et al., 2007).

Dentate gyrus is the point of contact of all sensory modalities helping in binding stimuli together and hence plays an important role in memory processing (Jonas and Lisman 2014). Structurally, it comprises of 3 distinct layers, cell-free molecular layer followed by principle granular layer consisting of tightly packed granule cells (Amaral, Scharfman, and Lavenex 2007). In humans, granular cell layer undergoes neurogenesis which is a rare characteristic for CNS neurons (Dieni, Chancey, and Overstreet-Wadiche 2013; Lopez et al., 2012). Within the granular layer lies polymorphic layer predominated by mossy cells (Amaral, Scharfman, and Lavenex 2007). Subiculum is the dorsal part of hippocampus lying below the fissure connecting it to entorhinal cortex. It is the major junction of information transfer between hippocampus and entorhinal cortex (Köhler 1985).

1.12.1 PATHWAYS OF HIPPOCAMPUS

Hippocampus plays a central role in episodic memory processing and spatial navigation and is the most studied part of the brain (Knierim 2015). The laminar arrangement of pyramidal cells and their unidirectional connections with defined flow of information makes it a favourable model to study synaptic connections (M. Witter 2012).

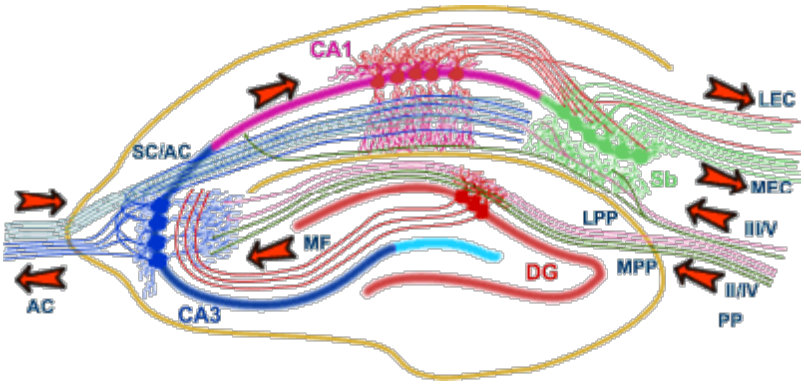

Figure 8: *Pathways of hippocampal network: Hippocampus forms a unidirectional flow of information from entorhinal cortex to dentate gyrus and CA3 via perforant pathway. CA3 receives inputs from dentate gyrus via mossy fibres and sends outputs to CA1 via schaffer collaterals as well as to CA1 via associational commissural pathway (ac). CA1 also receives input from perforant pathway (kesner 2013).*

The major input pathway to hippocampus is the perforant pathway connecting entorhinal cortex to CA regions of hippocampus (Kesner 2013). The axons of entorhinal cortex in perforant pathway principally consist of projections from superficial layers II and III of EC and only a minority from deeper IV and V layers (M. P. Witter 2007). Axons arising from layer II and IV of EC project to DG and CA3 pyramidal layer while layer III and V project to CA1 and subiculum (Swanson, Wyss, and Cowan 1978). The perforant pathway can either be medial perforant pathway or lateral perforant pathway depending of the medial or lateral projections from EC (Amaral, Scharfman, and Lavenex 2007). Mossy fibres pathway involves the mossy fibres of dentate gyrus projecting to CA3 region (Scharfman 2007). Multiple granule cells can synapse a single pyramidal cell in CA3 region (Vyleta, Borges-Merjane, and Jonas 2016). Schaffer collateral pathway involves the axons of CA3 projecting to CA1 which can either be ipsilateral or contralateral depending on the axon coming from the same or the other hippocampus (Martin, Shires, and da Silva 2019). CA3 fibres projecting to the CA1 pyramidal cells of different hemisphere are termed as commissural fibres (Dong et al., 2008). The principal output pathway from hippocampus to EC extends from CA1 to subiculum to EC (Xu et al., 2016). There exists a strict layout of connections between the CA1 and subiculum cells (Y. Sun et al., 2019). Distal end of CA1 projects to the proximal end of subiculum and further projections to EC follow a similar trend wherein proximal CA1 and distal subiculum project to medial EC and distal CA1 and proximal subiculum project to lateral EC (Amaral, Dolorfo, and Alvarez-Royo 1991). Projections to and from EC are associated with perirhinal and postrhinal cortices. Perirhinal cortex sends its projection to lateral EC initiating the lateral perforant pathway whereas postrhinal cortex is associated with medial entorhinal cortex merging into medial perforant pathway (R. P. Petersen et al., 2013).

1.12.2 PLACE CELLS

The ground breaking discovery of place cells by John O'Keefe and Dostrovsky in the year 1971 supported the cognitive map theory of hippocampus (O'Keefe 1976O'Keefe, J., & Dostrovsky, J. (1971). Hippocampal units were recorded while the animals explored an elevated maze with a circular platform in the centre. They discovered that the activity of some of the CA1 units was modulated by position of the subject in the arena and named

them as place cells (O'Keefe 1971). The spiking activity of place cells remained unaltered in response to sensory stimuli e.g., by turning the lights off or rotating the platform with respect to the distant room cues. They also documented a different class of cells which fired maximally at a place which was associated with a behaviour and termed them as 'misplace' cells. This suggested the role of place cells in cognitive maps acting as a neural substrate for cognitive representations (O'Keefe et al., 1979). Place field of a particular cell refers to the location where the given cell is active. In general, cells with spatial modulation their firingare present in multiple brain areas, but the strongest tuning can be found in hippocampal subfields, dentate gyrus, entorhinal cortex, and subiculum (Jacob et al., 2020; Knierim, Lee, and Hargreaves 2006; S.-M. Lee, Seol, and Lee 2022). Place cells are modulated by multiple sensory modalities (Acharya et al., 2016; Save, Nerad, and Poucet 2000). An ensemble of place cells can represent multiple environments depending on the configuration of spatial cues. This phenomenon of switching from one cognitive map to another is called remapping (Colgin, Moser, and Moser 2008). Depending on the alteration of environmental cues, remapping can be categorized into three types- rate, partial or global remapping. Any subtle changes in the environment altering the sensory input can modify the firing rate patterns of place cells consequently leading to rate remapping (Dupret et al., 2010). Switching the reward location or other episodic cue can lead to the change in the place fields of a subset of place cells called partial remapping. In global remapping, majority of place cells switch their place fields representing a complete new environment (Colgin, Moser, and Moser 2008).

Earlier single unit recordings from EC and subiculum showed weak spatial tuning of place cells whereas hippocampal proper showed higher spatial tuning which led to the idea that cognitive map computations occurred within the hippocampal network, particularly in DG and CA3 region (Sharp and Green 1994). Edward Moser and May Britt Moser who were studying hippocampus at the time asked whether the spatial coding originated upstream of hippocampus. A major input to hippocampus comes from entorhinal cortex (EC) present on the dorsal edge in rodent brain. Major part of EC projects to dentate gyrus connected to CA3 subfield which in turn is connected to CA1 (Brun et al., 2002; Fyhn et al., 2004). Additionally, CA1 has direct connection from medial EC. This anatomical connection prompted them to record from EC and they discovered a special class of spatially tuned cells

called grid cells (Hafting et al., 2005). Grid cells firing pattern forms nodes of a hexagon in a given space adding an additional metric in processing cognitive map. Further single unit recordings from entorhinal cortex showed sharply tuned firing fields in the dorsocaudal part of the EC as opposed to dispersed and wider fields in ventromedial part of EC (Fanselow and Dong 2010). It was concluded that the origin of the spatial maps is established well before the information is transferred to the hippocampus.

1.13 LOCAL FIELD POTENTIALS

Local field potentials represent the aggregated summed activity of excitatory and inhibitory potentials from a large population of neurons present near the recording site which can give a great insight about the network state activity (Herreras 2016). LFPs in brain can broadly be categorized into low frequency (1-30Hz) and high frequency oscillations (30Hz or higher) (Jacques et al., 2022). Low frequency oscillations include delta, theta, alpha, beta and low gamma whereas high frequency oscillations include the fast gamma (Jacques et al., 2022). Delta waves are the low frequency oscillations ranging from 0.1-4 Hz, theta oscillations are synchronous brain rhythms lying in 5-10Hz range, alpha frequency are dominated by 8-12 Hz, beta oscillations range from 15-30Hz, and low gamma oscillations have 30-50Hz frequency. High gamma oscillations are dominated by frequencies higher than 50 for up to 250 Hz (Başar 2013b). Low and high frequency oscillations are known to be differentially involved in signal transduction/processing across different brain regions (Cebolla and Cheron 2019). Low frequency oscillations are known to be involved in long range connections while the high frequency oscillations represent the local networking withing the brain regions reflecting the asynchronous neuronal activity (Crone, Korzeniewska, and Franaszczuk 2011; Miller et al., 2009). The interplay between low and high frequency oscillations in neural communication is explained by the amplitude and phase coupling of high and low frequency oscillations respectively (Munia and Aviyente 2019).

Recordings from different cortical regions have shown a relationship between LFP and latent dynamics representing the coordinated neural activity to be frequency dependent and region specific. In one of the studies in macaques, LFPs were recorded from parietal reach region during a reach/saccade task which showed a frequency specific modulation during reach vs saccade. Power spectrum analysis showed the involvement of low frequency

oscillation (1-15Hz) in movement type (saccade vs reach) while the high frequency oscillations (15-50Hz) encoded the direction of movement (Scherberger, Jarvis, and Andersen 2005).

1.13.1 LFP IN HIPPOCAMPUS

Local field potential in hippocampus reflect the summed activity of network of neurons and are known to be important in synchronising neural activity across networks (Teleńczuk, Teleńczuk, and Destexhe 2020). Majorly there are three types of hippocampal LFPs, theta rhythms, sharp wave/ripple complexes and gamma activity with different behavioural correlates in different species (Buzsáki 1986; Buzsáki et al., 1992; Teleńczuk, Teleńczuk, and Destexhe 2020). Information processing in cognition for example is a complex operation requiring a coordinated activity across multiple neural networks, effectively coordinated by neural oscillations (Noguchi et al., 2023). Hippocampus being an important component of spatial memory is an attractive model to study brain rhythms as a correlation of spatially modulated neuronal activity with field potentials can improve our understanding of memory processing.

1.13.2 THETA OSCILLATIONS

Theta rhythm is a low frequency oscillation characterised by a frequency range of 6-12Hz. It is present in all hippocampal subregions and is associated with active exploration and REM sleep (Givens 1996; Green and Arduini 1954). The amplitude and momentary rate of theta corresponds to the speed of the animal (Kennedy et al., 2022). The medial septum band of Broca is known to be theta pacemaker as lesion in this region abolished theta oscillations (Landfield, McGaugh, and Tusa 1972). In the mid-90s, several studies showed the correlation of theta rhythms with learning and hence it led to the theory that theta played an important part in learning (Greenstein, Pavlides, and Winson 1988). Simultaneously recorded hippocampal units have shown that theta cycles represent behavioural order of place cells which could be influenced by sensory or other environmental cues and are termed as theta sequences. They are considered as important temporal structure of neural representations and spatial memory patterns (Drieu and Zugaro 2019; Gupta et al., 2012). This theory was challenged by the experiments which abolished theta entrainment of spikes by blocking the medial septum activity and showed the intact spatial maps for novel environment. It was

hence concluded that theta was not required for the formation of place fields (Brandon et al., 2014). However, as has been pointed above, memory formation/processing is a complex process involving various cell ensembles to work in coordination. Nevertheless, multiple studies have shown the importance of theta sequences in such complex paradigm (L. Reddy et al., 2021; Y. Wang et al., 2015; Zielinski, Tang, and Jadhav 2020). Overall, it is proved that theta sequences integrate the information from different ensembles into functional units important in complex processing like memory formation (Zielinski, Tang, and Jadhav 2020).

1.13.3 SWRS IN HIPPOCAMPUS

Sharp wave ripples are irregularly occurring large amplitude oscillations with negative polarity coupled to high frequency ripple activity (100-250Hz) in the hippocampus during quiet wakefulness, slow wave sleep or consummatory behaviours (Buzsáki 1986). Hippocampus is the primary site of SWR generation as these events occur in hippocampal slices without any extrahippocampal connections (Rex et al., 2009). Sharp waves are known to be generated in CA3 region by the recurrent collateral system and transmitted to CA1 region via Shaffer collaterals (Schlingloff et al., 2014). Ripples on the other hand are generated locally in CA1 by the synchronous basket cell activity (Malerba et al., 2016). Simultaneous recordings from CA1 and CA3 have shown the phase locking of CA3 spikes to low amplitude sharp waves but not to the high frequency ripple oscillations demonstrating the involvement of CA3 in sharp waves but not ripples in CA1 region (Csicsvari et al., 1999). Despite having synchronous burst of activity, neurons are reactivated in a temporally sequential and compressed manner as they fired during a learning/behavioural task. This phenomenon is known as replay (Kudrimoti, Barnes, and McNaughton 1999; Jiang et al., 2017). Place cell recordings in rats have shown the increased cofiring of cell pairs during sleep sessions following a learning task which had overlapping place fields in the given environment (Giri et al., 2019; Ma and Bl 1994). This effect could be associated with synaptic modification during behavioural task which could serve as a mechanism of offline memory consolidation (Ma and Bl 1994). Importance of replays in memory processing has been strengthened by auditory spatial association task wherein selective replays could be stimulated by external cues during sleep sessions (Bendor and Wilson 2012). Intracranial recordings in humans during episodic task have shown the increased probability of ripples preceding the recall which was coupled to emergence of activation patterns in visual cortex

(D. Ji and Wilson 2007). In line with this idea, various animal models of memory deficit have shown impaired SWR activity. For example, in a mouse model of Alzheimer's disease, reduction in SWR occurrence and low slow gamma power have been linked to memory impairments (Funane et al., 2022). One of the suggested mechanisms of memory impairment in AD is the incoordination of SWR in hippocampus-EC network which preceded the memory deficit in an APP-KI mice (Funane et al.,, 2022). In a mouse model of heterozygous Scn2a gene which is associated with frequent mutations linked to intellectual disability in humans, reactivation strengths of replay sequences are diminished along with truncated sequences (Middleton et al., 2018).

Selective disruption of SWRs complexes after the hippocampal dependent learning task led to memory impairments in rats pointing towards the importance of these complexes in offline memory consolidation (Girardeau et al., 2009). Earlier it was speculated that the SWRs events were important in offline memory consolidation but recent evidence shows the role of awake ripples in memory encoding and processing (Tang and Jadhav 2019). In a spatial alternation learning task, disruption of awake ripples led to memory deficits throughout the training. Despite intact place fields and sharp wake ripples in the following rest session, awake SWRs interruption led to memory deficits supporting the idea that awake ripples play a major role in learning (Jadhav et al., 2012). Role of awake ripples in planning and future explorations has also been explored by jhadav et. al, wherein they found an inverse relationship between SWR occurrence and vicarious trial and error (VTE) behaviours after the animals learnt a reward specific location (Papale et al., 2016). The encoding of unrelated paths in awake SWR events while traversing a particular environment signifies the neural mechanism of possibility of future exploration or planning (Davidson, Kloosterman, and Wilson 2009). Intracellular recordings from CA1 region in freely moving animals have shown a prominent suppression of current induced spikes during SWR events (English et al., 2014). This increase in shunting inhibition by ripples leads to higher spike threshold which may only be attained by specific subset of cells involved in memory task (English et al., 2014).

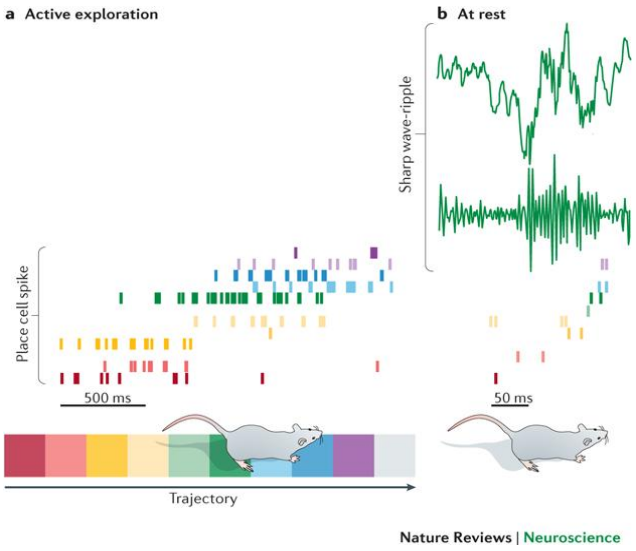

Figure 9: *Replays during sharp wave ripples a) during active exploration, each place cell (rows represent individual cells) fires at its place field in a particular sequence on the linear track, b) cells are active in a similar sequence during SWRs in a time compressed manner representing replay sequences (colgin 2016).*

1.13.4 HIPPOCAMPAL GAMMA OSCILLATIONS

Gamma oscillations are high frequency rhythms ranging from ~30 to about 150 Hz (Colgin and Moser 2010). These rhythms are nested within low frequency and high amplitude theta rhythms (Wulff et al., 2009). Theta oscillations are stable across active behaviours unlike gamma oscillations which occur in bursts within theta cycles(Lisman and Jensen 2013). Given the high frequency, gamma oscillations are important to coordinate neuronal networking associated with fast and complex operations which are beyond the temporal resolution of conscious decision making (Başar 2013a). Gamma oscillations are not associated with firing of all pyramidal neurons but engage a subset of neural assemblies referring to gating in the information processing stream (Colgin et al., 2009; J. Csicsvari et al., 2003).

1.14 EXPERIMENTAL EVIDENCE OF SEPSIS-ASSOCIATED COGNITIVE IMPAIRMENTS

As has been described above, sepsis leads to various forms of insults to brain which eventually leads to SABD and these changes are not confined to the acute phase but rather manifest into post-sepsis syndrome in survivors (Barichello et al., 2019). Post-sepsis syndrome is associated with a constellation of symptoms like memory impairments, delirium, cognitive fatigue, depression and sleep disturbances (Tsuruta and Oda 2016, 2016;

Wilcox et al., 2022). Up to 50% of septic shock survivors develop cognitive impairments which leads to the deterioration in the quality of life of patients and an enhanced burden on the caregivers (van der Slikke et al., 2020). There is abundance of evidence showing the impact of sepsis on various types of memories including long-term and short-term memories, fear memories, learning tasks and also procedural memories in humans (Barichello et al., 2019; Comim et al., 2011; Semmler et al., 2007, 2007). These long-term outcomes mainly depend on multiple factors including pre-sepsis status, presence of delirium, delay in antibiotic therapy and the given hospital conditions (Li, Ji, and Yang 2022). Human studies have demonstrated poor memory outcomes and decreased hippocampal volumes in sepsis patients (Yuan 2020). In animals models, sepsis-mediated decline in spatial memories as early as 24 hrs post sepsis-induction has been described (P. C. Alexandre et al., 2013; Gamal et al., 2015). Consequences of LPS-induced sepsis on behavioural and neuroanatomical alterations are not limited to the acute phase but have shown to be prevalent for up to 1-3 months in rodents (Barichello et al., 2007; Semmler et al., 2007). Impairment of aversive and extinction memories has been shown in CLP model of sepsis (Comim et al., 2011). In a cecal ligation and perforation model of sepsis, rodents showed cognitive impairments in the form of poor performance in latency retention in the inhibitory avoidance task after 10 and 30 days of surgery (Barichello et al., 2007). Induction of sepsis by cecum slurry injection in C57/B6 mice showed muscle weakness and cognitive assessment using novel object recognition until 2 weeks (Laitano et al., 2021). Persistent cognitive and physical impairments in these models of sepsis confer their potential to be used for elucidating therapeutic targets of sepsis-associated cognitive impairments. Mechanisms of long-terms memory outcomes in sepsis patients are still poorly understood. The postulated mechanisms of memory deficits in sepsis survivors may include neuroinflammation, neuronal death or disrupted neurotransmission. Is has been experimentally proven that targeting these factors led to improvement in memory outcomes (Comim et al., 2009; Gasparotto et al., 2018; Yang, Wang, and Andersson 2020). The detailed known mechanisms have been discussed in the section 1.6. In summary, during the acute phase of sepsis, proinflammatory cytokine storm should be targeted with antibiotics and during the chronic phase, the focus should be directed towards restoration of neurotransmitter levels, BBB dysfunction, suppressing the neuroinflammation,

phosphorylation of tau and amyloid β. These steps could eventually result in better outcomes in sepsis survivors (Sekino, Selim, and Shehadah 2022).

2. AIMS AND HYPOTHESES

The broader aim of the present study is to understand the effect of sepsis on hippocampal brain oscillations and dynamics of hippocampal cell population.

2.1 The first aim is to study hippocampal brain oscillations in the acute phase of sepsis under urethane anaesthesia. Central nervous system is one of the first organs to be affected during sepsis and the underlying detailed mechanisms are poorly understood. Cortical EEG recordings in laboratory rodents have shown fragmentation of NREM and suppression of REM state in both CLP and endotoxemia models of sepsis (Baracchi et al.,, 2011, Ingiosi and Opp, 2016). Also, power spectrum analyses have shown decreased delta power in NREM in these models. Studies in the subfield of 'sepsis and sleep' majorly focus on architecture of vigilance states and the power spectrum analyses. However, these types of analysis are limited to specific frequency bands or brain states and they consequently leave a gap in the knowledge of dynamic interaction between brain states. Given the importance of sleep quality in determining the outcomes in septic shock survivors, it is important to understand the properties of brain oscillations during acute phase of sepsis in the central nervous system. Therefore, in the present study, we recorded local field potentials from the CA3 region of hippocampus during sepsis under urethane anaesthesia to understand the dynamics of brain oscillatory states with respect to each other and to propose an electrophysiological mechanism of sepsis-induced state fragmentation. The ability of urethane to spare high amplitude NREM and low amplitude REM-like activity makes it a feasible model to understand the dynamics of intrinsically generated oscillatory activity free from external sensory inputs.

Hypothesis- We hypothesized that acute inflammation may lead to alteration in oscillatory and non-oscillatory properties of brain states (REM-like and NREM-like). These changes could eventually be associated with fluctuation in attractor state dynamics leading to state-fragmentation.

2.2 The second aim is to study hippocampal oscillations in non-anaesthetized behaving animals under sepsis. In order to confirm our findings in behaving animals and eventually correlate it to other behavioural deficits, we performed similar sleep state analysis in behaving rats in a paradigm explained in the section below.

Hypothesis- We hypothesised that LPS causes changes in power spectrum profile of brain states leading to fragmentation of sleep-wake patterns in awake model of sepsis.

2.3 The third aim is to understand the impact of sepsis on dynamics of hippocampal cell population. There is profound evidence of long term-cognitive impairments associated with septic shock survivors. Sepsis-associated memory impairments in chronic phase after recovery have also been shown in laboratory models of sepsis. Molecular studies showing elevated pro-inflammatory markers in hippocampus during both acute and chronic phase of infection suggested this region as one of sepsis targets (Annane 2009). Despite its susceptibility towards sepsis and its importance in memory formation and consolidation, information processing in hippocampal neuronal networks during sepsis has not been described. In the present study, we intended to bridge this gap by studying the dynamics of hippocampal neuronal populations during sepsis.

Hypothesis- We hypothesised that LPS may lead to changes in excitation and inhibition balance of neural activity. We expect an altered firing rate dynamics of excitatory pyramidal and inhibitory interneurons.

3. MATERIALS AND METHODS

3.1 Animals: Adult male Long-Evans rats weighing 400-500 grams were used. All methods were carried out in accordance with relevant guidelines and regulations. All protocols were approved by the Ethical Committee of the Ministry of Education, Youth and Sports of the Czech Republic (approval no. MSMT-12084/2019) according to the Guide for the Care and Use of Laboratory Animals (Protection of Animals from Cruelty Law, Act No. 246/92, Czech Republic) and in accordance with ARRIVE guidelines. The animals were housed individually in transparent polycarbonate cages and were kept in a 12:12 light/dark cycle with food and water *ad libitum*. Experiments were carried out during the light phase (Kala et al., 2023).

3.2 Experimental setup: 1. To investigate the effects of acute systemic inflammation under urethane anesthesia, two groups of rats were used (LPS and CTRL, N = 6 each, Figure 10). One hour after induction of urethane anesthesia, rats in both groups were injected with sterile saline (2ml/kg, i.p.). Then, baseline hippocampal activity was recorded for three hours. After this, rats in the LPS group were injected intraperitoneally with 10 mg/kg lipopolysaccharide (LPS) and were recorded for another three hours. Rats in the CTRL group received a second saline injection instead. After the second recording period, blood serum samples and brains were collected for IL-1β quantification and histological verification of electrode placement. All animals survived until the end of the recording period.

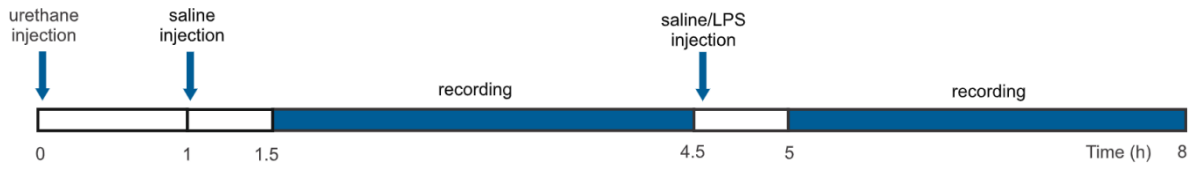

Figure 10: *Experimental design. Urethane anesthetized rats were injected with saline and baseline LFP was recorded for 3-hours, followed by a single dose of LPS (LPS, n=6) or saline (CTRL, n=6) and another a 3-hour recording.*

2. To understand the impact of systemic inflammation on hippocampal CA1 population dynamics and memory consolidation, a with-in subject design was used and each animal served as a control and LPS animal (N=7). Animals were pre-trained on a familiar linear track and implanted with movable 16-tetrode hyperdrives above the dorsal hippocampal region. The animals were then allowed to recover for about 5-6 days post-surgery and trained on

the familiar linear track for about 8-10 days. During this course of time, tetrodes were lowered carefully to reach hippocampal CA1 pyramidal layer. On the experimental day, signal was fine tuned to capture CA1 pyramidal neurons, and a pre-sleep session was recorded for about an hour. This was followed by recording hippocampal local field potentials while the animals traversed the familiar linear track. Another sleep session (post sleep 1) was recorded for an hour followed by exposing these animals to a novel linear track. Animals were then injected with saline (control day) followed by a long 6 hrs. recording. Next day, these animals were allowed to explore the familiar linear track. On day 3, similar protocol was performed but with a new novel track and saline was replaced by an i.p injection of 5 mg/kg LPS. The brain samples were collected for cytokine quantification and histological verification of tetrode bundles.

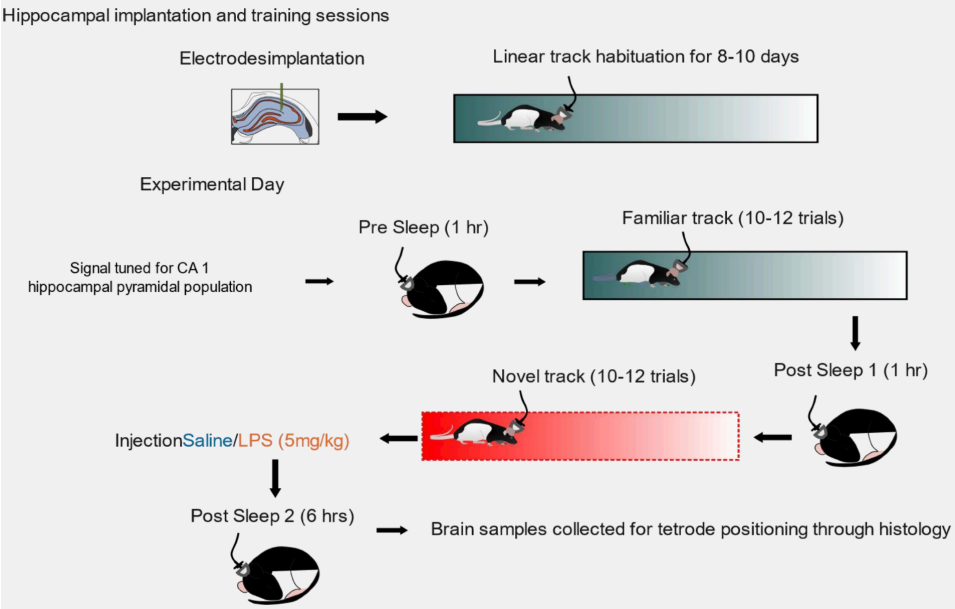

Figure 11: *Experimental design: To record local field potentials and hippocampal spikes in wake behaving animals, signal was tuned for CA1 hippocampal cells and one hour of pre sleep session was recorded. The animals were allowed to explore a familiar linear track while simultaneously recording local field potentials. Another session of sleep (referred as post sleep 1) was recorded followed by exploration and recording in a novel track. This was followed by an injection of saline (day 1) or LPS (day 3). A long recording pf 6 hrs (post sleep 2) was performed.*

3.3 Electrode implantation surgery*:* Local field potentials were recorded from the rats implanted with eight independently movable tetrodes above the hippocampal region (3.8

mm caudal, 3.2 mm lateral of bregma). Each tetrode consisted of four twisted 17-µm polyimide-coated platinum-iridium wires coated with platinum to reduce the impedance to 120 –200 kΩ at 1 kHz. First, rats were anaesthetized using a mixture of ketamine (Narkamon, 100 mg/kg, i.p.) and xylazine (Rometar, 10 mg/kg, i.p.) and 1.5-2% isoflurane in O_2. They were fixed in a stereotaxic frame and body temperature was maintained at 37 °C using a heating pad. An incision was made in the scalp to expose the skull, after which a craniotomy was made over the dorsal hippocampus (3.8 mm caudal, 3.2 mm lateral of bregma). After removal of the dura mater, the tetrode bundle was carefully lowered into the cortex. Individual tetrodes were slowly lowered into CA3 over the course of a 2-week recovery period. The hyperdrive was fixed to the skull using dental acrylic and stainless-steel screws. One screw, located above the frontal cortex, served as a reference. Rats were given carprofen (Rimadyl, 5 mg/kg, s.c.) and Marbofloxacin (Marbocyl, 5 mg/kg, s.c.) during recovery (Kala et al., 2023).

***3.4 Training sessions**:* For the awake behaving experiments (Obj 2), animals were allowed to explore a 170 cm long familiar linear track back and forth for about 15-20 mins for 8-10 days before the experiment. Novel linear track, also 170 cm long consisted of different visual and tactic cues and was only introduced on the day of recording (Kala et al., 2023).

3.5 Data acquisition: Recordings under urethane anesthesia (obj. 1) were performed using OpenEphys recording system. Hippocampal local field potentials were amplified using an Intan RHD2132 headstage amplifier, digitized and recorded at a sampling rate of 2,000 Hz and a high-pass filter set at 1Hz (Siegle et al., 2017).

Recordings in wake behaving animals were performed using a 64-channel axona data acquisition system (Axona Ltd). The tetrodes were lowered (30-40µm) very carefully for about 8-10 days post surgery. The signal was tuned to capture sharp wave ripples which show negatively deflecting waves with high frequency ripple activity which are the hallmarks of hippocampus. On the day of recording, the signal was fine tuned to reach CA1 pyramidal layer to capture spikes.

3.6 Spike detection and sorting: Analysing activity at single-cell level, extracellular recordings in brain rely on detecting spikes and classifying them into different non-overlapping clusters. Extracellular waveforms of different cells vary in various aspects

including morphological, biophysical and the relative distance from the recorded electrode. Waveform features including the width and height of the detected spikes are extracted which are later assigned into clusters of similar waveforms and this procedure is called spike sorting.

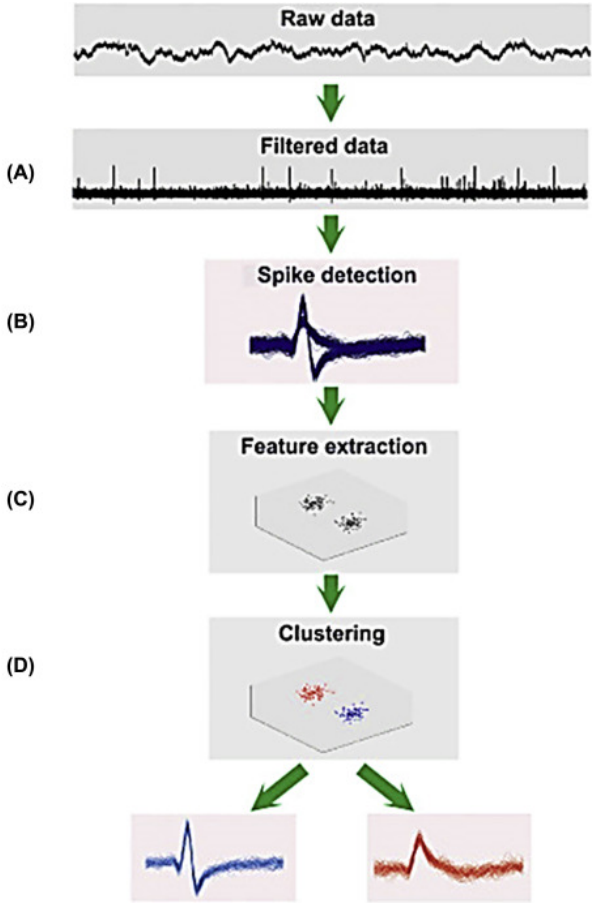

Figure 12: *Steps showing spike clustering and sorting: a) the first step involves the high pass filtering of raw signal, b) spikes are detected using amplitude thresholding, c) important features of waveforms like peak, shape, height and width are extracted using dimensionality reduction methods and d) these features are fed to a classification algorithm enabling the detection of different clusters of spikes, (rey, pedreira, and quian quiroga 2015).*

The extracellular signals from tetrodes were pre-amplified using a head stage (4 x 16 channels, Axona Ltd, St. Albans, Hertfordshire, UK) and continuously digitized at 24 kHz. Two red LED bundles were mounted on the preamplifier head-stage to track the location of the animal in the linear tracks. The data were resampled to 20KHz, and power was computed in 800-9000 Hz frequency range in sliding windows of 12.8ms. Spike detection was done using an amplitude thresholding method. If the amplitude exceeded 5 SD of the signal, local minima were detected and aligned across this point which was referred to as the trigger

points. In the present study, we used a hybrid of automatic (Klustakwik) and manual clustering software (Sgclust) for spike extraction and sorting. Based on the extracted features, spikes were assigned into clusters using principal component analysis, a dimensional reduction analysis which leads to the transformation of the waveform to a single number represented by the first component of PCA with maximum variability. After complex reduction, the clusters can be manually sorted using sgclust visual software depending on the overlapping waveforms, inter-cluster distances and auto correlograms. Putative pyramidal neurons and interneurons were distinguished by auto correlograms, waveforms and firing rates.

3.7 Cytokine quantification and histology: After recordings and testing, blood samples were collected, and serum was separated by centrifugation at 1,000 × g for 10 min. Levels of IL-1β were quantified using an ELISA kit (RAB0277, Sigma) according to manufacturer's protocol. Then, rats were killed using an overdose of sodium pentobarbital (50 mg/kg) and perfused transcardially with ringer solution followed by 4% paraformaldehyde in phosphate-buffered saline. Brains were collected and cut in 50µm thick coronal sections. Electrode placement was verified using Nissl staining. Electrode traces from electrodes outside of hippocampal CA3 and CA1 were excluded from analysis (Kala et al., 2023).

3.8 Data Analysis: In urethane-anesthetised recording (obj. 1), for vigilance state classification and later state-space analysis, a sliding window FFT analysis (2 s window, 1 s step) was performed on separately for all recorded channels using Welch's method in MATLAB 2014b (Hamming window, 50% overlap, 0.25 Hz resolution), yielding 1 epoch per second. Then, spectral ratios were calculated for overall power in two overlapping frequency ranges for each time window. Ratio 1 was calculated as R1 = (1-2 Hz)/(1-9 Hz) and Ratio 2 was calculated as R2 = (1-15 Hz)/(1-45 Hz). Frequency ranges were chosen based on literature and on the approximate frequencies of delta and theta peaks in our recorded baseline spectra (Diniz Behn et al., 2010; Gervasoni et al., 2004). Normalized signal amplitude was calculated using the same sliding window approach, where mean absolute signal amplitude was calculated for each window and normalized to mean absolute signal amplitude for the entire recording. The resulting power and amplitude time series for all channels were then combined into a single time series per rat for each of these variables using principal component analysis. The first principal component was used for state space

analyses, as described previously (Diniz Behn et al., 2010; Gervasoni et al., 2004). The Ratio 1 and Ratio 2 time series were generally well represented by this principal component, which explained over 89% of variance in both ratios at all time points. Epochs that contained artefacts were excluded from further analysis (0.18±0.06% of recording time). State labels for these epochs were set to be identical to the preceding, artefact-free epoch prior to smoothing (Kala et al., 2023).

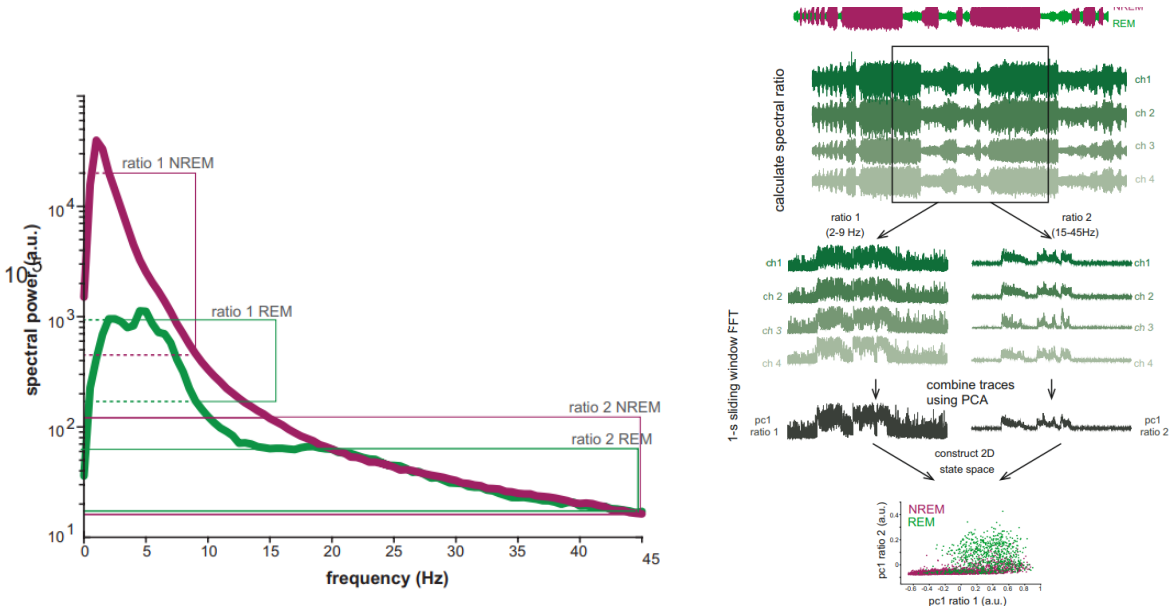

Figure 13: *Overview of state space classification*

3.9 Vigilance state classification and episode detection: Brain activity under urethane anaesthesia showed two distinct alternating states: a NREM-like state that was dominated by low frequency, high-amplitude waves, and a REM-like state with faster activity and a lower signal amplitude. Epochs were automatically classified as belonging to one of these states based on the calculated principal component values for R1, R2, and amplitude using k-means clustering. Inclusion of the amplitude parameter in the clustering procedure ensured reliable state identification, even when spectral ratios were affected by

experimental treatment.

After initial clustering, ultra-short periods of NREM-like or REM-like activity were removed: a state transition was only considered if the first epoch of the new state was followed by at least 3 more epochs of the same state. Otherwise, the epoch was labelled as belonging to the preceding state. This smoothing procedure ensured that any unrealistically short, artefactual state changes caused by normal within-state signal variability were removed. NREM-like and REM-like episodes were calculated as periods of each state that were at least 10 epochs long, and were followed by at least 10 epochs of the other state. Short episodes were considered as 20 – 120 s long, whereas episodes of 600 s or more were considered long. Epoch-to-epoch transition probability was calculated based on the percentage of epoch that was followed by the same or a different state. Episode transitions were characterized by fitting a logistic curve using MATLAB's fit function with the following equation $f(x) = offset + (range / (1 + e^{-slope*x}))$. Curves were fit to a 30-s period of LFP trace centred on the episode state transition after smoothing using a 5-s window moving average.

3.10 State-space analysis: Inflammation-related spectral changes were analysed in a 2-dimensional state-space based on R1 and R2. This type of analysis may reveal within- and between state dynamics that are not captured using less sensitive single-band approaches (Diniz Behn et al., 2010; Gervasoni et al., 2004). Cluster positions were defined using the median pc1R1 and pc1R2 values for each state.

Within-state jitter was analysed using epoch-to-epoch distances in state-space. Jitter was defined as distance between two subsequent epochs. As such, overall jitter was calculated as $j = \sqrt{((pc1R1_{n+1}-pc1R1_n)^2 + (pc1R2_{n+1}-pc1R2_n)^2)}$, and jitter along a single dimension such as R1 simply as $j_{R1} = pc1R1_{n+1} – pc1R1_n$ (Kala et al., 2023).

3.11 Analysis of periodic and aperiodic spectrum components*:* To further investigate how power spectrum changes lead to the observed state-space effects, aperiodic and periodic components of the power spectrum were parametrized using the FOOOF algorithm (v. 1.0.0) in Python 3.7 (Donoghue et al., 2020; Haller et al., 2018). First, average power spectra for each state were calculated from the sliding window FFT described earlier. One representative channel was analysed per rat and the same channel was used for the pre- and post-injection time points. For each spectrum, the frequency range from 1 to 45 Hz was used with the following algorithm settings: peak width limits 0.5 and 12 Hz, maximum

number of peaks 6, minimum peak height 0.2, peak threshold 2.0, and aperiodic mode: knee. Broad band gamma oscillations in the 15-30 Hz frequency range are not adequately captured by these settings. For these oscillations, the calculated aperiodic component was subtracted from the power spectrum first, after which peaks were fit with a minimum peak height 0.1, peak threshold 2.0, minimum peak width 0.5, but without a maximum peak width (Kala et al., 2023).

Aperiodic spectral components were modelled using the following aperiodic fit $AP(f) = 10^{b} * (1/(k+f^{\chi}))$ fit (AP) where f is frequency, b is offset, k is the knee parameter, and χ is the spectrum slope. The knee parameter represents the bending point where the aperiodic fit transitions from horizontal to negatively sloped. Knee frequency is dependent on the value of k and spectrum slope χ and was calculated as $k_{freq} = k^{(1/\chi)}$. Periodic components of the spectrum, representing putative oscillations, were modelled as Gaussian curves over and above the aperiodic background spectrum. Each oscillation has a center frequency (c), peak width (w), and center peak height (a), yielding the following for each frequency f $G(f) = a * \exp(-(f-c)^2/(2*w^2))$ (Kala et al., 2023).

3.12 Sleep scoring using AccuSleep: Sleep scoring in non-anesthetized animals (obj 2) was done using a robust open source AccuSleep interface with a combination of LFP reference channel and EMG. Scoring was performed in 5s long epochs.

3.13 Linearized Firing Rate Maps: The linearized 1D maze was 170 cm long and divided into 57 bins of 3 cm each. Using the tracking information, occupancy map of the animal was generated by calculating the time spent in each bin with a running threshold of more than 3cm/s. Firing rate maps were generated for each spike by dividing the cell count per bin to the time spent in the respective bin. These vectors were smoothed using a gaussian filter of 1 SD.

3.14 Sleep analysis using FFT: To analyse the effect of LPS on power in different frequency bands, classical FFT analysis (5 s window) was performed separately for all recorded channels using Welch's method in MATLAB 2021a (Hamming window, 50% overlap, 0.25 Hz resolution), yielding 1 epoch per second. For each channel, power values ranging from 0.1-25Hz were normalised to the pre sleep session 1 to obtain the percentage change from baseline. The normalised values were then averaged across channels.

3.15 Firing rate dynamics*:* To understand the dynamics of cell activity across vigilance states, the population activity was summed in 1s time bins and z scored. The z scored firing rates were smoothed with a moving average window of 10s. The mean firing rates of the population activity were analyzed for CA1 pyramidal cells and interneurons separately.

3.16 Detection of candidate frames: Putative sharp wave ripple events were detected from NREM signal. Pyramidal population activity was calculated in 1ms time bins and convoluted by 15 ms gaussian kernel. The population activity exceeding 2 SD and ranging between 100-800 ms long was considered as a putative sharp wave ripple event.

3.1 Statistics: Statistical analyses were performed using JASP 0.13.1, 0.14.1.0, MATLAB 2014b and MATLAB 2021a. Time- and treatment group effects were analysed using repeated measures ANOVA. Where sphericity assumptions were violated, the Greenhouse-Geisser correction was used to adjust p-values. Within-group changes in oscillatory and aperiodic activity were analysed using Wilcoxon's signed rank test. As these tests were applied to different aspects of the same peaks or background spectra, Bonferroni correction was used to adjust p-values for the 3 comparisons per set of tests. Bootstrapped correlations using Spearman's method and mean ± standard deviation was reported for the obtained rho values (Kala et al., 2023).

4. RESULTS

4.1 LPS increases serum IL-1β levels

IL-1β levels were measured to confirm systemic inflammation. Serum IL-1β concentrations in LPS-injected rats were at least 3 times higher than controls (398±32.24 pg/ml vs 122±63.64 pg/ml, n=6, independent sample t-test t (10) =3.88, p<0.01, Fig. 14) (Kala et al., 2023).

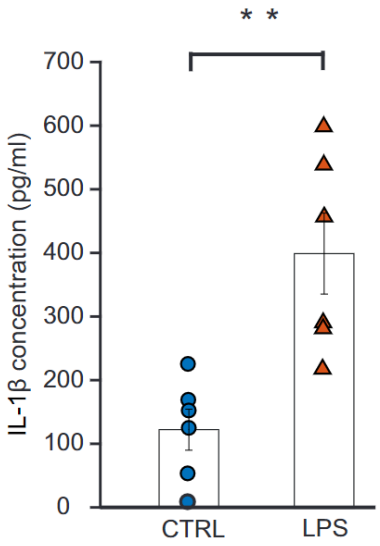

Figure 14: *LPS injection increased serum IL -1β. Each point represents IL -1β serum concentration in CTRL or LPS rats 8-9 hours after saline or LPS injection. Bar graphs show mean ± s.e.m. **p < 0.01*

4.2 LPS injection causes altered sleep state structure

Rats showed two distinct brain activity patterns under urethane: a NREM-like state dominated by high amplitude slow waves, and a REM-like state with low-amplitude, higher frequency activity (Fig. 15A-D). The states were long and stable at baseline and in saline-injected controls (Fig. 15A-C), but much shorter after LPS injection (Fig. 15D).

Fragmentation manifested as more REM episodes (rmANOVA; time effect: F(1,10)=8.357, p=0.016; group effect: F(1, 10)=5.277, p=0.044; group*time interaction : F(1,10) =8.719,

p=0.014, Fig. 15E), but also increased NREM episode numbers (rmANOVA; time effect: F(1,10)=8.357, p=0.016; group effect: F(1, 10)=5.277, p=0.044; group*time interaction : F(1,10) =8.719, p=0.014, Fig. 15F).

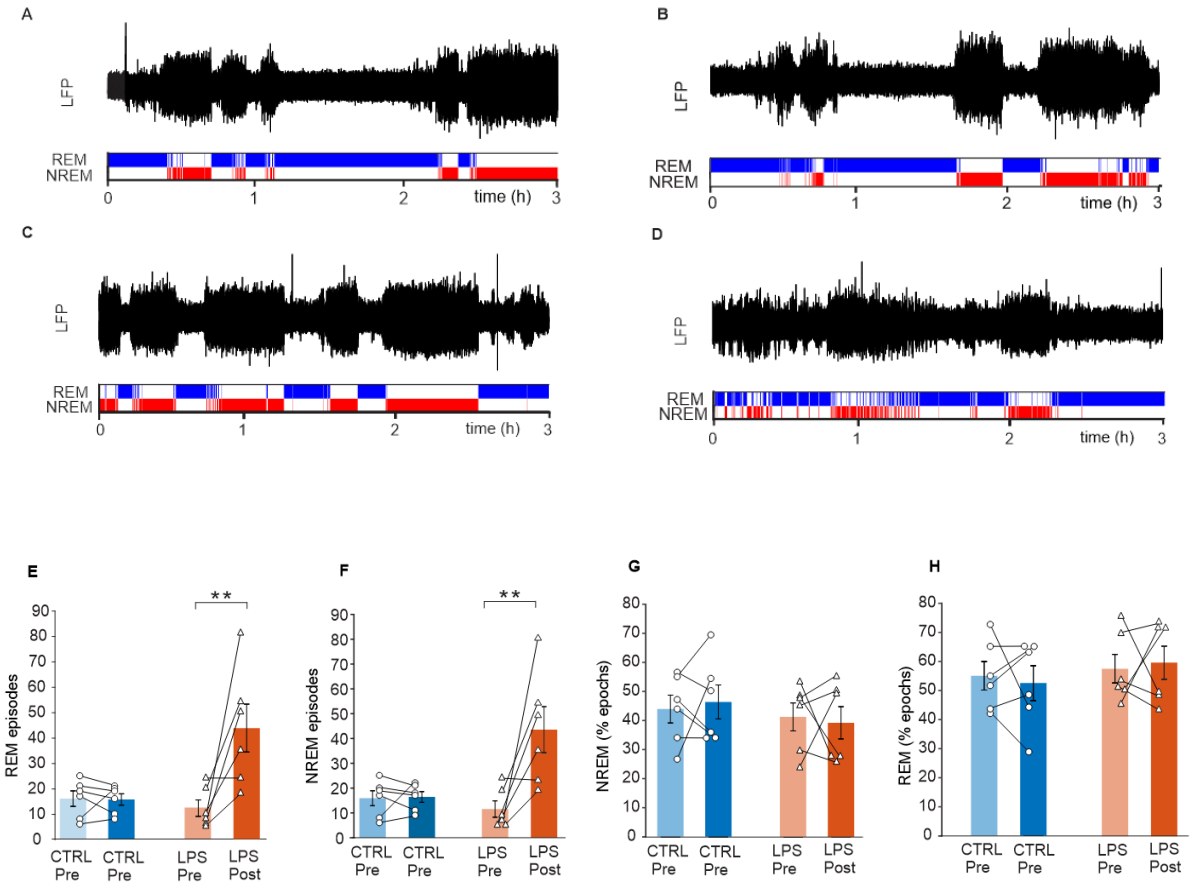

Figure 15: *LPS causes sleep state fragmentation in rats without affecting the total time spent in either state.*

A-D. Representative traces and hypnograms showing REM in blue and NREM in red. Sleep states were long and stable before (A) or after saline injection (B) in controls (CTRL) and before LPS injection (C) in the LPS group. After LPS injection (D), sleep states were heavily fragmented.

*E. Number of REM episodes before and after injection. Each data point shows the number of episodes in individual CTRL and LPS animals pre and post injection (CTRL, n = 6; LPS, n = Bars show mean ± s.e.m. **p<0.01*

*F. Number of NREM episodes in CTRL and LPS animals pre and post injection. **p<0.01*

G. Total time spent in NREM as percentage of recording time in CTRL and LPS animals pre and post injection.

H. Total time spent in REM as percentage of recording time in CTRL and LPS animals pre and post injection.

Despite increased episode numbers, time spent in NREM (rmANOVA; time effect: $F(1,10)=0.002$, $p=0.96$; group effect: $F(1, 10)=0.77$, $p=0.39$; group*time interaction: $F(1,10)=0.199$, $p=0.66$) and REM (rmANOVA; time effect: $F(1, 10)=0.002$, $p=0.96$, group effect: $F(1,10)=0.77$, $p=0.39$; group*time interaction: $F(1,10)=0.199$, $p=0.66$) were unaltered by LPS injection(Fig.15G-H).

Extensive sleep instability was further apparent in episode length distribution (Fig. 16A). At baseline and after saline injection rats had few short episodes (20-120 s) and a relatively many long episodes (≥600 s). After LPS injection, however, brain activity patterns consisted of many short episodes and only a few long ones. Relative amounts of short episodes were significantly higher in NREM after LPS injection (rmANOVA, time effect (rmANOVA; $F(1,10)=4.67$, $p=0.05$, group effect: $F(1,10)=0.25$, $p=0.62$, group*time interaction: $F(1,10)=19.78$, $p<0.01$), but not in REM (rmANOVA, group effect: $F(1,10)=6.58$, $p=0.02$), time effect: $F(1,10)=4.01$, $p=0.07$, group*time interaction: $F(1,10)=2.56$, $p=0.14$; Fig. 16B,C). Post-hoc analyses showed a significant increase in the percentage of short NREM episodes in the LPS group post injection (81.44±4.58% of NREM episodes vs 46.59±10.37% pre-injection) and a significant baseline difference in short REM episodes between controls (70.12±1.94%) and the LPS group (41.52±11.88%). Changes in long episodes were the opposite to those in short episodes (Fig. 16D,E). The occurrence of long NREM episodes was significantly reduced after LPS injection (5.90±1.55%), compared to baseline (39.97±10.48%), even though episode numbers are generally low (rmANOVA, time-effect: $F(1,10)=8.28$, $p=0.01$, group*time interaction: $F(1,10)=9.40$, $p=0.01$, group effect: $F(1,10)=0.79$, $p=0.39$). Effects on long REM episodes were similar (rmANOVA, time effect: $F(1,10)=9.78$, $p=0.01$, group*time interaction: $F(1,10)=8.39$, $p=0.01$, group effect: $F(1,10)=0.89$, $p=0.36$). Post-hoc analysis showed significantly fewer long REM episodes in the LPS group post-injection (6.51±2.12%) compared to pre-injection (44.16±10.42%). These results point to instability in both the REM and NREM state (Kala et al., 2023).

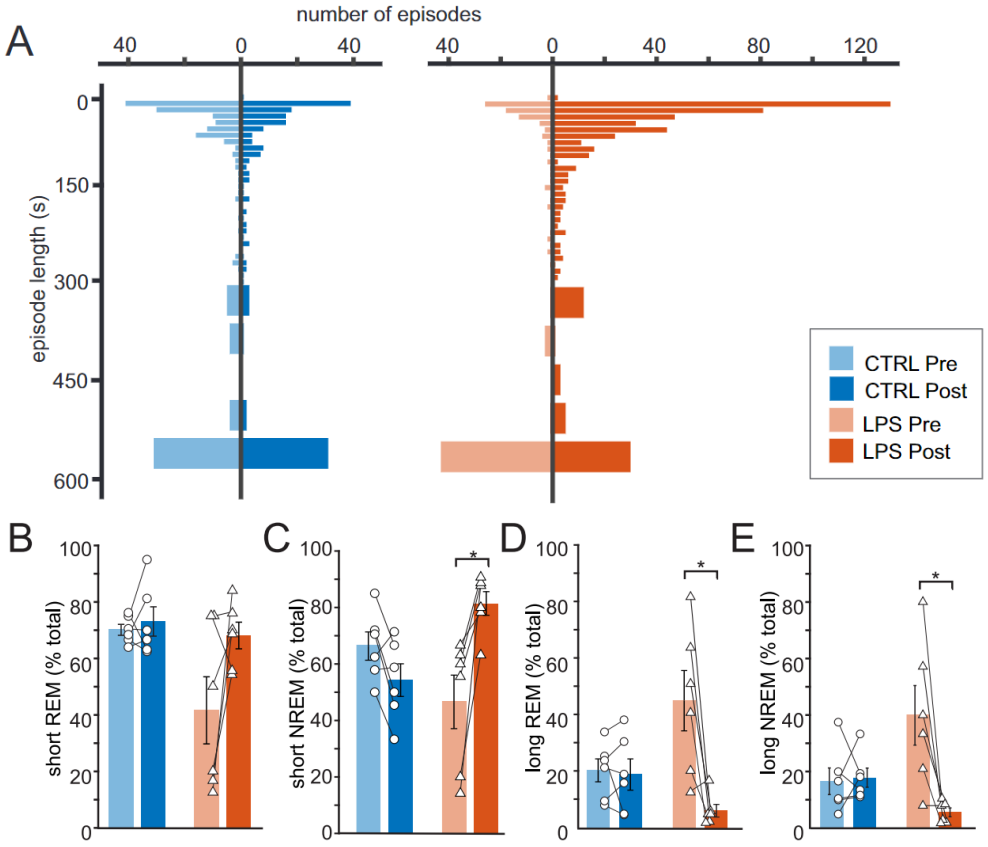

Figure 16: *LPS leads to an increase in short and a decrease in long sleep state episodes.*

A. Histograms depicting the overall distribution of episode lengths in CTRL (left) and LPS rats (right), pre and post injection. Each bar in the histogram shows the number of episodes per 10- or 50-s bin.

B-C. Proportions of short 20-120 s episodes of REM (B) or NREM (C) in CTRL and LPS rats, pre and post injection (n = 6 per group).

*D-E. Proportions of long ≥600 s episodes of REM (D) or NREM (E) in CTRL and LPS rats, pre and post injection. Bar graphs show mean ± s.e.m. *p<0.05.*

State instability was also apparent on the epoch-to-epoch level, where the probability of state transition from one epoch to the next was similarly increased for NREM-to-REM transitions (rmANOVA; time effect: $F(1,10)=16.72$, $p<0.01$; group effect: $F(1,10)=4.61$, $p=0.06$; group*time interaction: $F(1,10)=10.53$, $p<0.01$) and REM-to-NREM transitions (rmANOVA; time effect: $F(1,10)=16.12$, $p<0.01$; group effect: $F(1, 10)=4.77$, $p = 0.05$; group*time interaction: $F(1,10)=10.68$, $p<0.01$, Fig. 17). Post-hoc analysis showed significantly increased transition probabilities in both directions after LPS injection (NREM-to-REM: 0.17±0.05% pre vs. 0.62±0.10% post; REM-to-NREM: 0.17±0.05% pre vs.

0.62±0.09% post, Fig. 17). State transition probabilities remained at baseline levels in controls (NREM-to-REM: 0.22±0.05% vs 0.27±0.05%; REM-to-NREM: 0.27±0.05% vs 0.27±0.05%) (Kala et al., 2023).

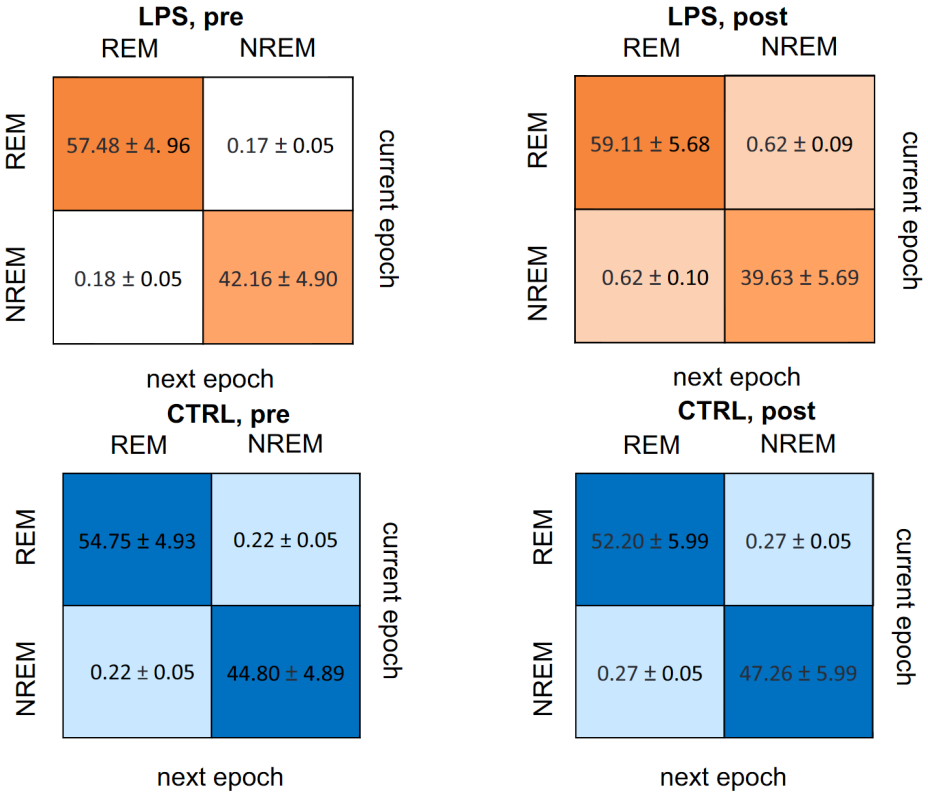

Figure 17: *LPS increased transition probability from REM to NREM and from NREM to REM. Each cell shows average transition probability per epoch from REM to REM, REM to NREM, NREM to REM or NREM to NREM states pre and post injection in control and LPS animals.*

Although a higher number of state transitions were found after LPS, transition characteristics were not significantly different from those in controls or at baseline (Fig. 18). Thus, LPS injection leads to instability of NREM and REM to a similar degree, without affecting time spent in either state or transition characteristics between the states (Kala et al., 2023).

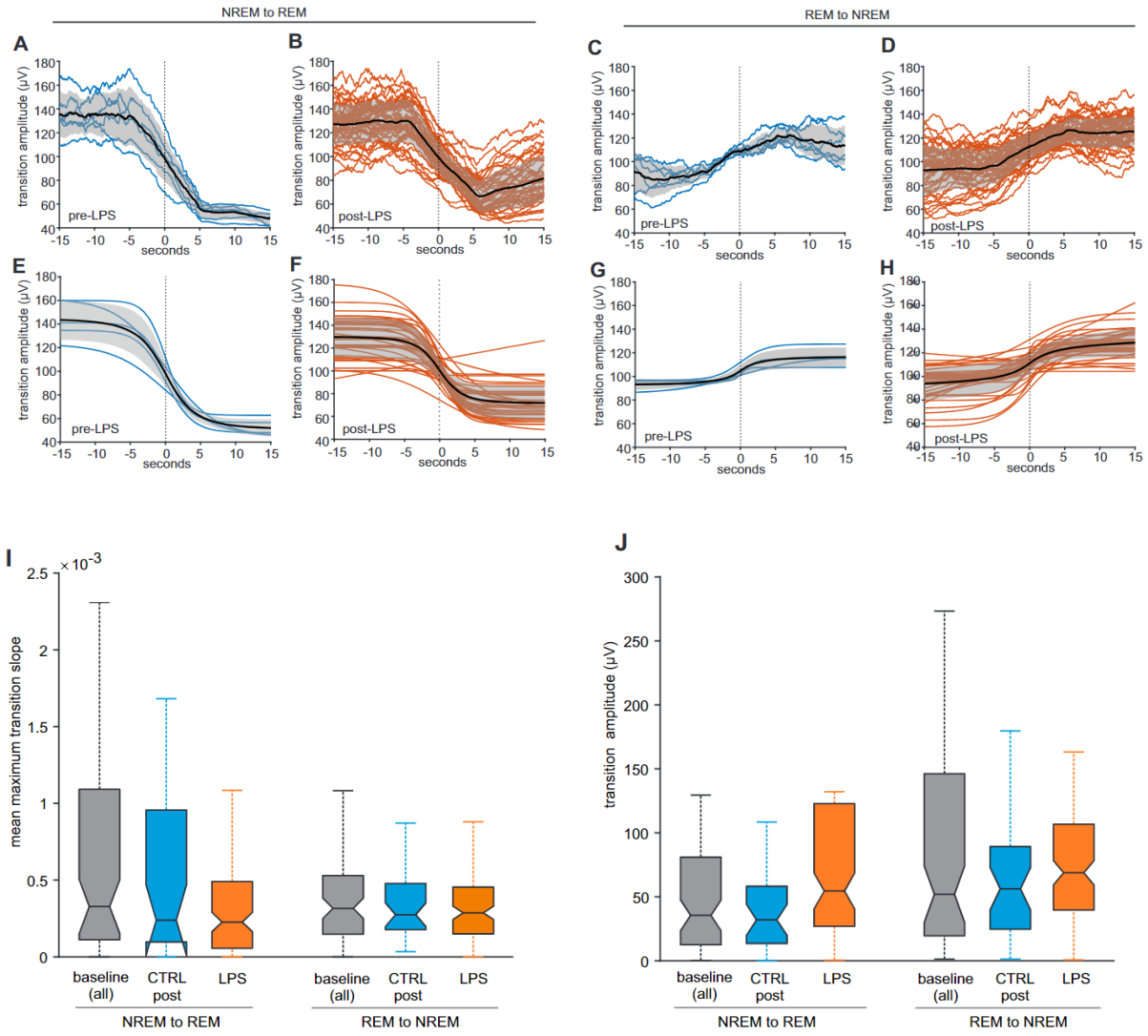

Figure 18: *State transition characteristics before and after LPS injection. A-D: Smoothed EEG traces for state transitions for a representative animal at before (A,C) and after LPS injection (B,D). NREM-to-REM transitions are shown in A and B, REM-to-NREM transitions are shown in B and D. Mean traces are shown in black, with standard deviation in grey.*

E-H: Fitted curves used to calculate transition dynamics in NREM-to-REM (E,F) and REM-to-NREM transitions (G,H) at before (E,G) and after LPS injection (F,H) for the traces shown in A-D. Mean fitted curves are shown in black, with standard deviation in grey.

I: Box plots showing medians and quartiles for maximum transition slope for all NREM-to-REM and REM-to-NREM transitions in all pre-injection recordings (N = 80 and N = 79, resp., 12 rats), post-injection in controls (CTRL, N = 37 and N = 34, resp., 6 rats), and after LPS injection (N = 123 and N = 116, resp., 6 rats).

J: Box plots showing medians and quartiles for transition amplitudes for all NREM-to-REM and REM-to-NREM transitions in all pre-injection recordings (N = 80 and N = 79, resp., 12 rats), post-injection in controls (CTRL, N = 37 and N = 34, resp., 6 rats), and after LPS injection (N = 123 and N = 116, resp., 6 rats).

4.3 LPS leads to increased spectral similarity between REM and NREM

Changes in spectral characteristics were assessed based on spectral power ratio 1 (R1, 1-2 Hz/1-9 Hz) and ratio 2 (R2, 1-15 Hz/1-45 Hz), which are distinct in the two observed states (Fig. 19A, B). State-space analysis based on these ratios resulted in two distinct state clusters of epochs in the control and LPS group at baseline and after injection (Fig. 19C-F).

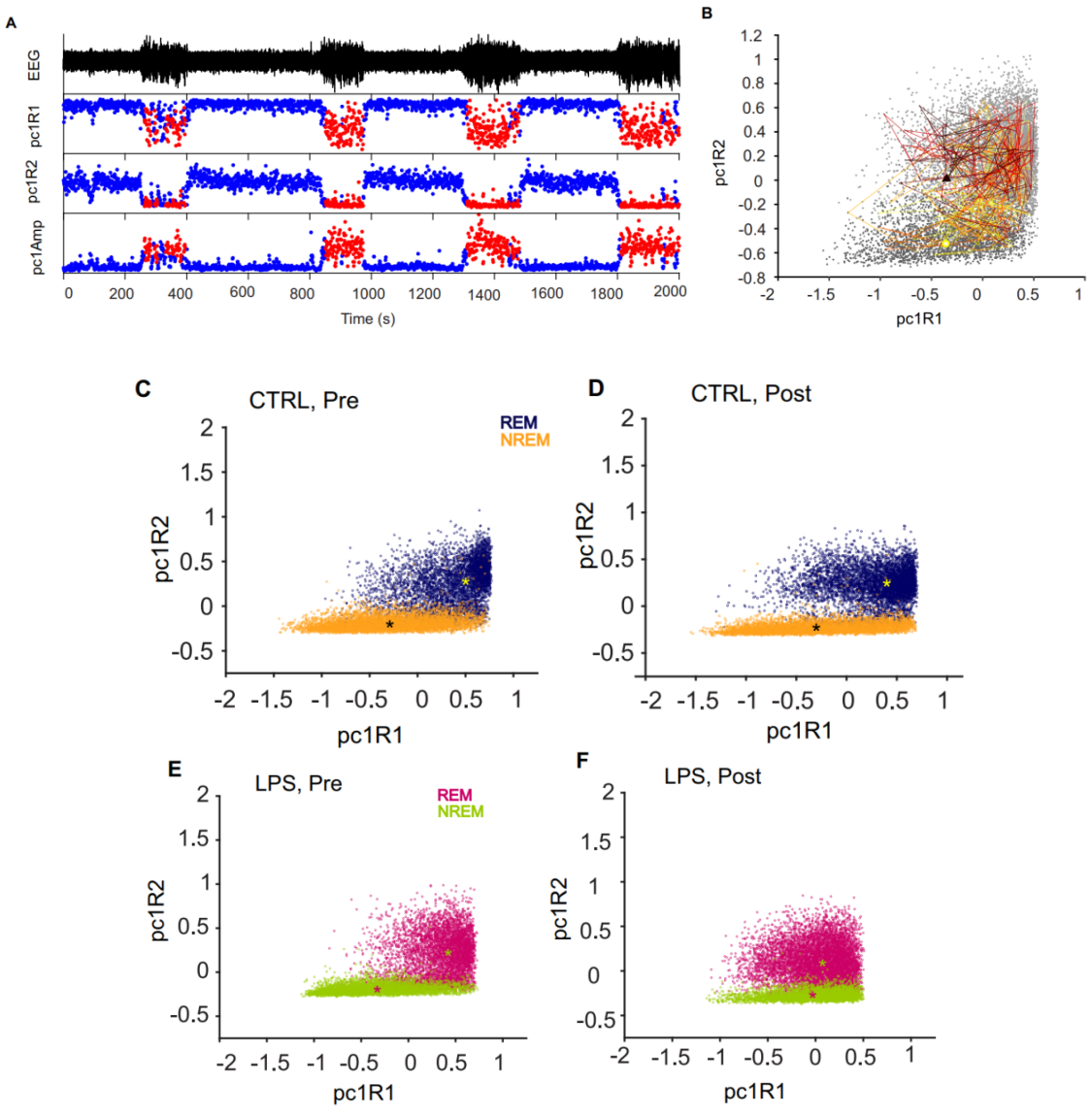

Figure 19: *LPS leads to reduced cluster distance between REM and NREM states.*

A. First principal components of spectral ratios R1 and R2 in time, as well as the amplitude component used for state classification, with the accompanying EEG trace. Epochs classified as NREM are shown in red, epoch classified as REM in blue.

B. Example of a 400-s long trajectory in 2-D state space. The shown trace starts in the NREM cluster (circle) and eventually ends in the REM cluster after covering much of the recording's state-space. Epochs that are not part of this trajectory are shown in grey.

C-F. Scatter plots showing REM and NREM epochs in 2-D state space in CTRL (C, D) and LPS (E, F) groups, pre and post injection. The asterisk marks the cluster median.

After LPS injection (Fig. 19F), the location of the NREM and REM clusters within state-space shifted, resulting in a decreased inter-cluster distance. The magnitude and direction of the changes in cluster location after LPS injection and in controls is shown in Fig. 20A. The centroid of REM cluster shifted significantly in LPS group compared to controls ($t(10)=2.33$, $p=0.04$, Fig. 20B), with a mean vector direction towards the origin and magnitudes of 0.23±0.05 a.u. and 0.10±0.03 a.u., respectively (Fig. 20B)**.** NREM cluster shifts were not significantly different in controls (0.16±0.04 a.u.) and in LPS rats (0.35±0.06 a.u., $t(10)=1.45$, $p=0.17$), due to higher variability. The mean NREM vector is directed away from origin, towards the REM cluster.
As a result of the observed shifts in cluster medians, the distance between the two clusters decreased (Fig. 20C). We calculated the distance between REM and NREM clusters before and after injection in control and LPS groups (rmANOVA, time effect: $F(1,10)=26.47$, $p< 0.001$, group*time interaction $F(1,10)=17.09$, $p<0.01$, group effect: $F(1,10)=0.3$, $p=0.59$). Post-hoc analysis showed significantly smaller distances between REM and NREM clusters in the LPS group post-injection (0.87±0.19 a.u.) compared to baseline (1.30±0.15 a.u.). Decreased inter-state cluster distances indicate increased spectral similarity between the states (Kala et al., 2023).

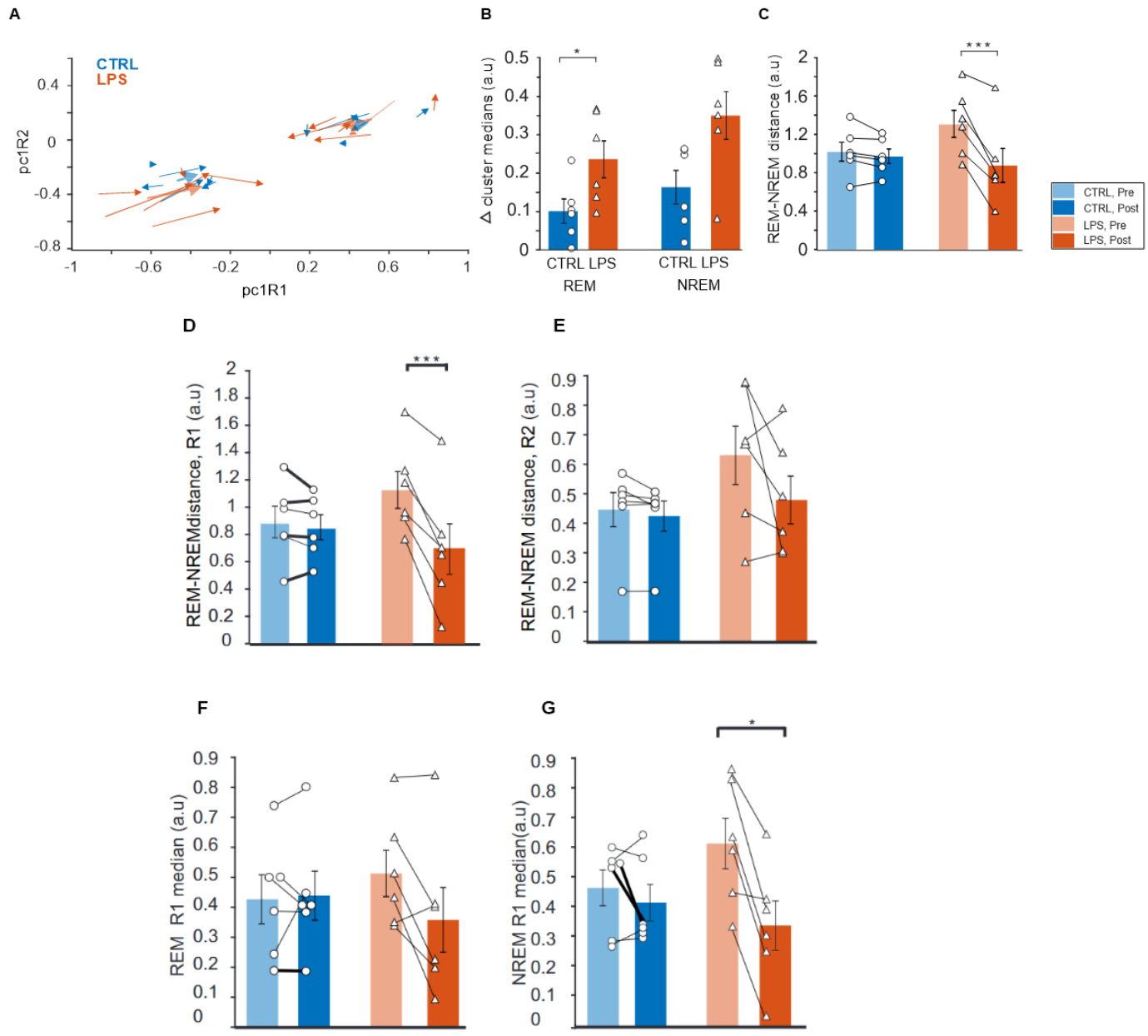

Figure 20: *LPS leads to spectral changes in the 1-9 Hz frequency range in both REM and NREM.*

A. Quiver plot showing the directional shift of the REM and NREM cluster medians before and after injection in CTRL (blue) and LPS animals (orange). The starting point of each arrow shows cluster medians before the injection, and the arrow head the medians after injection.

B. Size of the shift in cluster medians in REM and NREM. Each data point represents change in cluster position after the treatment in individual CTRL or LPS animals. Bars show mean ± s.e.m.

*C. The distance between REM and NREM clusters in CTRL or LPS animals pre and post injection. *p<0.05; ***p<0.001.*

*D-E: Each data point represents the distance between REM and NREM cluster medians along R1 (D) or R2 (E) in CTRL (circles) and LPS (triangles) animals pre or post injection. Bars represent mean ± s.e.m. ***p<0.001*

*F-G: Each data point represents median of R1 of REM (F) or NREM (G) in CTRL (circles) and LPS (triangles) animals' pre or post injection. Bars represent mean ± s.e.m. **p<0.05; ***p<0.001.*

4.4 State similarity in low spectrum frequencies

Decreased distance between REM and NREM clusters could be the result of changes in R1, R2, or in both. By decomposing the 2-dimensional inter-cluster distance into R1 and R2 components, we determined the spectral range most affected by LPS. Distance between REM and NREM clusters was significantly decreased along R1 (rmANOVA; time effect $F(1,10)=39.26$, $p<0.001$, group effect $F(1, 10)=0.03$, $p=0.84$, group*time interaction, $F(1,10)=27.55$, $p<0.001$). Post-hoc analysis showed that the distance between clusters was significantly smaller in the LPS group post injection (0.69 ± 0.20 a.u.) compared to baseline (1.13 ± 0.14 a.u., Fig. 20D). By contrast, there was no significant change in the distance between the clusters along R2 (rmANOVA; time effect, $F(1,10)=2.85$, $p=0.12$, group*time interaction, $F(1, 10)=1.59$, $p=0.23$, group effect, $F(1,10)=1.64$, $p=0.22$, Fig. 20E).

Hence, LPS-mediated spectral similarity between REM and NREM is resulting from changes in the 1-9 Hz frequency range (Kala et al., 2023).

4.5 NREM contributes more to spectral similarity in lower frequencies than REM

Reduced distance between REM and NREM clusters along R1 may be state-specific or both states could contribute. In REM, we observed no significant changes in median R1 values (rmANOVA; time effect: $F(1,10)=3.16$, $p=0.10$, group effect: $F(1,10)=0.0002$, $p=0.98$, time*group interaction: $F(1,10)=4.31$, $p=0.06$, Fig. 20F).

NREM R1 values were significantly affected, however (rmANOVA, time effect: $F(1, 10)=15.02$, $p<0.01$), time*group interaction: $F(1,10)=7.27$, $p=0.02$, group effect ($F(1, 10)=0.13$, $p=0.72$). Post-hoc analysis showed a significant increase in R1 medians in the LPS group post-injection (0.61 ± 0.09 a.u.) compared to baseline (0.34 ± 0.09 a.u., Fig. 20G) (Kala et al., 2023).

4.6 LPS caused increased within-state instability in REM and NREM

The observed state fragmentation and altered REM-NREM dynamics could be caused by inflammation-related state instability. Here, we used distance between subsequent epochs in state-space as a measure of within-state jitter or instability.

Trajectories of short time-series sampled from the LFP near a cluster median generally remained within the limits of the surrounding cluster (Fig. 21), but show high second-to-second variability: subsequent epochs were not located in close proximity within spectrum-based state space. This was the case in both the LPS and control groups, although there was more overlap between longer trajectories of both states after LPS injection. This is in part caused by increased state transitions captured in longer timeframes, but also by decreased inter-cluster distances and generally high spatial variability (Kala et al., 2023).

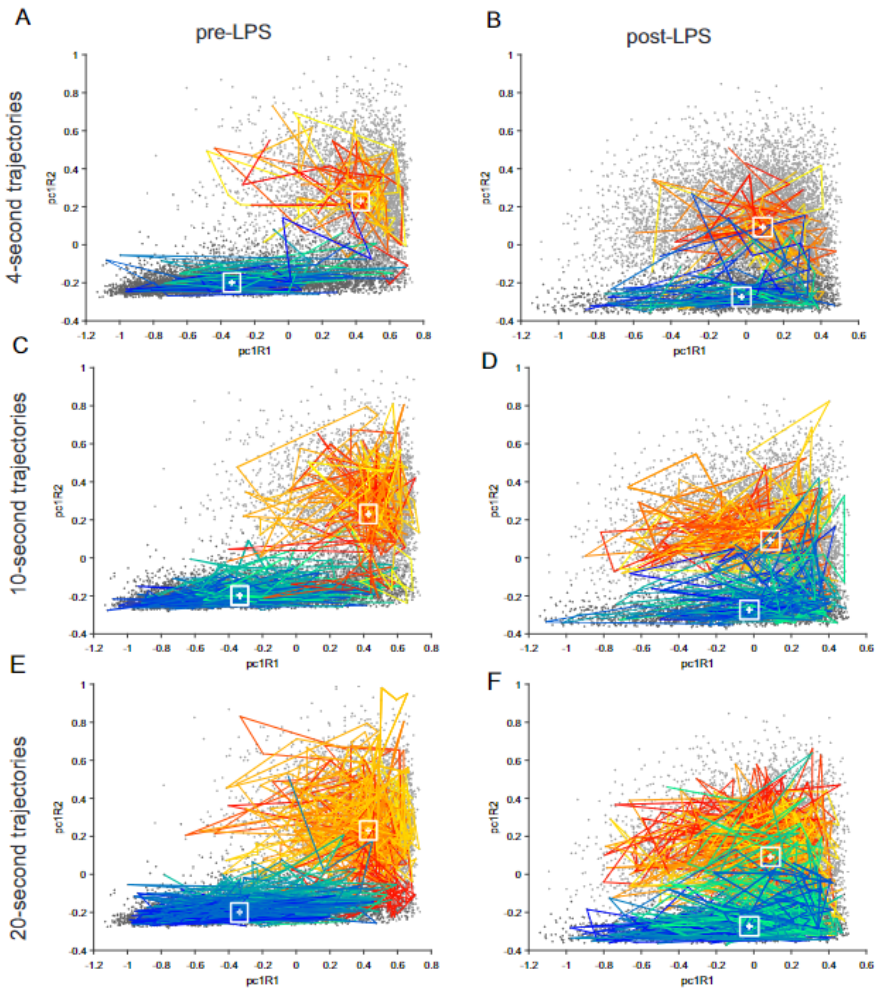

Figure 21: *Representative 4-, 10-, and 20-second-long trajectories in state space. A-f white boxes indicate the region around the state cluster median where the detected*

incoming and outgoing trajectories end resp. Start. 15 incoming and 15 outgoing trajectories are shown for each state. Plotted trajectories were chosen at random. Trajectories starting or ending in nrem are shown in blue-green, and rem trajectories are shown in red-yellow. Although second-to-second positions in state space vary widely and points that are neighbouring in time are not always closely spaced together in state space, overall trajectories sampled around a cluster median remain mostly within the boundaries of that cluster. This is the case at baseline, but also after LPS injection. Similar patterns were observed for short trajectories (4 s, a-b) and longer trajectories (10 s, c-d, 20 s e-f).

Jitter along R1 was not significantly affected by LPS injection in either REM (rmANOVA; time effect: $F(1,10)=1.20$, $p=0.29$; group effect: $F(1,10)=0.80$, $p=0.39$; time*group interaction: $F(1,10)=0.01$, $p=0.92$, Fig. 22A), or NREM (time effect: $F(1,10)=0.92$, $p=0.36$; group effect: $F(1,10)=0.86$, $p=0.37$; time*group interaction: $F(1,10)=0.0005$, $p=0.98$, Fig. 22B).

However, jitter along R2 was significantly increased in both REM and NREM after LPS injection. In REM, post-hoc analyses showed significantly higher jitter in LPS rats after injection (0.087±0.03 a.u.) compared to baseline (0.074±0.03 a.u.) (rmANOVA, time*group interaction: $F(1,10)=7.93$, $p=0.01$, group effect $F(1,10)=0.96$, $p=0.34$, time effect: $F(1,10)=1.17$, $p=0.30$; Fig. 22C). Effects on R2 jitter in NREM were similar (rmANOVA, time*group interaction: $F(1,10)=7.15$, $p=0.02$, group effect: $F(1,10)=0.96$, $p=0.34$, time effect: $F(1,10)=1.17$, $p=0.30$, Fig. 22D), although post-hoc analyses showed no significant differences (Kala et al., 2023).

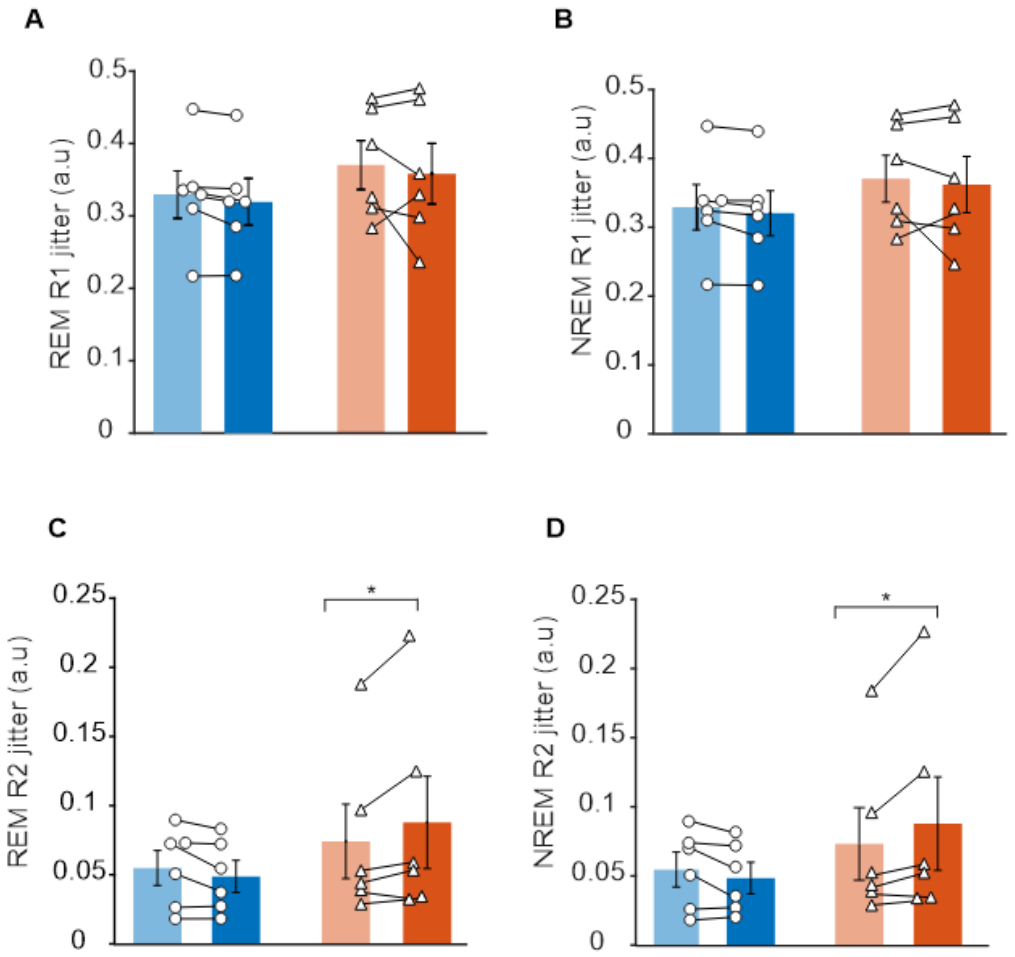

Figure 22: *LPS leads to within-state instability in high frequency range r2 (1-15 hz/1-45 hz). A-b: median jitter values of REM (a) and NREM (b) along R1 in Ctrl (circles) and LPS (triangles) animals pre or post injection. Bars represent mean ± sem. C-d: median jitter of REM (a) or NREM (b) along R2 in ctrl (circles) and LPS (triangles) animals pre or post injection. Bars represent mean ± sem. *p<0.05.*

4.7 Effects of LPS on periodic and background power spectrum components

To investigate possible sources of the changes in R1, power spectra were analysed for representative channels. NREM spectra showed markedly reduced power below 3 Hz in LPS-injected rats, but not controls (Fig. 24A). REM spectra showed the opposite effect: increased power in the <3 Hz range, as well as a smaller, variable increase in the 7-9 Hz range (Fig. 24B). Power spectra in the control group remained at baseline levels.

Post-LPS changes in spectral power could be caused by altered EEG oscillations and background (aperiodic) components of the power spectrum. To better understand post-LPS R1 in REM and NREM, aperiodic and periodic components of the power spectrum for each

state were modelled separately. Like in non-anaesthetized recordings (Leemburg et al.,, 2018), REM spectra had overall shallower slopes than NREM spectra at baseline (REM vs. NREM exponents: 1.42±0.28 vs. 1.95±0.18; Fig. 23A-B), and after LPS (REM vs. NREM exponents: 1.67±0.22 vs. 2.09±0.19; Fig. 23A-B) (Kala et al., 2023).

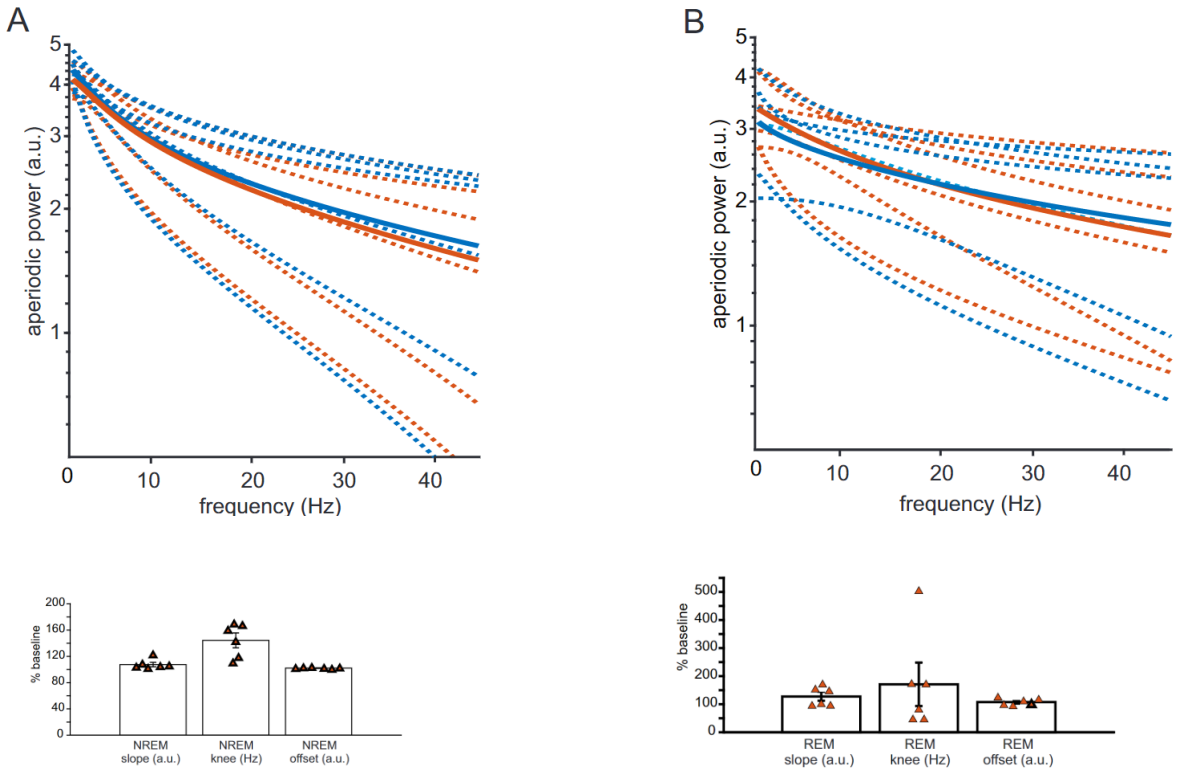

Figure 23: *Effects of LPS injection on aperiodic spectrum components*
A-B, Aperiodic component of the FOOOF model in NREM (A) and REM (B) pre (blue, solid lines) and post LPS injection (orange, dashed lines). Thin lines show aperiodic components of individual spectra, thick lines show group averages.
C-D, Post LPS changes in individual variables determining the aperiodic spectral component: slope, knee frequency and offset in NREM (C) and REM (D). Bars and error bars show mean + s.e.m, triangles show values for individual rats.

Aperiodic NREM spectrum components were not significantly affected by LPS (Fig. 23). Slopes remained at baseline levels (Wilcoxon signed rank test, W=21, p=0.09 after Bonferroni correction, Fig. 23C), as did offsets (W = 21, p=0.09 after Bonferroni correction). Knee frequencies were more variable than the other parameters and were slightly, but non-significantly, increased by LPS (144.39±11.36%, W=21, p=0.09 after Bonferroni correction, Fig. 24C). Effects of LPS on aperiodic REM spectrum components were similar (Fig. 24B). Slopes were not significant changed by LPS (W=16, p=0.94 after Bonferroni correction, Fig.

24D). Knee frequencies (W=15, p=1.31 after Bonferroni correction, Fig. 24D) and offsets were likewise unaffected (W=16, p=0.94 after Bonferroni correction, Fig. 24D).

At baseline, NREM spectra showed one major periodic component in the delta frequency range with a center frequency of 1.56±0.06 Hz and peak widths between 0.2 and 0.8 Hz (Fig. 24C-D). After LPS injection, center frequencies of this oscillation increased and peak widths became more variable (Fig. 24E-F), leading to overall faster and more variable NREM delta oscillations. As such, spectral power in frequencies above 2 Hz increased, resulting in the observed R1 shift. NREM spectra did not contain other oscillatory components (Kala et al., 2023).

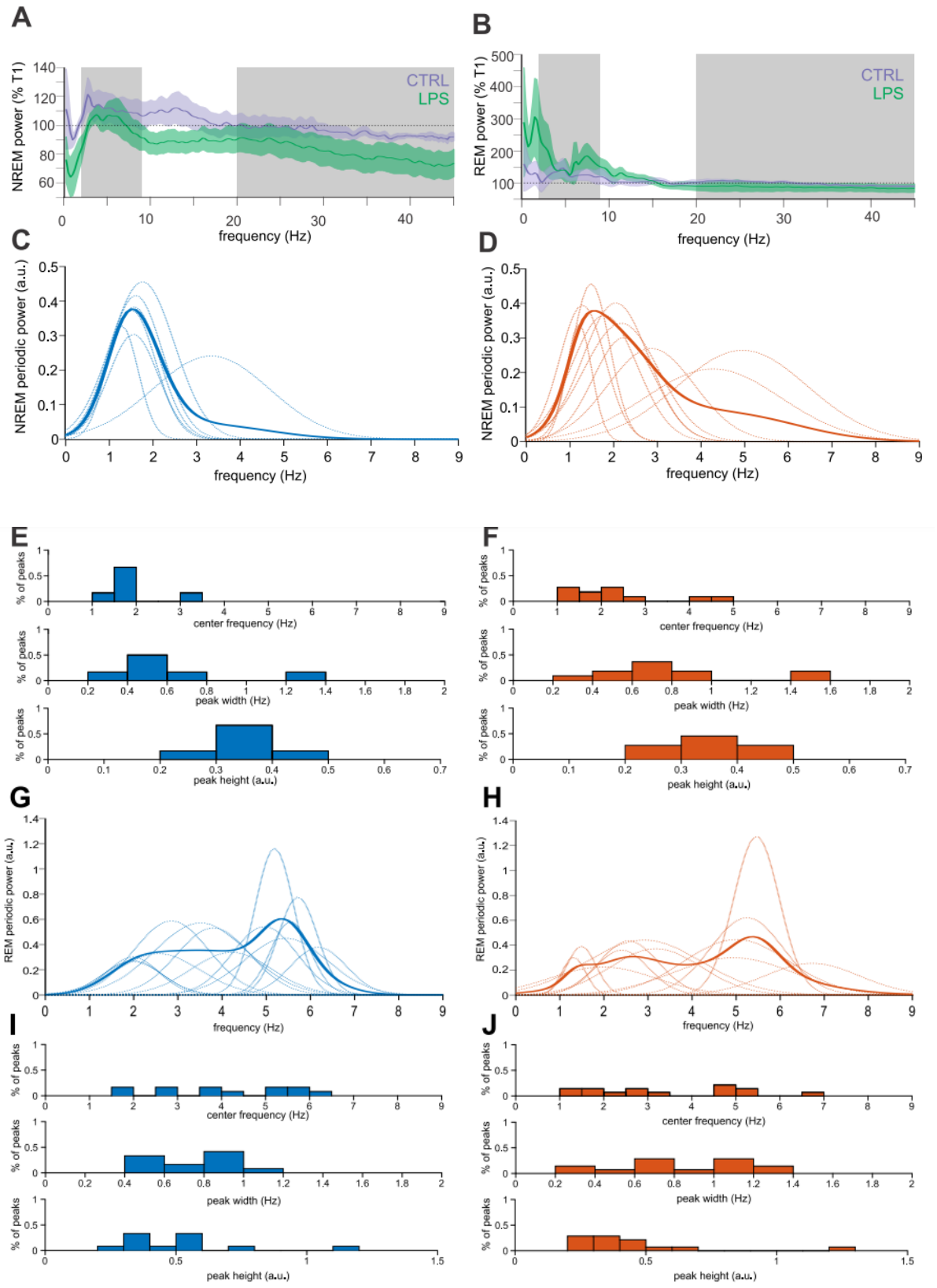

Figure 24: *Effects of LPS injection on oscillations in the 15-45 hz frequency range a-b detected oscillations in the 15-45 hz frequency range in REM pre (a) and post LPS injection (b). Dashed lines show detected peaks from individual spectra, thick lines show*

averages for each timepoint.
C-D pre (C) and post LPS (D) peak frequencies of detected oscillations in the 15-45 hz frequency range.
E-f pre (E) and post LPS (F) peak widths of detected oscillations in the 15-45 hz frequency range.
G-h pre (G) and post LPS (H) peak amplitudes of detected oscillations in the 15-45 hz frequency range

REM spectra showed multiple oscillations: a delta-like oscillation with a peak frequency in the 1-2 Hz range, and theta-like oscillations with a peak frequency around 5–6 Hz (Fig. 24G-H). These lower frequency oscillations remained present after LPS, but peak frequencies were lower, and more oscillations had peak frequencies lower than 2 Hz. Additionally, REM peak widths became more variable and overall peak heights slightly lower (Fig. 24I-J). This slowing of oscillatory components resulted in more power in the 1-2 Hz range and less in frequencies over 2 Hz was decreased. This effect, opposite to that found in the NREM spectrum, resulted in decreased inter-state distances between clusters in state-space along Ratio 1 (Kala et al.,2023).

4.8 Relations between inflammation severity, state fragmentation, and state similarity

Overall state fragmentation was positively correlated with higher IL-1β serum concentrations at the end of the experiment (Spearman's rho 0.682±0.202, p=0.009 for all rats, Spearman's rho 0.736±0.238, p=0.058 for LPS-injected animals only, mean ± stdev, Fig. 25 A-B). Inflammation severity, rather than the septic state per se resulted in state fragmentation.

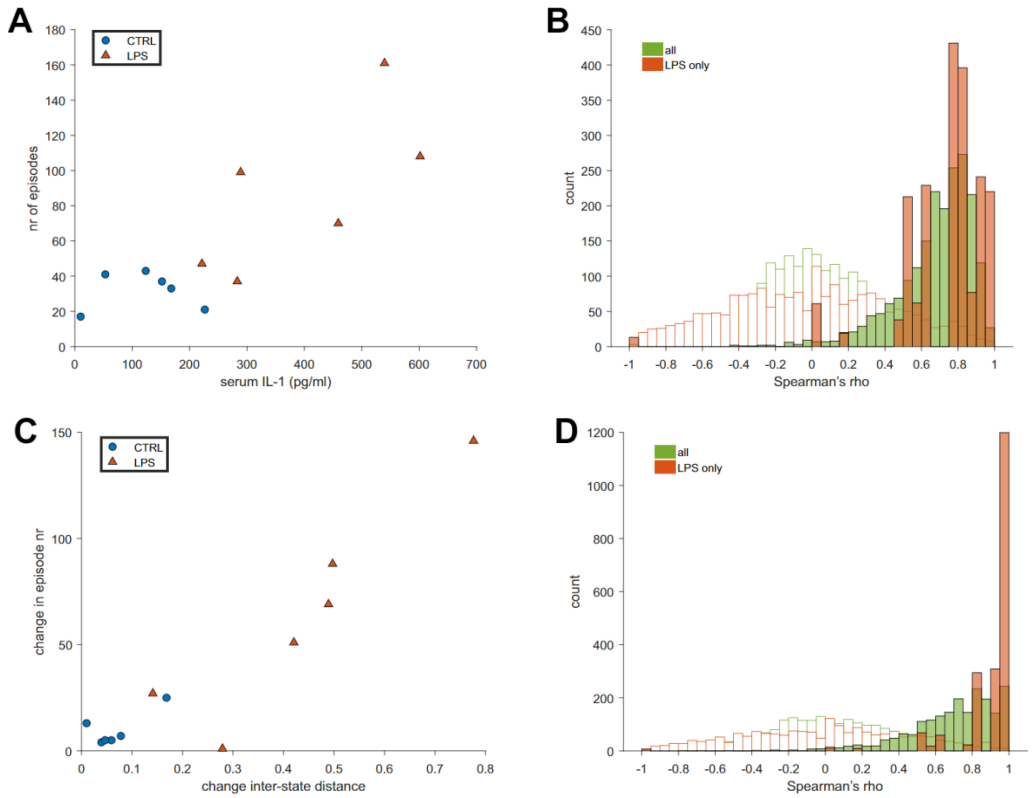

Figure 25: *Relations between inflammation severity, fragmentation, and inter-state distance*

A, Relation between IL-1β concentration and state fragmentation, expressed as the total number of NREM and REM episodes.

B, Bootstrapped results of Spearman correlations between IL-1β concentration and number of episodes. Filled bars show the results for all animals (green) and LPS only (orange). Open bars show the corresponding randomly sampled results.

C, Relation between the change in state fragmentation, expressed as the total number of NREM and REM episodes, and change in inter-state distance.

D, Bootstrapped results of Spearman correlations between change in number of episodes and change in inter-state distance. Filled bars show the results for all animals (green) and LPS only (orange). Open bars show the corresponding randomly sampled results.

Further, increases in state fragmentation were correlated with changes in inter-state distances. That is, animals with the largest decreases in inter-state distance also showed the largest increases in state fragmentation (Spearman's rho 0.700±0.233, p=0.0188 for all rats, Spearman's rho 0.909±0.173, p=0.175 for LPS-injected animals only, mean ± stdev, Fig. 25C-D) (Kala et al., 2023).

After studying the effects of LPS on brain oscillations in an anesthetised model, we confirmed these findings about sleep-state fragmentation and quality in awake behaving animals. The LPS dosage used in the urethane model was 10 mg/kg which caused a significantly higher mortality in awake behaving animals. The dose optimised for awake behaving animals was reduced to 5mg/kg which caused approximately 30% mortality signifying the severity of the given dose. Our next main objective was to focus on the LPS-mediated alteration of hippocampal cell population (CA1 pyramidal cells and interneurons). At the level of memory consolidation, the brain activity from these animals was recorded while exploring familiar or novel track. To understand the impact of LPS on memory consolidation, memory reactivation of familiar and novel track was accessed separately in the sleep session following behaviour.

4.9 LPS leads to NREM-Wake fragmentation and suppression of REM state in rats

The global oscillatory states in brain cortical areas during physiological conditions can be categorised into wakefulness, NREM and REM states based on frequency and amplitude of EEG waveforms and on EMG activity. Like in the urethane model, after LPS injection the experimental group showed fragmentation of network states as compared with long and stable vigilance states in the control group (Fig. 26A, B). Fragmentation manifested as shortening of average lengths of NREM (CTRL- 77.13±22.17, LPS 31.26±11.22, independent sample t-test $t(10)=4.126$, $p=0.002$), REM(CTRL- 60.07±9.02, LPS- 24.27±15.69, independent sample t-test $t(8)=4.085$, $p=0.004$) and WAKE (CTRL- 68.26±9.99, LPS-41.98±15.14, independent sample t-test $t(10)=3.238$, $p=0.009$) episodes in LPS group compared to the control group (Fig. 25C). Likewise, number of NREM (CTRL- 134.33±29.28, LPS-297.26±63.04, independent sample t-test $t(10)=-5.24$, $p<0.001$) and WAKE (CTRL- 134.54±25.66. LPS-286.34±64.79, independent sample t-test $t(10)=-4.870$, $p<0.001$) episodes increased significantly in the LPS group compared to the control group (Fig. 26D). However, number of REM episodes decreased significantly in the LPS group (CTRL-46.15±22.15, LPS- 5.01±4.57, independent sample t-test $t(10)=7.598$, $p<0.001$) compared to the control group (Fig. 26D. Despite NREM and wake fragmentation, time spent in NREM or wake was not affected but time spent in REM state (CTRL- 13.20±4.23, LPS-0.73±1.16, independent sample t-test

t(10)=6.340, p<0.001) was severely reduced in the LPS group compared to the control group (Fig.26E).

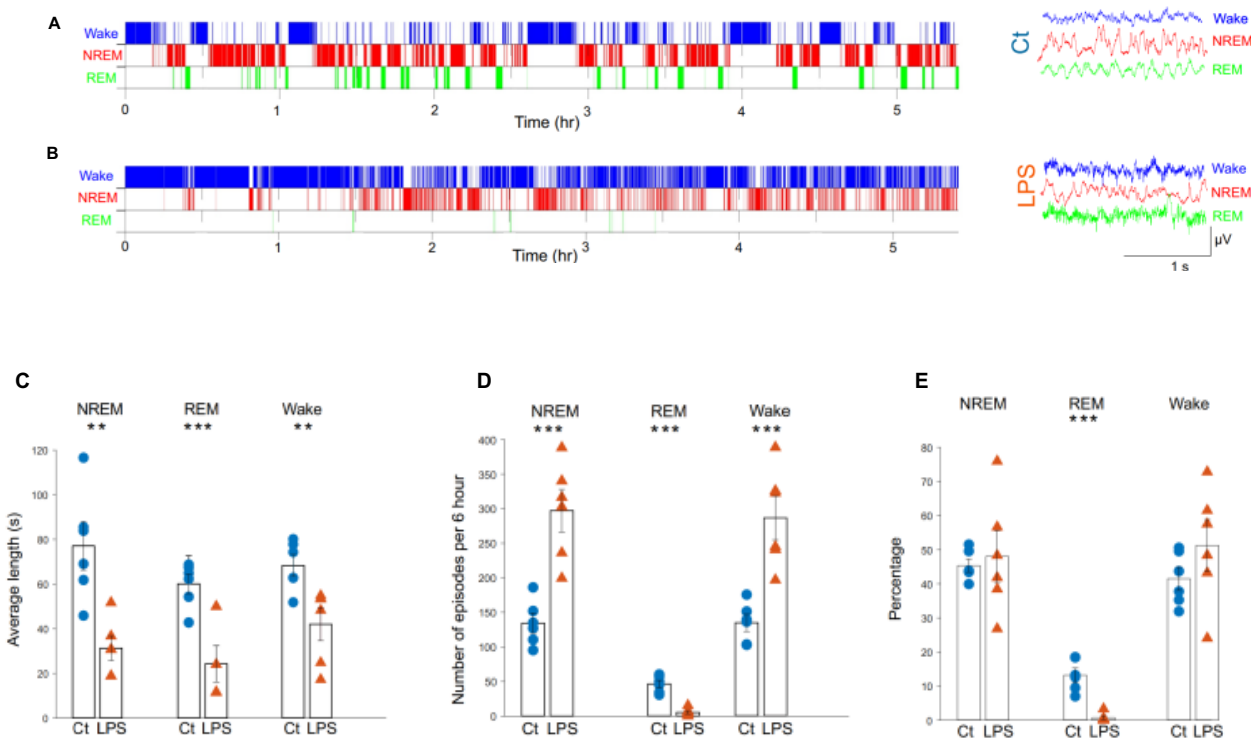

Figure 26: *LPS causes sleep-wake instability and suppression of REM state*

A-B. Representative traces and hypnograms showing WAKE in blue, NREM in red and REM in green.

*C. NREM, REM and WAKE states were long and stable in control group (CTRL). After LPS injection, the states were much shorter in length. Each data point shows the average length of episodes in individual CTRL and LPS animals (n = 6; Bars show mean ± s.e.m. **p<0.01, ***p<0.001)*

*D. Number of NREM, REM and Wake episodes in CTRL and LPS group. Each data point shows the number of episodes in individual CTRL and LPS animals (CTRL, n = 6; LPS, n = 6, Bars show mean ± s.e.m. ***p<0.001).*

*E. LPS does not lead to alteration in time spent in NREM or WAKE but significantly reduces the time spent in REM state. Each data point represents total time spent in NREM, REM and WAKE as percentage of recording time in CTRL and LPS animals (CTRL, n=6; LPS, n=6, Bars show mean ± s.e.m. ***p<0.001).*

4.10 LPS causes overall dampened power for up to 25Hz

Power spectrum analyses of the 6-hr long recording showed an overall dampened power of oscillations up to 25Hz frequency in the LPS group (Fig. 27A, B). Power of delta encompassing 1-4Hz frequency band showed significant decrease in the LPS group (27C, 95±6 vs 74±4, n=5, independent sample t-test t (8) =5.02, p<0.001). Theta power also showed similar pattern of decrease in the LPS group (27D, 102±4 vs 77±5, n=5, independent sample t-test t (8) =4.97, p=0.004).

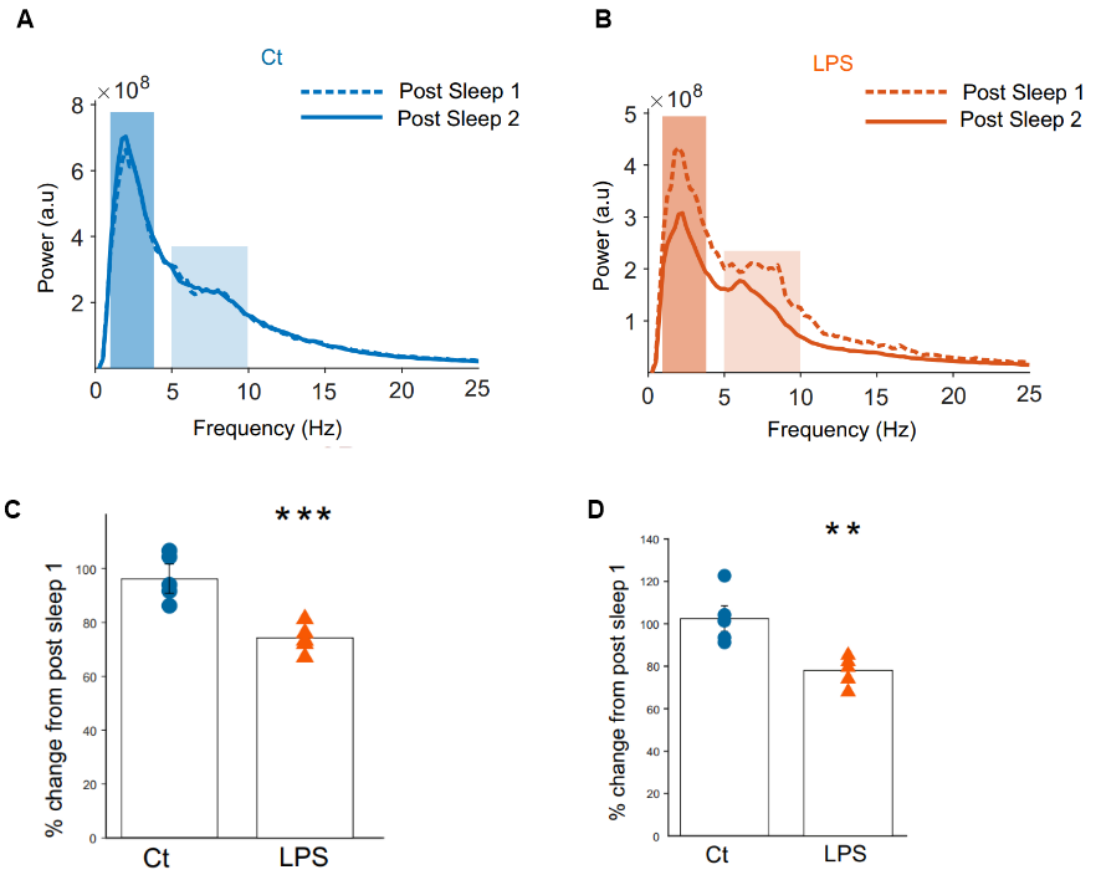

Figure 27: *LPS leads to decrease in delta (1-4Hz) and theta (5-10Hz) power in NREM state.*

A-B: Representative power spectra of NREM state in control (A) and LPS animal (B) in post sleep 1 and post sleep 2.

*C: Each data point shows percentage change from post sleep 1 (baseline) of NREM delta power of individual animals in control (circles) and LPS group (triangles). Bars represent mean ± SEM. ***p<0.001.*

*D: Each data point shows percentage change from post sleep 1 (baseline) of NREM theta power of individual animals in control (circles) and LPS group (triangles). Bars represent mean ± SEM. **p<0.01.*

4.11 LPS suppresses CA1 hippocampal pyramidal and interneuron activity

To describe the effect of LPS on discharge frequency of CA1 pyramidal cells and interneurons, the z-scored firing rates of population activity were analysed per hour. The CA1 pyramidal activity decreased significantly in the LPS group (rmANOVA; time effect: $F(1,11)=3.463$, $p<0.003$; group effect: $F(1,11)=7.083$, $p=0.022$; time*group interaction: $F(1,11)=0.429$, $p=0.92$, Fig. 28C). Posthoc analysis showed significant decrease in population firing at 5^{th} and 6^{th} hour of LPS injection. Likewise, the discharge activity of interneurons decreased significantly in the LPS group (rmANOVA; time effect: $F(1,11)=6.849$, $p<0.001$; group effect: $F(1,11)=6.815$, $p=0.026$; time*group interaction: $F(1,11)=9.152$, $p<0.001$, Fig. 28E). Posthoc analysis showed a significant increase in interneuron activity for up to 3 hrs after the novel exposure in control animals which eventually stabilised at later time points. In the LPS group however, the novelty induced increase in firing activity was absent, but it rather led to a significant decrease in activity after 1 hr of LPS injection which remained dampened until 6 hrs of recording.

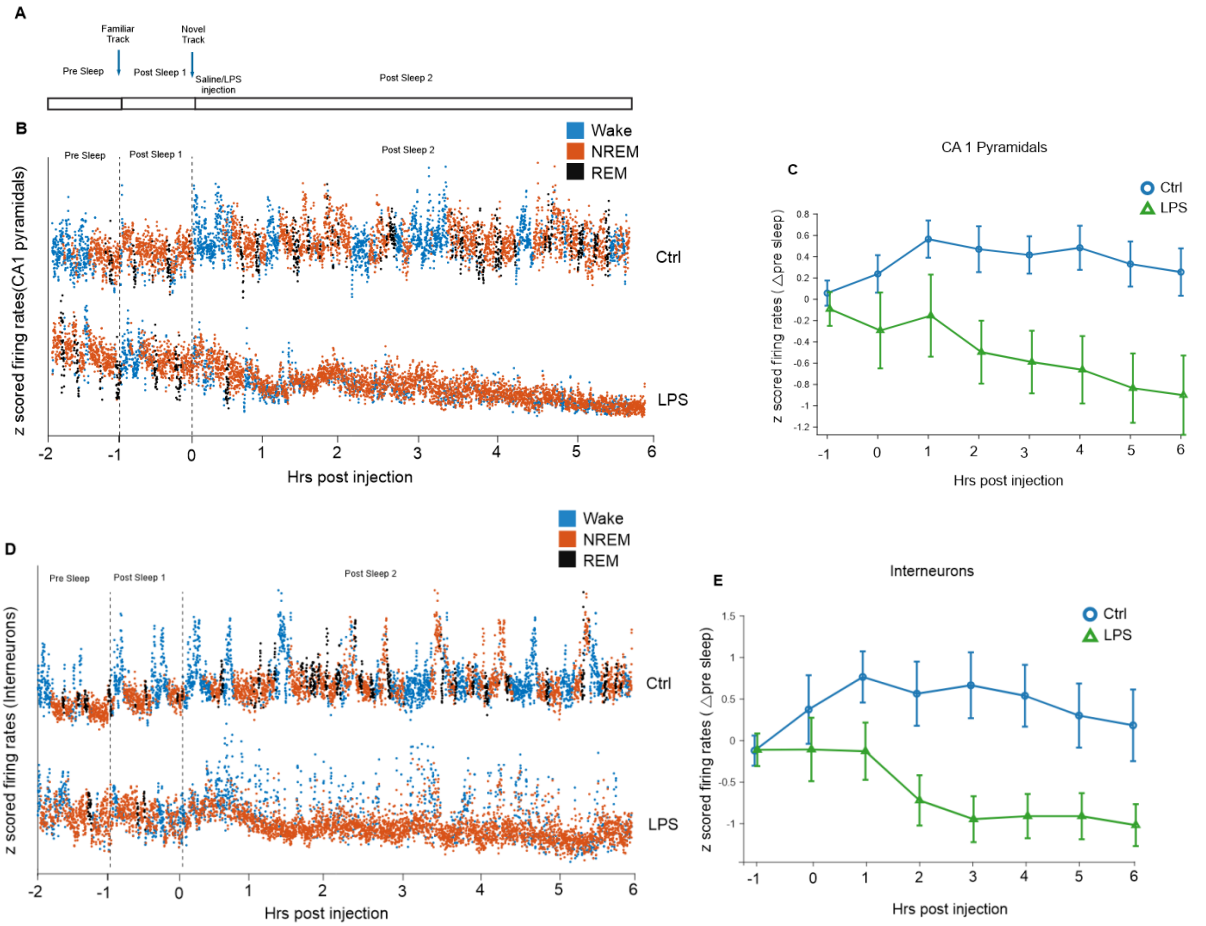

Figure 28: *LPS leads to decrease in population firing of CA1 pyramidal neurons and interneurons.*

A. Schematic of experimental design. Animals were recorded for one hour of pre sleep followed byrunning trials in familiar track. Another hour of sleep session, referred to as post sleep1 was recorded. The animals were then exposed to a novel track followed by recording 6 hrs long sleep session called post sleep2.

B. Example of population firing rate of CA1 pyramidal neurons for the entire recording during control and LPS day. The shown trace shows the z-scored firing rate activity in time smoothed for 10 second epochs. Wake is shown in blue, NREM in orange and REM in black.

C. Each point represents the mean firing rate of CA1 pyramidal neurons per hour. Controls are represented by blue circles and LPS by green triangles, $p<0.001$.

D. Example of population firing rate of interneurons for the entire recording during control and LPS day. The shown trace shows the z-scored firing rate activity in time smoothed for 10 second epochs. Wake is shown in blue, NREM in orange and REM in black.

E. Each point represents the mean firing rate of interneurons per hour. Controls are represented by blue circles and LPS by green triangles, p<0.001.

4.12 LPS leads to increase in sharp wave ripple density during NREM

Sharp wave ripple events are considered to be one of the central processes of memory consolidation at the network level. To investigate the effect of LPS on memory consolidation, we used sharp wave ripple events as electrophysiological marker of this step of memory processing and analysed their rate during sleep sessions. LPS group showed marked increase in the occurrence of SWRs during NREM state throughout the sleep sessions compared to the control group (rmANOVA; time effect: F (1,11)=13.593, p<0.001; group effect: F(1,11)=0.476, p=0.504; time*group interaction: F(1,11)=3.502, p=0.026, Fig. 29A,B). Posthoc analysis showed significantly elevated occurrence of SWR events after the LPS injection during NREM episodes (Fig. 29C).

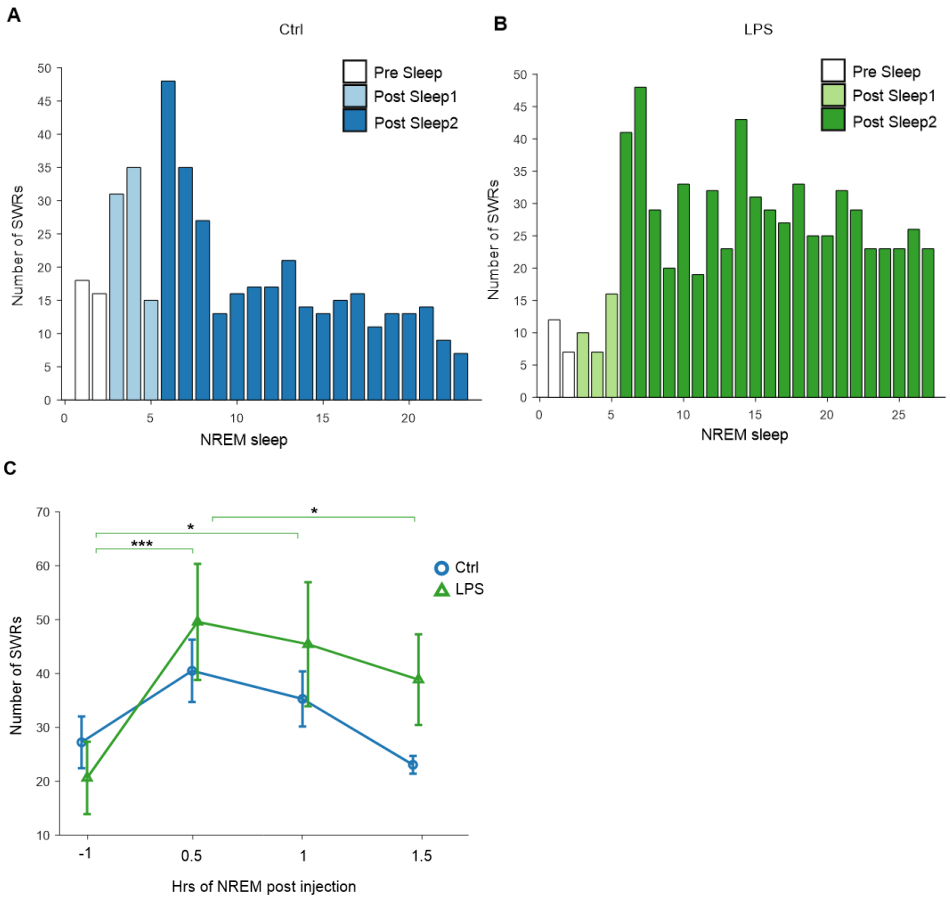

Figure 29: *LPS leads to increase in sharp wave ripple events after LPS injection.*

A-B. Each bar represents the average number of SWR events per 10 minutes of NREM sleep session in control (A) and LPS group (B). Bars in white represent SWRs during NREM in pre sleep session, light blue bars represent SWRs during NREM in post sleep 1 session in controls and dark blue bars show number of SWRs during NREM in post sleep 2 session in controls. Bars in light green represent SWRs during NREM in post sleep 1 in LPS group and dark green bars show SWRs during NREM in post sleep 2 session in LPS group.

*C. Number of SWRs averaged across 30 mins of NREM. Each data point represents number of SWRs per 10 mins of NREM. Controls are represented by blue circles and LPS by green triangles, *p<0.05, **p<0.01, ***p<0.001.*

5.DISCUSSION

In the current study, we used a high dose of LPS to mimic the acute phase of sepsis. In the first part of the project, we used 10 mg/kg of LPS under urethane anaesthesia to characterize the effects of sepsis on hippocampal oscillatory activity in REM-like and NREM-like states. The dosage used was based on previous studies. We found an extensive state fragmentation in the LPS group manifested by about 75% decrease of each state duration and a reciprocal increased number of the episodes. Additionally, we found that the overall time spent in each state remained unaltered indicating that the observed state fragmentation is unlikely a result of specific state suppression. We further analysed dynamics of transitions from REM to NREM and NREM to REM to understand the characteristics of state switching. We found no effect of LPS on the dynamics of state transitions *per se*. Using a 2-D state space approach, we further analysed spectral characteristics of REM-like and NREM-like states and found that LPS led to an increased spectral similarity between the states by decreasing their corresponding cluster distance. The decreased inter-cluster distance was majorly contributed by the shift of NREM cluster. In the frequency domain, the increased similarity between the states was driven by low frequency component (1-9 Hz). As a measure of state stability, we further quantified a within-state jitter representing the inner velocities of REM-like and NREM-like clusters and found in both cases their significantly increase. Increased within-states jitter was modulated by high frequency component encompassing 15-45 Hz frequency range. Parametrizing the periodic and aperiodic component of NREM and REM spectra showed that LPS caused alteration in oscillatory component and not in the aperiodic background spectra. Power spectrum analysis of NREM spectra showed decreased power at low frequency oscillations (<3 Hz) in LPS group compared to control group. REM spectra showed an opposite trend of increased power at lower frequency (<3 Hz) compared to controls. We also found a positive correlation between the levels of IL-1β and state fragmentation. Furthermore, state fragmentation was positively correlated with inter-state distance and therefore with their spectral similarity.

Next, we confirmed the analogous findings on state fragmentation in awake behaving animals. In this study, we used 5mg/kg dose of LPS as 10mg/kg dosage was associated with

high mortality under this protocol. 5mg/kg dose led to about 30% mortality signifying the high severity and hence the suitability of the model. LPS in awake behaving animals led to fragmentation of wake, NREM and REM states. Time spent in wake or NREM did not differ, but time spent in REM was severely reduced in the LPS group compared to the controls. Power spectrum analysis of sleep states showed an overall dampened power for at least up to 25 Hz. State space analysis in awake behaving animals (5mg/kg LPS) showed similar outcomes as the urethane injected animals (10mg/kg) confirming that the lower dose retained the spectral similarity outcomes (data not shown). In the next part of the study, we analyzed the response of CA1 hippocampal population activity (pyramidal cells and interneurons) during sepsis. We found an overall inhibition in both pyramidal and interneuron activity. CA1 pyramidal activity decreased significantly after 4 hrs of LPS injection. Decrease in interneuron activity on the other hand preceded the pyramidal cells and was prominently dampened after 1 hour of LPS injection. Furthermore, we analysed the occurrence of sharp wave ripples in NREM sleep sessions after LPS injection. Surprisingly, the number of SWRs in the LPS group were significantly elevated throughout the recording.

Fragmentation associated findings -namely vigilance state discontinuity, unaltered time spent in NREM, and REM suppression in the current study are in line with the previous work shown in rodents under the influence of LPS or CLP model of sepsis (Baracchi et al., 2011; Lancel et al., 1995). In contrast with our results Lancel et al., showed that delta power in NREM was enhanced in the LPS injected rats. However, the dosage used in the study was very low (30 or 100 micrograms/kg LPS) and hence these differences in power in various frequency bands could be attributed to the low dose of LPS which supposedly elicited a weaker immune system response. Similar outcomes on reduced power of delta and theta band in the current study were shown in a CLP model of sepsis which confirmed that the dosage used in the present study was enough to capture a sepsis-associated alteration in oscillatory activity (Baracchi et al., 2011). In previously described studies, it is unclear whether the changes in power spectra during sepsis conditions were driven by oscillatory activity or by a background spectrum as parameterization of these components was not performed. These analyses were often limited to particular states or frequency bands without assessing the shifts in the peak frequencies. In the first objective of this study, we used an LPS model of sepsis under urethane anaesthesia. This model captures the fine

kinetics of oscillatory activity during sepsis as urethane exerts minimum effects on respiratory and cardiovascular systems sparing the REM-like and NREM-like activity. We decomposed the power spectra into aperiodic and periodic components and found the periodic component to be the main contributor of sepsis-associated changes. We used a 2D state space approach to understand and characterize the dynamics of two states with respect to each other under septic conditions. We calculated the power in two frequency bands, R1 (1 - 9Hz) and R2 (9 – 45 Hz) for each 1 second recording. These epochs were then classified into REM or NREM based on their positioning in the 2-D state space allowing us to study the relation between the states and within state dynamics. The distance between the clusters decreased in the LPS group signifying increased spectral similarity. We observed that the overall decrease in distance between the states was driven by opposing shifts in the lower frequency band, R1. These alterations were manifested by decreased delta power in NREM and a shift towards faster oscillations. In case of REM, LPS led to increased delta and theta power shift towards the slower activity. Next, we analysed the stability of the REM-like and NREM-like states by calculating jitter which represented the median velocity of the two clusters. We observed an increase in the jitter parameters which was driven by high frequency oscillations, R2. Alteration in oscillatory spectra can be directly related to the stability and hence to fragmentation of states during septic shock conditions. NREM and REM represent global brain states with attractor properties requiring stability to maintain the respective states. The relationship between the states can be illustrated by energy landscape with two local minima separated by high energy saddles. Inter-state and intra-state stability characterised by the distance between the two states and with-in state velocity respectively may drive the overall stability of brain states. Sepsis-mediated changes in spectral characteristics of REM and NREM state may alter the energy landscape of brain states leading to increased spectral similarity and instability facilitating more state transitions. We observed a direct correlation between state fragmentation and inter-cluster distance and hence conclude that these changes may be associated with higher fragmentation in sepsis animals or patients. Furthermore, we also found that the state fragmentation was positively correlated to the levels of IL-1β fragmentation pointing towards the possibility of severity induced state fragmentation.

In unanaesthetised recordings, sepsis caused similar vigilance state fragmentation but additionally also led to REM suppression which has been previously described both during sepsis as well as low dose immune challenge (Baracchi et al., 2011; Lancel et al., 1995). It has been shown that REM active lateral hypothalamus GABAergic neurons are silenced in response to peripheral LPS injection which could be a potential mechanism of REM suppression during inflammatory conditions (Borniger and de Lecea 2021). Since NREM delta power is known to be a hallmark of homeostatic sleep drive (Long et al., 2021), decreased delta power in NREM because of LPS may indicate the disruption of sleep homeostasis. Power of delta often depends on duration and intensity of sleep state (Long et al., 2021). In the current study, we found extensively short durations of sleep states which might indicate the possible cause of failure to attain high delta power and hence sleep intensity. In summary, LPS causes spectral similarity and instability of vigilance states which may decrease the threshold of state switching leading to state fragmentation and an eventual failure of sleep homeostasis and quality.

Effect of sepsis on hippocampus in the context of inflammation, volume or memory functions have been previously described both in human studies and animal models of sepsis (Basak et al., 2021; Yuan 2020). In a CLP model of sepsis, in-vitro studies have shown decreased expression of hippocampal PV interneurons which has been linked to impaired cognitive outcomes in septic shock survivors (M. Ji et al., 2020; L. Zhang et al., 2023). Structural damage to CA1 hippocampal dendritic arbors and decreased spines in the apical dendrites have also been documented during sepsis (Huerta et al., 2016). Despite the importance of hippocampus in memory processing and spatial navigation accompanied by increased vulnerability during sepsis, studies involving hippocampal cellular response during sepsis are rare. In the current work, we recorded spiking activity of hippocampal CA1 cells in awake subjects in an attempt to decipher electrophysiological correlates of memory impairment during sepsis. We analysed the dynamics of firing frequency of CA1 pyramidal and interneurons and found a differential time-dependent response. Firing rates of interneurons decreased after about 1 hour after LPS injection which was followed by a decreased pyramidal cell activity approximately 4 hrs post LPS injection. In-vitro studies have shown decreased expression of CA1 cell population (CA1 and interneurons) in sepsis models at various timescales (Comim et al., 2013; M. Ji et al., 2020; M.-H. Ji et al., 2015; L.

Zhang et al., 2023). Furthermore, we also analysed sharp wave ripple events, which are considered as a hallmark of memory consolidation. In NREM sleep epochs we found their increase after LPS injection which remained elevated until the end of recording sessions. Under physiological conditions, SWRs frequency, occurrence and durations are modulated by temperature changes in brain (P. C. Petersen, Vöröslakos, and Buzsáki 2022). Sepsis is often associated with hyperthermia (Granger et al., 2013; Lancel et al., 1995). Elevated temperature in the acute phase of sepsis may be one of the plausible explanations for increased occurrence of SWRs. Alternatively, it is postulated that sepsis leads to decreased hippocampal and cortical cholinergic innervation in animal models of sepsis (Barichello et al., 2023). An inverse relationship between the number of sharp wave ripple complexes and acetylcholine levels using fiber photometry readouts in mice was recently shown (Y. Zhang et al., 2021). Sepsis-mediated disruption in cholinergic pathway may be a contributing factor in increased number of SWR events. Our findings add new hypothesis that relates changes in SWR occurrence to observed decreased inhibition in hippocampal circuitry. Dampened activity in population of interneurons in our data seems to cause an overall circuitry inhibition, as reflected in suppressed spiking in pyramidal cell population. Despite we did not record in CA3 region, where the SWR activity originates, we assume that CA3 network is likely to be affected as the adjacent CA1 region we recorded from. Decreased interneuron activity thus might disinhibit pyramidal cell ensembles that become more prone to reactivate during NREM epochs of sleep.

Neuroinflammation forms the core basis of brain dysfunction in many types of dementias and hence is a major player in sepsis-mediated-memory-disturbances as well. Memory impairments are very well described in sepsis patients and animal models. On the other hand, role of sleep despite playing a vital role in maintaining a wide spectra of brain and immune functions in determining the outcomes in sepsis patients remains poorly understood. Disrupted sleep patterns driven by altered oscillatory activity may be responsible for poor outcomes in sepsis patients both in the survival rate in the acute phase and by long term neurological consequences in those who survive. Analysis of hippocampal place cell activity during sepsis may indicate the mechanism of sepsis-induced memory impairment at network level. Remedying sleep-wake dynamics in hippocampal network may

thus serve as a potential therapeutic target in improving the survival and eventually memory outcomes in sepsis patients.

6. references

1. Lever A, Mackenzie I. Sepsis: definition, epidemiology, and diagnosis. *BMJ*. 2007;335(7625):879-883. doi:10.1136/bmj.39346.495880.AE

2. Arwyn-Jones J, Brent AJ. Sepsis. *Surgery (Oxford)*. 2019;37(1):1-8. doi:10.1016/j.mpsur.2018.11.007

3. Huang M, Cai S, Su J. The Pathogenesis of Sepsis and Potential Therapeutic Targets. *IJMS*. 2019;20(21):5376. doi:10.3390/ijms20215376

4. Wilcox ME, Daou M, Dionne JC, et al. Protocol for a scoping review of sepsis epidemiology. *Systematic Reviews*. 2022;11(1):125. doi:10.1186/s13643-022-02002-6

5. Khanina A, Cairns KA, McGloughlin S, et al. Improving sepsis care for hospital inpatients using existing medical emergency response systems. *Infection, Disease & Health*. 2020;25(2):63-70. doi:10.1016/j.idh.2019.10.003

6. Ramachandran G. Gram-positive and gram-negative bacterial toxins in sepsis. *Virulence*. 2014;5(1):213-218. doi:10.4161/viru.27024

7. Minasyan H. Sepsis: mechanisms of bacterial injury to the patient. *Scand J Trauma Resusc Emerg Med*. 2019;27:19. doi:10.1186/s13049-019-0596-4

8. Novosad SA. Vital Signs: Epidemiology of Sepsis: Prevalence of Health Care Factors and Opportunities for Prevention. *MMWR Morb Mortal Wkly Rep*. 2016;65. doi:10.15585/mmwr.mm6533e1

9. Porat A, Bhutta BS, Kesler S. Urosepsis. In: *StatPearls*. StatPearls Publishing; 2023. Accessed June 12, 2023. http://www.ncbi.nlm.nih.gov/books/NBK482344/

10. Megha KB, Joseph X, Akhil V, Mohanan PV. Cascade of immune mechanism and consequences of inflammatory disorders. *Phytomedicine*. 2021;91:153712. doi:10.1016/j.phymed.2021.153712

11. Gaddis ML, Gaddis GM. detecting Sepsis in an emergency department: SirS vs. qSofa.

12. Laupland KB, Zahar JR, Adrie C, et al. Determinants of temperature abnormalities and influence on outcome of critical illness. *Crit Care Med*. 2012;40(1):145-151. doi:10.1097/CCM.0b013e31822f061d

13. Marik PE, Taeb AM. SIRS, qSOFA and new sepsis definition. *J Thorac Dis*. 2017;9(4):943-945. doi:10.21037/jtd.2017.03.125

14. Singer M, Deutschman CS, Seymour CW, et al. The Third International Consensus Definitions for Sepsis and Septic Shock (Sepsis-3). *JAMA*. 2016;315(8):801. doi:10.1001/jama.2016.0287

15. Hernandez G, Bruhn A, Castro R, et al. Persistent Sepsis-Induced Hypotension without Hyperlactatemia: A Distinct Clinical and Physiological Profile within the Spectrum of Septic Shock. *Crit Care Res Pract*. 2012;2012:536852. doi:10.1155/2012/536852

16. Jarczak D, Kluge S, Nierhaus A. Sepsis—Pathophysiology and Therapeutic Concepts. *Front Med*. 2021;8:628302. doi:10.3389/fmed.2021.628302

17. Buras JA, Holzmann B, Sitkovsky M. Animal Models of sepsis: setting the stage. *Nat Rev Drug Discov*. 2005;4(10):854-865. doi:10.1038/nrd1854

18. Park BS, Lee JO. Recognition of lipopolysaccharide pattern by TLR4 complexes. *Exp Mol Med*. 2013;45(12):e66-e66. doi:10.1038/emm.2013.97

19. Lewis AJ, Seymour CW, Rosengart MR. Current Murine Models of Sepsis. *Surg Infect (Larchmt)*. 2016;17(4):385-393. doi:10.1089/sur.2016.021

20. Poli-de-Figueiredo LF, Garrido AG, Nakagawa N, Sannomiya P. EXPERIMENTAL MODELS OF SEPSIS AND THEIR CLINICAL RELEVANCE. *Shock*. 2008;30(7):53. doi:10.1097/SHK.0b013e318181a343

21. Cai L, Rodgers E, Schoenmann N, Raju RP. Advances in Rodent Experimental Models of Sepsis. *International Journal of Molecular Sciences*. 2023;24(11):9578. doi:10.3390/ijms24119578

22. Ghanta S, Kwon MY, Perrella MA. Induction of Sepsis Via Fibrin Clot Implantation. In: Walker WE, ed. *Sepsis: Methods and Protocols*. Methods in Molecular Biology. Springer US; 2021:17-25. doi:10.1007/978-1-0716-1488-4_3

23. Wen H. Sepsis Induced by Cecal Ligation and Puncture. *Methods in molecular biology (Clifton, NJ)*. 2013;1031:117. doi:10.1007/978-1-62703-481-4_15

24. Seemann S, Zohles F, Lupp A. Comprehensive comparison of three different animal models for systemic inflammation. *J Biomed Sci*. 2017;24:60. doi:10.1186/s12929-017-0370-8

25. Toscano MG, Ganea D, Gamero AM. Cecal Ligation Puncture Procedure. *J Vis Exp*. 2011;(51):2860. doi:10.3791/2860

26. Rincon JC, Efron PA, Moldawer LL, Larson SD. Cecal Slurry Injection in Neonatal and Adult Mice. *Methods Mol Biol*. 2021;2321:27-41. doi:10.1007/978-1-0716-1488-4_4

27. Sun GD, Zhang Y, Mo SS, Zhao MY. Multiple Organ Dysfunction Syndrome Caused by Sepsis: Risk Factor Analysis. *Int J Gen Med*. 2021;14:7159-7164. doi:10.2147/IJGM.S328419

28. Sygitowicz G, Sitkiewicz D. Molecular mechanisms of organ damage in sepsis: an overview. *The Brazilian Journal of Infectious Diseases*. 2020;24(6):552. doi:10.1016/j.bjid.2020.09.004

29. Goligorsky MS, Sun D. Glycocalyx in Endotoxemia and Sepsis. *The American Journal of Pathology*. 2020;190(4):791-798. doi:10.1016/j.ajpath.2019.06.017

30. Stanzani G, Duchen MR, Singer M. The role of mitochondria in sepsis-induced cardiomyopathy. *Biochimica et Biophysica Acta (BBA) - Molecular Basis of Disease*. 2019;1865(4):759-773. doi:10.1016/j.bbadis.2018.10.011

31. Dolmatova EV, Wang K, Mandavilli R, Griendling KK. The effects of sepsis on endothelium and clinical implications. *Cardiovasc Res*. 2020;117(1):60-73. doi:10.1093/cvr/cvaa070

32. Chousterman BG, Swirski FK, Weber GF. Cytokine storm and sepsis disease pathogenesis. *Semin Immunopathol*. 2017;39(5):517-528. doi:10.1007/s00281-017-0639-8

33. Haussner F, Chakraborty S, Halbgebauer R, Huber-Lang M. Challenge to the Intestinal Mucosa During Sepsis. *Frontiers in Immunology*. 2019;10. Accessed July 17, 2023. https://www.frontiersin.org/articles/10.3389/fimmu.2019.00891

34. Yoseph BP, Klingensmith NJ, Liang Z, et al. Mechanisms of intestinal barrier dysfunction in sepsis. *Shock*. 2016;46(1):52-59. doi:10.1097/SHK.0000000000000565

35. Turner JR. Intestinal mucosal barrier function in health and disease. *Nat Rev Immunol*. 2009;9(11):799-809. doi:10.1038/nri2653

36. Hu Q, Hao C, Tang S. From sepsis to acute respiratory distress syndrome (ARDS): emerging preventive strategies based on molecular and genetic researches. *Biosci Rep*. 2020;40(5):BSR20200830. doi:10.1042/BSR20200830

37. Rios F, Iscar T, Cardinal-Fernández P. What every intensivist should know about acute respiratory distress syndrome and diffuse alveolar damage. *Rev bras ter intensiva*. 2017;29:354-363. doi:10.5935/0103-507X.20170044

38. Wang D, Yin Y, Yao Y. Advances in sepsis-associated liver dysfunction. *Burns Trauma*. 2014;2(3):97-105. doi:10.4103/2321-3868.132689

39. Highton AJ, Schuster IS, Degli-Esposti MA, Altfeld M. The role of natural killer cells in liver inflammation. *Semin Immunopathol*. 2021;43(4):519-533. doi:10.1007/s00281-021-00877-6

40. Caraballo C, Jaimes F. Organ Dysfunction in Sepsis: An Ominous Trajectory From Infection To Death. *Yale J Biol Med*. 2019;92(4):629-640.

41. Ferrer R, Martin-Loeches I, Phillips G, et al. Empiric Antibiotic Treatment Reduces Mortality in Severe Sepsis and Septic Shock From the First Hour: Results From a Guideline-Based Performance Improvement Program. *Critical Care Medicine*. 2014;42(8).

42. Carrara M, Ferrario M, Bollen Pinto B, Herpain A. The autonomic nervous system in septic shock and its role as a future therapeutic target: a narrative review. *Ann Intensive Care*. 2021;11:80. doi:10.1186/s13613-021-00869-7

43. Boldt J, Menges T, Kuhn D, Diridis C, Hempelmann G. Alterations in circulating vasoactive substances in the critically ill —a comparison between survivors and non-survivors. *Intensive Care Med*. 1995;21(3):218-225. doi:10.1007/BF01701475

44. Dünser MW, Hasibeder WR. Sympathetic Overstimulation During Critical Illness: Adverse Effects of Adrenergic Stress. *J Intensive Care Med*. 2009;24(5):293-316. doi:10.1177/0885066609340519

45. Suzuki T, Suzuki Y, Okuda J, et al. Sepsis-induced cardiac dysfunction and β-adrenergic blockade therapy for sepsis. *J Intensive Care*. 2017;5:22. doi:10.1186/s40560-017-0215-2

46. Carrara M, Bollen Pinto B, Baselli G, Bendjelid K, Ferrario M. Baroreflex Sensitivity and Blood Pressure Variability can Help in Understanding the Different Response to Therapy During Acute Phase of Septic Shock. *Shock*. 2018;50(1):78-86. doi:10.1097/SHK.0000000000001046

47. Lu YC, Yeh WC, Ohashi PS. LPS/TLR4 signal transduction pathway. *Cytokine*. 2008;42(2):145-151. doi:10.1016/j.cyto.2008.01.006

48. Pålsson-McDermott EM, O'Neill LAJ. Signal transduction by the lipopolysaccharide receptor, Toll-like receptor-4. *Immunology*. 2004;113(2):153-162. doi:10.1111/j.1365-2567.2004.01976.x

49. CHAUDHRY H, ZHOU J, ZHONG Y, et al. Role of Cytokines as a Double-edged Sword in Sepsis. *In Vivo*. 2013;27(6):669-684.

50. Liu YC, Yu MM, Shou ST, Chai YF. Sepsis-Induced Cardiomyopathy: Mechanisms and Treatments. *Frontiers in Immunology*. 2017;8. Accessed July 18, 2023. https://www.frontiersin.org/articles/10.3389/fimmu.2017.01021

51. Denning NL, Aziz M, Gurien SD, Wang P. DAMPs and NETs in Sepsis. *Frontiers in Immunology*. 2019;10. Accessed July 21, 2023. https://www.frontiersin.org/articles/10.3389/fimmu.2019.02536

52. Cox LE, Walstein K, Völlger L, et al. Neutrophil extracellular trap formation and nuclease activity in septic patients. *BMC Anesthesiol*. 2020;20(1):15. doi:10.1186/s12871-019-0911-7

53. Diamond CE, Khameneh HJ, Brough D, Mortellaro A. Novel perspectives on non-canonical inflammasome activation. *Immunotargets Ther*. 2015;4:131-141. doi:10.2147/ITT.S57976

54. Sankowski R, Mader S, Valdés-Ferrer SI. Systemic Inflammation and the Brain: Novel Roles of Genetic, Molecular, and Environmental Cues as Drivers of Neurodegeneration. *Front Cell Neurosci*. 2015;9:28. doi:10.3389/fncel.2015.00028

55. Bourhy L, Mazeraud A, Bozza FA, Turc G, Lledo PM, Sharshar T. Neuro-Inflammatory Response and Brain-Peripheral Crosstalk in Sepsis and Stroke. *Front Immunol*. 2022;13:834649. doi:10.3389/fimmu.2022.834649

56. Dantzer R, O'Connor JC, Freund GG, Johnson RW, Kelley KW. From inflammation to sickness and depression: when the immune system subjugates the brain. *Nat Rev Neurosci*. 2008;9(1):46-56. doi:10.1038/nrn2297

57. Akrout N, Sharshar T, Annane D. Mechanisms of Brain Signaling During Sepsis. *Curr Neuropharmacol*. 2009;7(4):296-301. doi:10.2174/157015909790031175

58. McCANN SM, Kimura M, Karanth S, Yu WH, Mastronardi CA, Rettori V. The Mechanism of Action of Cytokines to Control the Release of Hypothalamic and Pituitary Hormones in Infection. *Annals of the New York Academy of Sciences*. 2000;917(1):4-18. doi:10.1111/j.1749-6632.2000.tb05368.x

59. Benfante R, Di Lascio S, Cardani S, Fornasari D. Acetylcholinesterase inhibitors targeting the cholinergic anti-inflammatory pathway: a new therapeutic perspective in aging-related disorders. *Aging Clinical and Experimental Research*. 2021;33. doi:10.1007/s40520-019-01359-4

60. Berthoud HR, Neuhuber WL. Functional and chemical anatomy of the afferent vagal system. *Auton Neurosci*. 2000;85(1-3):1-17. doi:10.1016/S1566-0702(00)00215-0

61. Bonaz B, Sinniger V, Pellissier S. The Vagus Nerve in the Neuro-Immune Axis: Implications in the Pathology of the Gastrointestinal Tract. *Frontiers in Immunology*. 2017;8. Accessed April 30, 2023. https://www.frontiersin.org/articles/10.3389/fimmu.2017.01452

62. Wang H, Liao H, Ochani M, et al. Cholinergic agonists inhibit HMGB1 release and improve survival in experimental sepsis. *Nat Med*. 2004;10(11):1216-1221. doi:10.1038/nm1124

63. Kelly MJ, Breathnach C, Tracey KJ, Donnelly SC. Manipulation of the inflammatory reflex as a therapeutic strategy. *Cell Reports Medicine*. 2022;3(7):100696. doi:10.1016/j.xcrm.2022.100696

64. Sekino N, Selim M, Shehadah A. Sepsis-associated brain injury: underlying mechanisms and potential therapeutic strategies for acute and long-term cognitive impairments. *Journal of Neuroinflammation*. 2022;19(1):101. doi:10.1186/s12974-022-02464-4

65. Laflamme N, Echchannaoui H, Landmann R, Rivest S. Cooperation between toll-like receptor 2 and 4 in the brain of mice challenged with cell wall components derived from gram-negative and gram-positive bacteria. *European Journal of Immunology*. 2003;33(4):1127-1138. doi:10.1002/eji.200323821

66. Yan X, Yang K, Xiao Q, Hou R, Pan X, Zhu X. Central role of microglia in sepsis-associated encephalopathy: From mechanism to therapy. *Front Immunol*. 2022;13:929316. doi:10.3389/fimmu.2022.929316

67. Daneman R, Prat A. The Blood–Brain Barrier. *Cold Spring Harb Perspect Biol*. 2015;7(1):a020412. doi:10.1101/cshperspect.a020412

68. Erikson K, Tuominen H, Vakkala M, et al. Brain tight junction protein expression in sepsis in an autopsy series. *Crit Care*. 2020;24(1):385. doi:10.1186/s13054-020-03101-3

69. Towner RA, Saunders D, Smith N, et al. Assessing long-term neuroinflammatory responses to encephalopathy using MRI approaches in a rat endotoxemia model. *GeroScience*. 2018;40(1):49-60. doi:10.1007/s11357-018-0009-z

70. Osellame LD, Blacker TS, Duchen MR. Cellular and molecular mechanisms of mitochondrial function. *Best Practice & Research Clinical Endocrinology & Metabolism*. 2012;26(6):711-723. doi:10.1016/j.beem.2012.05.003

71. Brand MD, Orr AL, Perevoshchikova IV, Quinlan CL. The role of mitochondrial function and cellular bioenergetics in ageing and disease: Mitochondrial function in ageing and disease. *Br J Dermatol*. 2013;169:1-8. doi:10.1111/bjd.12208

72. Garrabou G, Morén C, López S, et al. The Effects of Sepsis on Mitochondria. *The Journal of Infectious Diseases*. 2012;205(3):392-400. doi:10.1093/infdis/jir764

73. Schwartz DR, Malhtora A, Fink MP. Cytopathic Hypoxia in Sepsis: An Overview. *Sepsis*. 1999;2(4):279-289. doi:10.1023/A:1009830318674

74. Yan C, Ma Z, Ma H, et al. Mitochondrial Transplantation Attenuates Brain Dysfunction in Sepsis by Driving Microglial M2 Polarization. *Mol Neurobiol*. 2020;57(9):3875-3890. doi:10.1007/s12035-020-01994-3

75. Manfredini A, Constantino L, Pinto MC, et al. Mitochondrial dysfunction is associated with long-term cognitive impairment in an animal sepsis model. *Clinical Science*. 2019;133(18):1993-2004. doi:10.1042/CS20190351

76. Tsuruta R, Oda Y. A clinical perspective of sepsis-associated delirium. *Journal of Intensive Care*. 2016;4(1):18. doi:10.1186/s40560-016-0145-4

77. Bozza FA, Garteiser P, Oliveira MF, et al. Sepsis-associated encephalopathy: a magnetic resonance imaging and spectroscopy study. *J Cereb Blood Flow Metab*. 2010;30(2):440-448. doi:10.1038/jcbfm.2009.215

78. Pantzaris ND, Platanaki C, Tsiotsios K, Koniari I, Velissaris D. The use of electroencephalography in patients with sepsis: A review of the literature. *Journal of Translational Internal Medicine*. 2021;0(0):000010247820210007. doi:10.2478/jtim-2021-0007

79. Oddo M, Carrera E, Claassen J, Mayer SA, Hirsch LJ. Continuous electroencephalography in the medical intensive care unit*: *Critical Care Medicine*. 2009;37(6):2051-2056. doi:10.1097/CCM.0b013e3181a00604

80. Alessandri F, Badenes R, Bilotta F. Seizures and Sepsis: A Narrative Review. *J Clin Med*. 2021;10(5):1041. doi:10.3390/jcm10051041

81. Azabou E, Magalhaes E, Braconnier A, et al. Early Standard Electroencephalogram Abnormalities Predict Mortality in Septic Intensive Care Unit Patients. *PLoS One*. 2015;10(10):e0139969. doi:10.1371/journal.pone.0139969

82. Gilmore EJ, Gaspard N, Choi HA, et al. Acute brain failure in severe sepsis: a prospective study in the medical intensive care unit utilizing continuous EEG monitoring. *Intensive Care Med*. 2015;41(4):686-694. doi:10.1007/s00134-015-3709-1

83. Telias I, Wilcox ME. Sleep and Circadian Rhythm in Critical Illness. *Critical Care*. 2019;23(1):82. doi:10.1186/s13054-019-2366-0

84. Jung S, Kim J, Lee J, Rhee C, Na S, Yoon JH. Assessment of Noise Exposure and Its Characteristics in the Intensive Care Unit of a Tertiary Hospital. *Int J Environ Res Public Health*. 2020;17(13):4670. doi:10.3390/ijerph17134670

85. Baracchi F, Ingiosi AM, Raymond RM, Opp MR. Sepsis-induced alterations in sleep of rats. *Am J Physiol Regul Integr Comp Physiol*. 2011;301(5):R1467-1478. doi:10.1152/ajpregu.00354.2011

86. Sewal RK, Modi M, Saikia UN, Chakrabarti A, Medhi B. Increase in seizure susceptibility in sepsis like condition explained by spiking cytokines and altered adhesion molecules level with impaired blood brain barrier integrity in experimental model of rats treated with lipopolysaccharides. *Epilepsy Research*. 2017;135:176-186. doi:10.1016/j.eplepsyres.2017.05.012

87. Orihuela CJ, Fillon S, Smith-Sielicki SH, et al. Cell Wall-Mediated Neuronal Damage in Early Sepsis. *Infection and Immunity*. 2006;74(7):3783-3789. doi:10.1128/iai.00022-06

88. Annane D. Hippocampus: a future target for sepsis treatment! *Intensive Care Med*. 2009;35(4):585-586. doi:10.1007/s00134-009-1395-6

89. Alexandre PC, Reis PA, D`Ávila J, et al. Atorvastatin and simvastatin protects cognitive impairment in an animal model of sepsis. *Critical Care*. 2013;17(4):P108. doi:10.1186/cc13007

90. Gamal M, Moawad J, Rashed L, et al. Evaluation of the effects of Eserine and JWH-133 on brain dysfunction associated with experimental endotoxemia. *Journal of Neuroimmunology*. 2015;281:9-16. doi:10.1016/j.jneuroim.2015.02.008

91. Goodwin AJ, Ford DW. Readmissions Among Sepsis Survivors: Risk Factors and Prevention. *Clin Pulm Med*. 2018;25(3):79-83. doi:10.1097/CPM.0000000000000254

92. van der Slikke EC, An AY, Hancock REW, Bouma HR. Exploring the pathophysiology of post-sepsis syndrome to identify therapeutic opportunities. *EBioMedicine*. 2020;61:103044. doi:10.1016/j.ebiom.2020.103044

93. Li Y, Ji M, Yang J. Current Understanding of Long-Term Cognitive Impairment After Sepsis. *Front Immunol*. 2022;13:855006. doi:10.3389/fimmu.2022.855006

94. Bourhy L, Mazeraud A, Costa LHA, et al. Silencing of amygdala circuits during sepsis prevents the development of anxiety-related behaviours. *Brain*. 2022;145(4):1391-1409. doi:10.1093/brain/awab475

95. Seidel G, Gaser C, Götz T, Günther A, Hamzei F. Accelerated brain ageing in sepsis survivors with cognitive long-term impairment. *European Journal of Neuroscience*. 2020;52(10):4395-4402. doi:10.1111/ejn.14850

96. Semmler A, Frisch C, Debeir T, et al. Long-term cognitive impairment, neuronal loss and reduced cortical cholinergic innervation after recovery from sepsis in a rodent model. *Experimental Neurology*. 2007;204(2):733-740. doi:10.1016/j.expneurol.2007.01.003

97. Basak JM, Ferreiro A, Cohen LS, et al. Bacterial sepsis increases hippocampal fibrillar amyloid plaque load and neuroinflammation in a mouse model of Alzheimer's disease. *Neurobiology of Disease*. 2021;152:105292. doi:10.1016/j.nbd.2021.105292

98. Kirk RA, Kesner RP, Wang LM, et al. Lipopolysaccharide exposure in a rat sepsis model results in hippocampal amyloid-β plaque and phosphorylated tau deposition and corresponding behavioral deficits. *GeroScience*. 2019;41(4):467-481. doi:10.1007/s11357-019-00089-9

99. Gasparotto J, Girardi CS, Somensi N, et al. Receptor for advanced glycation end products mediates sepsis-triggered amyloid-β accumulation, Tau phosphorylation, and cognitive impairment. *Journal of Biological Chemistry*. 2018;293(1):226-244. doi:10.1074/jbc.M117.786756

100. Huang CY, Daniels R, Lembo A, et al. Life after sepsis: an international survey of survivors to understand the post-sepsis syndrome. *International Journal for Quality in Health Care*. 2019;31(3):191-198. doi:10.1093/intqhc/mzy137

101. Song IA, Park HY, Oh TK. Sleep Disorder and Long-Term Mortality Among Sepsis Survivors: A Nationwide Cohort Study in South Korea. *Nature and Science of Sleep*. 2021;13:979-988. doi:10.2147/NSS.S319769

102. Lee DA, Liu J, Hong Y, et al. Evolutionarily conserved regulation of sleep by epidermal growth factor receptor signaling. *Sci Adv*. 2019;5(11):eaax4249. doi:10.1126/sciadv.aax4249

103. Everson CA, Bergmann BM, Rechtschaffen A. Sleep deprivation in the rat: III. Total sleep deprivation. *Sleep*. 1989;12(1):13-21. doi:10.1093/sleep/12.1.13

104. Campbell IG. EEG Recording and Analysis for Sleep Research. *Curr Protoc Neurosci*. 2009;CHAPTER:Unit10.2. doi:10.1002/0471142301.ns1002s49

105. Zhang J, Wang B, Zhang C, Xiao Y, Wang MY. An EEG/EMG/EOG-Based Multimodal Human-Machine Interface to Real-Time Control of a Soft Robot Hand. *Front Neurorobot*. 2019;13:7. doi:10.3389/fnbot.2019.00007

106. Huang H, Zhang J, Zhu L, et al. EEG-Based Sleep Staging Analysis with Functional Connectivity. *Sensors (Basel)*. 2021;21(6):1988. doi:10.3390/s21061988

107. Memar P, Faradji F. A Novel Multi-Class EEG-Based Sleep Stage Classification System. *IEEE Transactions on Neural Systems and Rehabilitation Engineering*. 2018;26(1):84-95. doi:10.1109/TNSRE.2017.2776149

108. Gais S, Mölle M, Helms K, Born J. Learning-Dependent Increases in Sleep Spindle Density. *J Neurosci*. 2002;22(15):6830-6834. doi:10.1523/JNEUROSCI.22-15-06830.2002

109. Carley DW, Farabi SS. Physiology of Sleep. *Diabetes Spectrum*. 2016;29(1):5-9. doi:10.2337/diaspect.29.1.5

110. Patel AK, Reddy V, Shumway KR, Araujo JF. Physiology, Sleep Stages. In: *StatPearls*. StatPearls Publishing; 2023. Accessed July 18, 2023. http://www.ncbi.nlm.nih.gov/books/NBK526132/

111. Brooks PL, Peever JH. Unraveling the Mechanisms of REM Sleep Atonia. *Sleep*. 2008;31(11):1492-1497.

112. Khan F, Aadil F. Efficient Car Alarming System for Fatigue Detection during Driving. *International Journal of Innovation, Management and Technology*. 2012;3:480. doi:10.7763/IJIMT.2012.V3.280

113. Brown RE, Basheer R, McKenna JT, Strecker RE, McCarley RW. CONTROL OF SLEEP AND WAKEFULNESS. *Physiol Rev*. 2012;92(3):1087-1187. doi:10.1152/physrev.00032.2011

114. Lindsley DB, Bowden JW, Magoun HW. Effect upon the EEG of acute injury to the brain stem activating system. *Electroencephalography and Clinical Neurophysiology*. 1949;1(1):475-486. doi:10.1016/0013-4694(49)90221-7

115. Buchanan GF, Richerson GB. Central serotonin neurons are required for arousal to CO_2. *Proc Natl Acad Sci USA*. 2010;107(37):16354-16359. doi:10.1073/pnas.1004587107

116. Grady FS, Boes AD, Geerling JC. A Century Searching for the Neurons Necessary for Wakefulness. *Frontiers in Neuroscience*. 2022;16. Accessed July 18, 2023. https://www.frontiersin.org/articles/10.3389/fnins.2022.930514

117. Tsubokawa T, Katayama Y. Active Neural Processes within the Brain Stem in Production of Coma. *Neurologia medico-chirurgica*. 1985;25(7):503-514. doi:10.2176/nmc.25.503

118. Double KL, Crocker AD. Dopamine receptors in the substantia nigra are involved in the regulation of muscle tone. *Proc Natl Acad Sci U S A*. 1995;92(5):1669-1673.

119. Hauser T, Eldar E, Dolan R. Separate mesocortical and mesolimbic pathways encode effort and reward learning signals. *Proceedings of the National Academy of Sciences*. 2017;114:201705643. doi:10.1073/pnas.1705643114

120. Kim HF, Ghazizadeh A, Hikosaka O. Separate groups of dopamine neurons innervate caudate head and tail encoding flexible and stable value memories. *Front Neuroanat*. 2014;8:120. doi:10.3389/fnana.2014.00120

121. Monti JM. Serotonin control of sleep-wake behavior. *Sleep Medicine Reviews*. 2011;15(4):269-281. doi:10.1016/j.smrv.2010.11.003

122. Eban-Rothschild A, Rothschild G, Giardino WJ, Jones JR, de Lecea L. VTA dopaminergic neurons regulate ethologically relevant sleep–wake behaviors. *Nat Neurosci*. 2016;19(10):1356-1366. doi:10.1038/nn.4377

123. Chen L, Yin D, Wang TX, et al. Basal Forebrain Cholinergic Neurons Primarily Contribute to Inhibition of Electroencephalogram Delta Activity, Rather Than Inducing Behavioral Wakefulness in Mice. *Neuropsychopharmacol*. 2016;41(8):2133-2146. doi:10.1038/npp.2016.13

124. Kaur S, Junek A, Black MA, Semba K. Effects of Ibotenate and 192IgG-Saporin Lesions of the Nucleus Basalis Magnocellularis/Substantia Innominata on Spontaneous Sleep and Wake States and on Recovery Sleep after Sleep Deprivation in Rats. *J Neurosci*. 2008;28(2):491-504. doi:10.1523/JNEUROSCI.1585-07.2008

125. Boucetta S, Cissé Y, Mainville L, Morales M, Jones BE. Discharge Profiles across the Sleep–Waking Cycle of Identified Cholinergic, GABAergic, and Glutamatergic Neurons in the Pontomesencephalic Tegmentum of the Rat. *J Neurosci*. 2014;34(13):4708-4727. doi:10.1523/JNEUROSCI.2617-13.2014

126. Anaclet C, Pedersen NP, Ferrari LL, et al. Basal forebrain control of wakefulness and cortical rhythms. *Nat Commun*. 2015;6(1):8744. doi:10.1038/ncomms9744

127. Therapeutics AS for P and E. Correction to “Behavioral characterization of mice lacking histamine H3 receptors.” *Mol Pharmacol*. 2002;62(3):763-763. doi:10.1124/mol.62.3.763

128. de Lecea L. Hypocretins and the neurobiology of sleep–wake mechanisms. *Prog Brain Res*. 2012;198:15-24. doi:10.1016/B978-0-444-59489-1.00003-3

129. Inutsuka A, Yamanaka A. The physiological role of orexin/hypocretin neurons in the regulation of sleep/wakefulness and neuroendocrine functions. *Frontiers in Endocrinology*. 2013;4. Accessed July 18, 2023. https://www.frontiersin.org/articles/10.3389/fendo.2013.00018

130. Alexandre C, Andermann ML, Scammell TE. Control of arousal by the orexin neurons. *Curr Opin Neurobiol*. 2013;23(5):752-759. doi:10.1016/j.conb.2013.04.008

131. De la Herrán-Arita AK, Guerra-Crespo M, Drucker-Colín R. Narcolepsy and Orexins: An Example of Progress in Sleep Research. *Front Neurol*. 2011;2:26. doi:10.3389/fneur.2011.00026

132. Scammell TE, Arrigoni E, Lipton J. Neural Circuitry of Wakefulness and Sleep. *Neuron*. 2017;93(4):747-765. doi:10.1016/j.neuron.2017.01.014

133. Vanini G, Lydic R, Baghdoyan HA. GABA-to-ACh Ratio in Basal Forebrain and Cerebral Cortex Varies Significantly During Sleep. *Sleep*. 2012;35(10):1325-1334. doi:10.5665/sleep.2106

134. Zhao YN, Jiang JB, Tao SY, et al. GABAergic neurons in the rostromedial tegmental nucleus are essential for rapid eye movement sleep suppression. *Nat Commun*. 2022;13:7552. doi:10.1038/s41467-022-35299-x

135. Vyazovskiy VV, Olcese U, Lazimy YM, et al. Cortical firing and sleep homeostasis. *Neuron*. 2009;63(6):865-878. doi:10.1016/j.neuron.2009.08.024

136. Sherin JE, Elmquist JK, Torrealba F, Saper CB. Innervation of Histaminergic Tuberomammillary Neurons by GABAergic and Galaninergic Neurons in the Ventrolateral Preoptic Nucleus of the Rat. *J Neurosci*. 1998;18(12):4705-4721. doi:10.1523/JNEUROSCI.18-12-04705.1998

137. Melander T, Hökfelt T, Rökaeus A. Distribution of galaninlike immunoreactivity in the rat central nervous system. *Journal of Comparative Neurology*. 1986;248(4):475-517. doi:10.1002/cne.902480404

138. Borbély A. The two-process model of sleep regulation: Beginnings and outlook†. *Journal of Sleep Research*. 2022;31(4):e13598. doi:10.1111/jsr.13598

139. Stiller J, Postolache T. Sleep-wake and Other Biological Rhythms: Functional Neuroanatomy. *Clinics in sports medicine*. 2005;24:205-235, vii. doi:10.1016/j.csm.2004.12.008

140. Achermann P. The two-process model of sleep regulation revisited. *Aviat Space Environ Med*. 2004;75(3 Suppl):A37-43.

141. Vibha D, Shukla G. Two-Process Model of Sleep. *Indian Journal of Sleep Medicine*. 2014;9(3):91-95. doi:10.5958/0974-0155.2014.01108.5

142. Perelis M, Ramsey KM, Bass J. THE MOLECULAR CLOCK AS A METABOLIC RHEOSTAT. *Diabetes Obes Metab*. 2015;17(0 1):99-105. doi:10.1111/dom.12521

143. Waterhouse J, Fukuda Y, Morita T. Daily rhythms of the sleep-wake cycle. *Journal of Physiological Anthropology*. 2012;31(1):5. doi:10.1186/1880-6805-31-5

144. Easton A, Meerlo P, Bergmann B, Turek FW. The Suprachiasmatic Nucleus Regulates Sleep Timing and Amount in Mice. *Sleep*. 2004;27(7):1307-1318. doi:10.1093/sleep/27.7.1307

145. Kalsbeek A, Palm IF, La Fleur SE, et al. SCN outputs and the hypothalamic balance of life. *J Biol Rhythms*. 2006;21(6):458-469. doi:10.1177/0748730406293854

146. Reghunandanan V, Reghunandanan R. Neurotransmitters of the suprachiasmatic nuclei. *J Circadian Rhythms*. 2006;4:2. doi:10.1186/1740-3391-4-2

147. Welsh DK, Takahashi JS, Kay SA. Suprachiasmatic Nucleus: Cell Autonomy and Network Properties. *Annu Rev Physiol*. 2010;72:551-577. doi:10.1146/annurev-physiol-021909-135919

148. Ramkisoensing A, Meijer JH. Synchronization of Biological Clock Neurons by Light and Peripheral Feedback Systems Promotes Circadian Rhythms and Health. *Front Neurol*. 2015;6:128. doi:10.3389/fneur.2015.00128

149. Jessen NA, Munk ASF, Lundgaard I, Nedergaard M. The Glymphatic System – A Beginner's Guide. *Neurochem Res*. 2015;40(12):2583-2599. doi:10.1007/s11064-015-1581-6

150. Kaur J, Fahmy LM, Davoodi-Bojd E, et al. Waste Clearance in the Brain. *Frontiers in Neuroanatomy*. 2021;15. Accessed June 11, 2023. https://www.frontiersin.org/articles/10.3389/fnana.2021.665803

151. Louveau A, Plog BA, Antila S, Alitalo K, Nedergaard M, Kipnis J. Understanding the functions and relationships of the glymphatic system and meningeal lymphatics. *J Clin Invest*. 2017;127(9):3210-3219. doi:10.1172/JCI90603

152. Plog BA, Nedergaard M. The Glymphatic System in Central Nervous System Health and Disease: Past, Present, and Future. *Annual Review of Pathology: Mechanisms of Disease*. 2018;13(1):379-394. doi:10.1146/annurev-pathol-051217-111018

153. Iliff JJ, Wang M, Liao Y, et al. A paravascular pathway facilitates CSF flow through the brain parenchyma and the clearance of interstitial solutes, including amyloid β. *Science Translational Medicine*. 2012;4(147). doi:10.1126/scitranslmed.3003748

154. Reddy OC, van der Werf YD. The Sleeping Brain: Harnessing the Power of the Glymphatic System through Lifestyle Choices. *Brain Sci*. 2020;10(11):868. doi:10.3390/brainsci10110868

155. Reeves BC, Karimy JK, Kundishora AJ, et al. Glymphatic System Impairment in Alzheimer's Disease and Idiopathic Normal Pressure Hydrocephalus. *Trends Mol Med*. 2020;26(3):285-295. doi:10.1016/j.molmed.2019.11.008

156. Vasciaveo V, Iadarola A, Casile A, et al. Sleep fragmentation affects glymphatic system through the different expression of AQP4 in wild type and 5xFAD mouse models.

Acta Neuropathologica Communications. 2023;11(1):16. doi:10.1186/s40478-022-01498-2

157. Hinkerohe D, Smikalla D, Schoebel A, et al. Dexamethasone prevents LPS-induced microglial activation and astroglial impairment in an experimental bacterial meningitis co-culture model. *Brain Research*. 2010;1329:45-54. doi:10.1016/j.brainres.2010.03.012

158. Jha MK, Kim JH, Song GJ, et al. Functional dissection of astrocyte-secreted proteins: Implications in brain health and diseases. *Progress in Neurobiology*. 2018;162:37-69. doi:10.1016/j.pneurobio.2017.12.003

159. Ren X, Liu S, Lian C, et al. Dysfunction of the Glymphatic System as a Potential Mechanism of Perioperative Neurocognitive Disorders. *Frontiers in Aging Neuroscience*. 2021;13. Accessed June 11, 2023. https://www.frontiersin.org/articles/10.3389/fnagi.2021.659457

160. Dijk DJ, Landolt HP. Sleep Physiology, Circadian Rhythms, Waking Performance and the Development of Sleep-Wake Therapeutics. In: Landolt HP, Dijk DJ, eds. *Sleep-Wake Neurobiology and Pharmacology*. Handbook of Experimental Pharmacology. Springer International Publishing; 2019:441-481. doi:10.1007/164_2019_243

161. Kong N, Choi J, Seo WS. Evaluation of Sleep Problems or Disorders Using Sleep Questionnaires. *Chronobiol Med*. 2019;1(4):144-148. doi:10.33069/cim.2019.0028

162. Chokroverty S. Overview of sleep & sleep disorders. *SLEEP DISORDERS*. Published online 2010.

163. Sankri-Tarbichi AG. Obstructive sleep apnea-hypopnea syndrome: Etiology and diagnosis. *Avicenna J Med*. 2012;02(01):3-8. doi:10.4103/2231-0770.94803

164. Schwab RJ, Gupta KB, Gefter WB, Metzger LJ, Hoffman EA, Pack AI. Upper airway and soft tissue anatomy in normal subjects and patients with sleep-disordered breathing. Significance of the lateral pharyngeal walls. *Am J Respir Crit Care Med*. 1995;152(5):1673-1689. doi:10.1164/ajrccm.152.5.7582313

165. Lin CM, Davidson TM, Ancoli-Israel S. Gender Differences in Obstructive Sleep Apnea and Treatment Implications. *Sleep Med Rev*. 2008;12(6):481-496. doi:10.1016/j.smrv.2007.11.003

166. Johns MW. A New Method for Measuring Daytime Sleepiness: The Epworth Sleepiness Scale. *Sleep*. 1991;14(6):540-545. doi:10.1093/sleep/14.6.540

167. Steward KA, Silva MA, Maduri P, et al. Obstructive sleep apnea is associated with worse cognitive outcomes in acute moderate-to-severe traumatic brain injury: A TBI Model Systems study. *Sleep Medicine*. 2022;100:454-461. doi:10.1016/j.sleep.2022.09.012

168. O'Donoghue FJ, Wellard RM, Rochford PD, et al. Magnetic Resonance Spectroscopy and Neurocognitive Dysfunction in Obstructive Sleep Apnea before and after CPAP Treatment. *Sleep*. 2012;35(1):41-48. doi:10.5665/sleep.1582

169. Chavda V, Chaurasia B, Umana GE, Tomasi SO, Lu B, Montemurro N. Narcolepsy—A Neuropathological Obscure Sleep Disorder: A Narrative Review of Current Literature. *Brain Sciences*. 2022;12(11):1473. doi:10.3390/brainsci12111473

170. Frauscher B, Ehrmann L, Mitterling T, et al. Delayed Diagnosis, Range of Severity, and Multiple Sleep Comorbidities: A Clinical and Polysomnographic Analysis of 100 Patients of the Innsbruck Narcolepsy Cohort. *J Clin Sleep Med*. 2013;9(8):805-812. doi:10.5664/jcsm.2926

171. Siegel JM, Boehmer LN. Narcolepsy and the hypocretin system—where motion meets emotion. *Nat Clin Pract Neurol*. 2006;2(10):548-556. doi:10.1038/ncpneuro0300

172. Roth T, Dauvilliers Y, Mignot E, et al. Disrupted Nighttime Sleep in Narcolepsy. *Journal of Clinical Sleep Medicine*. 09(09):955-965. doi:10.5664/jcsm.3004

173. Dauvilliers Y, Arnulf I, Mignot E. Narcolepsy with cataplexy. *Lancet*. 2007;369(9560):499-511. doi:10.1016/S0140-6736(07)60237-2

174. Wise MS, Arand DL, Auger RR, Brooks SN, Watson NF. Treatment of Narcolepsy and other Hypersomnias of Central Origin. *Sleep*. 2007;30(12):1712-1727.

175. Bonnet MH, Arand DL. Hyperarousal and insomnia. *Sleep Medicine Reviews*. 1997;1(2):97-108. doi:10.1016/S1087-0792(97)90012-5

176. Finan PH, Smith MT. The comorbidity of insomnia, chronic pain, and depression: Dopamine as a putative mechanism. *Sleep Medicine Reviews*. 2013;17(3):173-183. doi:10.1016/j.smrv.2012.03.003

177. Basta M, Chrousos GP, Vela-Bueno A, Vgontzas AN. Chronic Insomnia and the Stress System. *Sleep Medicine Clinics*. 2007;2(2):279-291. doi:10.1016/j.jsmc.2007.04.002

178. Harvey AG. INSOMNIA: SYMPTOM OR DIAGNOSIS? *Clinical Psychology Review*. 2001;21(7):1037-1059. doi:10.1016/S0272-7358(00)00083-0

179. Nofzinger EA, Buysse DJ, Germain A, Price JC, Miewald JM, Kupfer DJ. Functional neuroimaging evidence for hyperarousal in insomnia. *Am J Psychiatry*. 2004;161(11):2126-2128. doi:10.1176/appi.ajp.161.11.2126

180. Riemann D, Spiegelhalder K, Feige B, et al. The hyperarousal model of insomnia: a review of the concept and its evidence. *Sleep Med Rev*. 2010;14(1):19-31. doi:10.1016/j.smrv.2009.04.002

181. Fu M, Zhu Y, Gong Z, et al. Benzodiazepine Receptor Agonists Prescribing for Insomnia Among Adults in Primary Health Care Facilities in Beijing, China. *JAMA Netw Open*. 2023;6(2):e230044. doi:10.1001/jamanetworkopen.2023.0044

182. Ibarra-Coronado EG, Pantaleón-Martínez AM, Velazquéz-Moctezuma J, et al. The Bidirectional Relationship between Sleep and Immunity against Infections. *J Immunol Res*. 2015;2015:678164. doi:10.1155/2015/678164

183. Shoham S, Davenne D, Cady AB, Dinarello CA, Krueger JM. Recombinant tumor necrosis factor and interleukin 1 enhance slow-wave sleep. *American Journal of Physiology-Regulatory, Integrative and Comparative Physiology*. 1987;253(1):R142-R149. doi:10.1152/ajpregu.1987.253.1.R142

184. Amin MN, Siddiqui SA, Ibrahim M, et al. Inflammatory cytokines in the pathogenesis of cardiovascular disease and cancer. *SAGE Open Med*. 2020;8:2050312120965752. doi:10.1177/2050312120965752

185. Freedman NS, Gazendam J, Levan L, Pack AI, Schwab RJ. Abnormal Sleep/Wake Cycles and the Effect of Environmental Noise on Sleep Disruption in the Intensive Care Unit. *Am J Respir Crit Care Med*. 2001;163(2):451-457. doi:10.1164/ajrccm.163.2.9912128

186. Mistraletti G, Carloni E, Cigada M, et al. Sleep and delirium in the Intensive Care Unit. *MINERVA ANESTESIOLOGICA*. 2008;74(6).

187. Young GB, Bolton CF, Archibald YM, Austin TW, Wells GA. The electroencephalogram in sepsis-associated encephalopathy. *J Clin Neurophysiol*. 1992;9(1):145-152. doi:10.1097/00004691-199201000-00016

188. Weinhouse GL, Schwab RJ. Sleep in the Critically ill Patient. *Sleep*. 2006;29(5):707-716. doi:10.1093/sleep/29.5.707

189. Gabor JY, Cooper AB, Crombach SA, et al. Contribution of the Intensive Care Unit Environment to Sleep Disruption in Mechanically Ventilated Patients and Healthy Subjects. *Am J Respir Crit Care Med*. 2003;167(5):708-715. doi:10.1164/rccm.2201090

190. Roth T, Kramer M, Trinder J. The Effect of Noise during Sleep on the Sleep Patterns of Different Age Groups. *Canadian Psychiatric Association Journal*. 1972;17(6_suppl2):197-201. doi:10.1177/07067437720176S231

191. Bourne RS, Mills GH. Melatonin: possible implications for the postoperative and critically ill patient. *Intensive Care Med*. 2006;32(3):371-379. doi:10.1007/s00134-005-0061-x

192. Ingiosi AM, Opp MR. Sleep and immunomodulatory responses to systemic lipopolysaccharide in mice selectively expressing interleukin-1 receptor 1 on neurons or astrocytes. *Glia*. 2016;64(5):780-791. doi:10.1002/glia.22961

193. Lancel M, Cronlein J, Muller-Preuss P, Holsboer F. Lipopolysaccharide increases EEG delta activity within non-REM sleep and disrupts sleep continuity in rats. *American Journal of Physiology-Regulatory, Integrative and Comparative Physiology*. 1995;268(5):R1310-R1318. doi:10.1152/ajpregu.1995.268.5.R1310

194. Barichello T, Sayana P, Giridharan VV, et al. Long-Term Cognitive Outcomes After Sepsis: a Translational Systematic Review. *Mol Neurobiol*. 2019;56(1):186-251. doi:10.1007/s12035-018-1048-2

195. Comim CM, Constantino LS, Petronilho F, Quevedo J, Dal-Pizzol F. Aversive memory in sepsis survivor rats. *J Neural Transm*. 2011;118(2):213-217. doi:10.1007/s00702-010-0502-8

196. McGaugh JL. The perseveration-consolidation hypothesis: Mueller and Pilzecker, 1900. *Brain Research Bulletin*. 1999;50(5-6):445-446. doi:10.1016/S0361-9230(99)00126-4

197. McGaugh JL. Memory--a Century of Consolidation. *Science*. 2000;287(5451):248-251. doi:10.1126/science.287.5451.248

198. Lømo T. The discovery of long-term potentiation. *Philos Trans R Soc Lond B Biol Sci*. 2003;358(1432):617-620. doi:10.1098/rstb.2002.1226

199. Mascetti L, Foret A, Schrouff J, et al. Concurrent Synaptic and Systems Memory Consolidation during Sleep. *Journal of Neuroscience*. 2013;33(24):10182-10190. doi:10.1523/JNEUROSCI.0284-13.2013

200. Tononi G, Cirelli C. Sleep and the Price of Plasticity: From Synaptic and Cellular Homeostasis to Memory Consolidation and Integration. *Neuron*. 2014;81(1):12-34. doi:10.1016/j.neuron.2013.12.025

201. Jenkins JG, Dallenbach KM. Obliviscence during Sleep and Waking. *The American Journal of Psychology*. 1924;35(4):605-612. doi:10.2307/1414040

202. Eriksen CW, Johnson HJ. Storage and decay characteristics of nonattended auditory stimuli. *Journal of Experimental Psychology*. 1964;68(1):28-36. doi:10.1037/h0048460

203. Goelet P, Castellucci VF, Schacher S, Kandel ER. The long and the short of long–term memory—a molecular framework. *Nature*. 1986;322(6078):419-422. doi:10.1038/322419a0

204. Schwartz B. *Psychology of Learning and Behavior, 3rd Ed*. W W Norton & Co; 1989:xvii, 379.

205. Barco A, Bailey CH, Kandel ER. Common molecular mechanisms in explicit and implicit memory. *Journal of Neurochemistry*. 2006;97(6):1520-1533. doi:10.1111/j.1471-4159.2006.03870.x

206. Cortina M, Liotti G. New approaches to understanding unconscious processes: Implicit and explicit memory systems. *International Forum of Psychoanalysis*. 2007;16(4):204-212. doi:10.1080/08037060701676326

207. Robbins SE. The COST of explicit memory. *Phenom Cogn Sci*. 2009;8(1):33-66. doi:10.1007/s11097-008-9088-0

208. Thompson RF, Kim JJ. Memory systems in the brain and localization of a memory. *Proceedings of the National Academy of Sciences*. 1996;93(24):13438-13444. doi:10.1073/pnas.93.24.13438

209. Duff MC, Covington NV, Hilverman C, Cohen NJ. Semantic Memory and the Hippocampus: Revisiting, Reaffirming, and Extending the Reach of Their Critical Relationship. *Frontiers in Human Neuroscience*. 2020;13. Accessed July 20, 2023. https://www.frontiersin.org/articles/10.3389/fnhum.2019.00471

210. Schacter DL, Chiu CYP, Ochsner KN. Implicit Memory: A Selective Review. *Annual Review of Neuroscience*. 1993;16(1):159-182. doi:10.1146/annurev.ne.16.030193.001111

211. Schott BH, Henson RN, Richardson-Klavehn A, et al. Redefining implicit and explicit memory: The functional neuroanatomy of priming, remembering, and control of retrieval. *Proceedings of the National Academy of Sciences*. 2005;102(4):1257-1262. doi:10.1073/pnas.0409070102

212. Pritz C, Itskovits E, Bokman E, et al. Principles for coding associative memories in a compact neural network. Iino Y, Behrens TE, eds. *eLife*. 2023;12:e74434. doi:10.7554/eLife.74434

213. Thorwart A, Livesey EJ. Three Ways That Non-associative Knowledge May Affect Associative Learning Processes. *Frontiers in Psychology*. 2016;7. Accessed July 21, 2023. https://www.frontiersin.org/articles/10.3389/fpsyg.2016.02024

214. Mochizuki-Kawai H. [Neural basis of procedural memory]. *Brain Nerve*. 2008;60(7):825-832.

215. Winocur G, Moscovitch M. Memory Transformation and Systems Consolidation. *Journal of the International Neuropsychological Society*. 2011;17(5):766-780. doi:10.1017/S1355617711000683

216. Eichenbaum H. The hippocampus and declarative memory: cognitive mechanisms and neural codes. *Behavioural Brain Research*. 2001;127(1):199-207. doi:10.1016/S0166-4328(01)00365-5

217. Ebbinghaus (1885) H. Memory: A Contribution to Experimental Psychology. *Ann Neurosci*. 2013;20(4):155-156. doi:10.5214/ans.0972.7531.200408

218. Klinzing JG, Niethard N, Born J. Mechanisms of systems memory consolidation during sleep. *Nat Neurosci*. 2019;22(10):1598-1610. doi:10.1038/s41593-019-0467-3

219. Pereira SIR, Lewis PA. The differing roles of NREM and REM sleep in the slow enhancement of skills and schemas. *Current Opinion in Physiology*. 2020;15:82-88. doi:10.1016/j.cophys.2019.12.005

220. Siegel JM. The REM Sleep–Memory Consolidation Hypothesis. *Science*. 2001;294(5544):1058-1063. doi:10.1126/science.1063049

221. Bendor D, Wilson MA. Biasing the content of hippocampal replay during sleep. *Nat Neurosci*. 2012;15(10):1439-1444. doi:10.1038/nn.3203

222. Runge K, Cardoso C, de Chevigny A. Dendritic Spine Plasticity: Function and Mechanisms. *Frontiers in Synaptic Neuroscience*. 2020;12. Accessed July 19, 2023. https://www.frontiersin.org/articles/10.3389/fnsyn.2020.00036

223. Squire LR, Genzel L, Wixted JT, Morris RG. Memory Consolidation. *Cold Spring Harb Perspect Biol*. 2015;7(8):a021766. doi:10.1101/cshperspect.a021766

224. Jiang X, Shamie I, K. Doyle W, et al. Replay of large-scale spatio-temporal patterns from waking during subsequent NREM sleep in human cortex. *Sci Rep*. 2017;7:17380. doi:10.1038/s41598-017-17469-w

225. Vaz AP, Wittig JH, Inati SK, Zaghloul KA. Replay of cortical spiking sequences during human memory retrieval. *Science*. 2020;367(6482):1131-1134. doi:10.1126/science.aba0672

226. Nadel L, Samsonovich A, Ryan L, Moscovitch M. Multiple trace theory of human memory: computational, neuroimaging, and neuropsychological results. *Hippocampus*. 2000;10(4):352-368. doi:10.1002/1098-1063(2000)10:4<352::AID-HIPO2>3.0.CO;2-D

227. Yassa M, Reagh Z. Competitive Trace Theory: A Role for the Hippocampus in Contextual Interference during Retrieval. *Frontiers in behavioral neuroscience*. 2013;7:107. doi:10.3389/fnbeh.2013.00107

228. Hirano M, Noguchi K. Dissociation between Specific Personal Episodes and other Aspects of Remote Memory in a Patient with Hippocampal Amnesia. *Percept Mot Skills*. 1998;87(1):99-107. doi:10.2466/pms.1998.87.1.99

229. Reagh ZM, Yassa MA. Repetition strengthens target recognition but impairs similar lure discrimination: evidence for trace competition. *Learn Mem*. 2014;21(7):342-346. doi:10.1101/lm.034546.114

230. Karni A, Tanne D, Rubenstein BS, Askenasy JJM, Sagi D. Dependence on REM Sleep of Overnight Improvement of a Perceptual Skill. *Science*. 1994;265(5172):679-682. doi:10.1126/science.8036518

231. Karni A, Sagi D. The time course of learning a visual skill. *Nature*. 1993;365(6443):250-252. doi:10.1038/365250a0

232. Weiss JT, Donlea JM. Roles for Sleep in Neural and Behavioral Plasticity: Reviewing Variation in the Consequences of Sleep Loss. *Front Behav Neurosci*. 2022;15:777799. doi:10.3389/fnbeh.2021.777799

233. Medic G, Wille M, Hemels ME. Short- and long-term health consequences of sleep disruption. *Nature and Science of Sleep*. 2017;9:151-161. doi:10.2147/NSS.S134864

234. Short MA, Banks S. The Functional Impact of Sleep Deprivation, Sleep Restriction, and Sleep Fragmentation. In: Bianchi MT, ed. *Sleep Deprivation and Disease*. Springer New York; 2014:13-26. doi:10.1007/978-1-4614-9087-6_2

235. Habeck C, Rakitin BC, Moeller J, et al. An event-related fMRI study of the neurobehavioral impact of sleep deprivation on performance of a delayed-match-to-sample task. *Cognitive Brain Research*. 2004;18(3):306-321. doi:10.1016/j.cogbrainres.2003.10.019

236. Lythe KE, Williams SCR, Anderson C, Libri V, Mehta MA. Frontal and parietal activity after sleep deprivation is dependent on task difficulty and can be predicted by the fMRI response after normal sleep. *Behavioural Brain Research*. 2012;233(1):62-70. doi:10.1016/j.bbr.2012.04.050

237. Dai C, Zhang Y, Cai X, et al. Effects of Sleep Deprivation on Working Memory: Change in Functional Connectivity Between the Dorsal Attention, Default Mode, and Fronto-Parietal Networks. *Front Hum Neurosci*. 2020;14:360. doi:10.3389/fnhum.2020.00360

238. Csipo T, Lipecz A, Owens C, et al. Sleep deprivation impairs cognitive performance, alters task-associated cerebral blood flow and decreases cortical neurovascular coupling-related hemodynamic responses. *Sci Rep*. 2021;11(1):20994. doi:10.1038/s41598-021-00188-8

239. Havekes R, Park AJ, Tudor JC, et al. Sleep deprivation causes memory deficits by negatively impacting neuronal connectivity in hippocampal area CA1. *Elife*. 2016;5:e13424. doi:10.7554/eLife.13424

240. Newbury CR, Crowley R, Rastle K, Tamminen J. Sleep Deprivation and Memory: Meta-Analytic Reviews of Studies on Sleep Deprivation Before and After Learning. *Psychol Bull*. 2021;147(11):1215-1240. doi:10.1037/bul0000348

241. Benkirane O, Delwiche B, Mairesse O, Peigneux P. Impact of Sleep Fragmentation on Cognition and Fatigue. *IJERPH*. 2022;19(23):15485. doi:10.3390/ijerph192315485

242. Lee ML, Katsuyama ÂM, Duge LS, et al. Fragmentation of Rapid Eye Movement and Nonrapid Eye Movement Sleep without Total Sleep Loss Impairs Hippocampus-Dependent Fear Memory Consolidation. *Sleep*. 2016;39(11):2021-2031. doi:10.5665/sleep.6236

243. Ward CP, McCoy JG, McKenna JT, Connolly NP, McCarley RW, Strecker RE. Spatial learning and memory deficits following exposure to 24 h of sleep fragmentation or intermittent hypoxia in a rat model of obstructive sleep apnea. *Brain Research*. 2009;1294:128-137. doi:10.1016/j.brainres.2009.07.064

244. Whitmore NW, Bassard AM, Paller KA. Targeted memory reactivation of face-name learning depends on ample and undisturbed slow-wave sleep. *npj Sci Learn*. 2022;7(1):1. doi:10.1038/s41539-021-00119-2

245. Whitmore NW, Harris JC, Kovach T, Paller KA. Improving memory via automated targeted memory reactivation during sleep. *Journal of Sleep Research*. 2022;31(6). doi:10.1111/jsr.13731

246. Liguori C, Placidi F, Izzi F, Spanetta M, Mercuri NB, Di Pucchio A. Sleep dysregulation, memory impairment, and CSF biomarkers during different levels of neurocognitive functioning in Alzheimer's disease course. *Alzheimers Res Ther*. 2020;12(1):5. doi:10.1186/s13195-019-0571-3

247. Anand KS, Dhikav V. Hippocampus in health and disease: An overview. *Ann Indian Acad Neurol*. 2012;15(4):239-246. doi:10.4103/0972-2327.104323

248. Corkin S. Lasting Consequences of Bilateral Medial Temporal Lobectomy: Clinical Course and Experimental Findings in H.M. *Semin Neurol*. 1984;4(2):249-259. doi:10.1055/s-2008-1041556

249. Squire LR. The Legacy of Patient H.M. for Neuroscience. *Neuron*. 2009;61(1):6-9. doi:10.1016/j.neuron.2008.12.023

250. Milner B, Corkin S, Teuber HL. Further analysis of the hippocampal amnesic syndrome: 14-year follow-up study of H.M. *Neuropsychologia*. 1968;6(3):215-234. doi:10.1016/0028-3932(68)90021-3

251. Scoville WB, Milner B. LOSS OF RECENT MEMORY AFTER BILATERAL HIPPOCAMPAL LESIONS. *J Neurol Neurosurg Psychiatry*. 1957;20(1):11-21.

252. Cherubini E, Miles R. The CA3 region of the hippocampus: how is it? what is it for? how does it do it? *Frontiers in Cellular Neuroscience*. 2015;9. Accessed July 19, 2023. https://www.frontiersin.org/articles/10.3389/fncel.2015.00019

253. Fogwe LA, Reddy V, Mesfin FB. Neuroanatomy, Hippocampus. In: *StatPearls*. StatPearls Publishing; 2023. Accessed July 19, 2023. http://www.ncbi.nlm.nih.gov/books/NBK482171/

254. Witter M. Chapter 5 - Hippocampus. In: Watson C, Paxinos G, Puelles L, eds. *The Mouse Nervous System*. Academic Press; 2012:112-139. doi:10.1016/B978-0-12-369497-3.10005-6

255. Amaral DG, Scharfman HE, Lavenex P. The dentate gyrus: fundamental neuroanatomical organization (dentate gyrus for dummies). *Prog Brain Res*. 2007;163:3-22. doi:10.1016/S0079-6123(07)63001-5

256. Maccaferri G. Stratum oriens horizontal interneurone diversity and hippocampal network dynamics. *J Physiol*. 2005;562(Pt 1):73-80. doi:10.1113/jphysiol.2004.077081

257. Deller T, Adelmann G, Nitsch R, Frotscher M. The alvear pathway of the rat hippocampus. *Cell Tissue Res*. 1996;286(3):293-303. doi:10.1007/s004410050699

258. Slomianka L, Amrein I, Knuesel I, Sørensen JC, Wolfer DP. Hippocampal pyramidal cells: the reemergence of cortical lamination. *Brain Struct Funct*. 2011;216(4):301-317. doi:10.1007/s00429-011-0322-0

259. Jonas P, Lisman J. Structure, function, and plasticity of hippocampal dentate gyrus microcircuits. *Front Neural Circuits*. 2014;8:107. doi:10.3389/fncir.2014.00107

260. Nelson S, Chris M. Structural and Functional Properties of Hippocampal Neurons. In: Andersen P, Morris R, Amaral D, Bliss T, O'Keefe J, eds. *The Hippocampus Book*. Oxford University Press; 2006:0. doi:10.1093/acprof:oso/9780195100273.003.0005

261. Maccaferri G. Modulation of hippocampal stratum lacunosum-moleculare microcircuits. *The Journal of Physiology*. 2011;589(8):1885-1891. doi:10.1113/jphysiol.2010.201079

262. Jinno S, Klausberger T, Marton LF, et al. Neuronal Diversity in GABAergic Long-Range Projections from the Hippocampus. *J Neurosci*. 2007;27(33):8790-8804. doi:10.1523/JNEUROSCI.1847-07.2007

263. Dieni C, Chancey J, Overstreet-Wadiche L. Dynamic functions of GABA signaling during granule cell maturation. *Frontiers in Neural Circuits*. 2013;6. Accessed July 19, 2023. https://www.frontiersin.org/articles/10.3389/fncir.2012.00113

264. Lopez C, Pelkey K, Chittajallu R, et al. Competition from newborn granule cells does not drive axonal retraction of silenced old granule cells in the adult hippocampus. *Frontiers in Neural Circuits*. 2012;6. Accessed July 19, 2023. https://www.frontiersin.org/articles/10.3389/fncir.2012.00085

265. Köhler C. Intrinsic projections of the retrohippocampal region in the rat brain. I. The subicular complex. *Journal of Comparative Neurology*. 1985;236(4):504-522. doi:10.1002/cne.902360407

266. Knierim JJ. The hippocampus. *Current Biology*. 2015;25(23):R1116-R1121. doi:10.1016/j.cub.2015.10.049

267. Kesner R. Neurobiological foundations of an attribute model of memory. *Comparative Cognition & Behavior Reviews*. 2013;8:29-59. doi:10.3819/ccbr.2013.80003

268. Witter MP. The perforant path: projections from the entorhinal cortex to the dentate gyrus. In: Scharfman HE, ed. *Progress in Brain Research*. Vol 163. The Dentate Gyrus: A Comprehensive Guide to Structure, Function, and Clinical Implications. Elsevier; 2007:43-61. doi:10.1016/S0079-6123(07)63003-9

269. Swanson LW, Wyss JM, Cowan WM. An autoradiographic study of the organization of intrahippocampal association pathways in the rat. *J Comp Neurol*. 1978;181(4):681-715. doi:10.1002/cne.901810402

270. Scharfman HE. The CA3 "Backprojection" to the Dentate Gyrus. *Prog Brain Res*. 2007;163:627-637. doi:10.1016/S0079-6123(07)63034-9

271. Vyleta NP, Borges-Merjane C, Jonas P. Plasticity-dependent, full detonation at hippocampal mossy fiber–CA3 pyramidal neuron synapses. Raman IM, ed. *eLife*. 2016;5:e17977. doi:10.7554/eLife.17977

272. Martin SJ, Shires KL, da Silva BM. Hippocampal Lateralization and Synaptic Plasticity in the Intact Rat: No Left–Right Asymmetry in Electrically Induced CA3-CA1 Long-Term Potentiation. *Neuroscience*. 2019;397:147-158. doi:10.1016/j.neuroscience.2018.11.044

273. Dong Z, Han H, Cao J, Zhang X, Xu L. Coincident Activity of Converging Pathways Enables Simultaneous Long-Term Potentiation and Long-Term Depression in Hippocampal CA1 Network In Vivo. *PLOS ONE*. 2008;3(8):e2848. doi:10.1371/journal.pone.0002848

274. Xu X, Sun Y, Holmes TC, López AJ. Non-canonical connections between the subiculum and hippocampal CA1. *J Comp Neurol*. 2016;524(17):3666-3673. doi:10.1002/cne.24024

275. Sun Y, Jin S, Lin X, et al. CA1-projecting subiculum neurons facilitate object–place learning. *Nat Neurosci*. 2019;22(11):1857-1870. doi:10.1038/s41593-019-0496-y

276. Amaral DG, Dolorfo C, Alvarez-Royo P. Organization of CA1 projections to the subiculum: A PHA-L analysis in the rat. *Hippocampus*. 1991;1(4):415-435. doi:10.1002/hipo.450010410

277. Petersen RP, Moradpour F, Eadie BD, et al. Electrophysiological identification of medial and lateral perforant path inputs to the dentate gyrus. *Neuroscience*. 2013;252:154-168. doi:10.1016/j.neuroscience.2013.07.063

278. O'Keefe J. Place units in the hippocampus of the freely moving rat. *Experimental Neurology*. 1976;51(1):78-109. doi:10.1016/0014-4886(76)90055-8

279. Jacob PY, Van Cauter T, Poucet B, Sargolini F, Save E. Medial entorhinal cortex lesions induce degradation of CA1 place cell firing stability when self-motion information is used. *Brain Neurosci Adv*. 2020;4:2398212820953004. doi:10.1177/2398212820953004

280. Knierim JJ, Lee I, Hargreaves EL. Hippocampal place cells: Parallel input streams, subregional processing, and implications for episodic memory. *Hippocampus*. 2006;16(9):755-764. doi:10.1002/hipo.20203

281. Lee SM, Seol JM, Lee I. Subicular neurons represent multiple variables of a hippocampal-dependent task by using theta rhythm. *PLoS Biol*. 2022;20(1):e3001546. doi:10.1371/journal.pbio.3001546

282. Acharya L, Aghajan ZM, Vuong C, Moore JJ, Mehta MR. Causal Influence of Visual Cues on Hippocampal Directional Selectivity. *Cell*. 2016;164(1-2):197-207. doi:10.1016/j.cell.2015.12.015

283. Save E, Nerad L, Poucet B. Contribution of multiple sensory information to place field stability in hippocampal place cells. *Hippocampus*. 2000;10(1):64-76. doi:10.1002/(SICI)1098-1063(2000)10:1<64::AID-HIPO7>3.0.CO;2-Y

284. Colgin LL, Moser EI, Moser MB. Understanding memory through hippocampal remapping. *Trends in Neurosciences*. 2008;31(9):469-477. doi:10.1016/j.tins.2008.06.008

285. Dupret D, O'Neill J, Pleydell-Bouverie B, Csicsvari J. The reorganization and reactivation of hippocampal maps predict spatial memory performance. *Nat Neurosci*. 2010;13(8):995-1002. doi:10.1038/nn.2599

286. Sharp PE, Green C. Spatial correlates of firing patterns of single cells in the subiculum of the freely moving rat. *J Neurosci*. 1994;14(4):2339-2356. doi:10.1523/JNEUROSCI.14-04-02339.1994

287. Brun VH, Otnæss MK, Molden S, et al. Place Cells and Place Recognition Maintained by Direct Entorhinal-Hippocampal Circuitry. *Science*. 2002;296(5576):2243-2246. doi:10.1126/science.1071089

288. Fyhn M, Molden S, Witter MP, Moser EI, Moser MB. Spatial representation in the entorhinal cortex. *Science*. 2004;305(5688):1258-1264. doi:10.1126/science.1099901

289. Hafting T, Fyhn M, Molden S, Moser MB, Moser EI. Microstructure of a spatial map in the entorhinal cortex. *Nature*. 2005;436(7052):801-806. doi:10.1038/nature03721

290. Fanselow MS, Dong HW. Are The Dorsal and Ventral Hippocampus functionally distinct structures? *Neuron*. 2010;65(1):7. doi:10.1016/j.neuron.2009.11.031

291. Herreras O. Local Field Potentials: Myths and Misunderstandings. *Frontiers in Neural Circuits*. 2016;10. Accessed July 20, 2023. https://www.frontiersin.org/articles/10.3389/fncir.2016.00101

292. Jacques C, Jonas J, Colnat-Coulbois S, Maillard L, Rossion B. Low and high frequency intracranial neural signals match in the human associative cortex. Ploner M, Büchel C, Ploner M, eds. *eLife*. 2022;11:e76544. doi:10.7554/eLife.76544

293. Başar E. Brain oscillations in neuropsychiatric disease. *Dialogues Clin Neurosci*. 2013;15(3):291-300.

294. Cebolla AM, Cheron G. Understanding Neural Oscillations in the Human Brain: From Movement to Consciousness and Vice Versa. *Frontiers in Psychology*. 2019;10. Accessed July 20, 2023. https://www.frontiersin.org/articles/10.3389/fpsyg.2019.01930

295. Crone NE, Korzeniewska A, Franaszczuk PJ. Cortical gamma responses: Searching high and low. *International Journal of Psychophysiology*. 2011;79(1):9-15. doi:10.1016/j.ijpsycho.2010.10.013

296. Miller KJ, Zanos S, Fetz EE, den Nijs M, Ojemann JG. Decoupling the Cortical Power Spectrum Reveals Real-Time Representation of Individual Finger Movements in Humans. *J Neurosci*. 2009;29(10):3132-3137. doi:10.1523/JNEUROSCI.5506-08.2009

297. Munia TTK, Aviyente S. Time-Frequency Based Phase-Amplitude Coupling Measure For Neuronal Oscillations. *Sci Rep*. 2019;9(1):12441. doi:10.1038/s41598-019-48870-2

298. Scherberger H, Jarvis MR, Andersen RA. Cortical Local Field Potential Encodes Movement Intentions in the Posterior Parietal Cortex. *Neuron*. 2005;46(2):347-354. doi:10.1016/j.neuron.2005.03.004

299. Teleńczuk M, Teleńczuk B, Destexhe A. Modelling unitary fields and the single-neuron contribution to local field potentials in the hippocampus. *The Journal of Physiology*. 2020;598(18):3957-3972. doi:10.1113/JP279452

300. Buzsáki G. Hippocampal sharp waves: their origin and significance. *Brain Res*. 1986;398(2):242-252. doi:10.1016/0006-8993(86)91483-6

301. Buzsáki G, Horváth Z, Urioste R, Hetke J, Wise K. High-frequency network oscillation in the hippocampus. *Science*. 1992;256(5059):1025-1027. doi:10.1126/science.1589772

302. Noguchi A, Yamashiro K, Matsumoto N, Ikegaya Y. Theta oscillations represent collective dynamics of multineuronal membrane potentials of murine hippocampal pyramidal cells. *Commun Biol*. 2023;6(1):1-14. doi:10.1038/s42003-023-04719-z

303. Green JD, Arduini AA. Hippocampal electrical activity in arousal. *Journal of Neurophysiology*. 1954;17(6):533-557. doi:10.1152/jn.1954.17.6.533

304. Givens B. Stimulus-evoked resetting of the dentate theta rhythm: relation to working memory. *NeuroReport*. 1996;8(1):159.

305. Kennedy JP, Zhou Y, Qin Y, et al. A Direct Comparison of Theta Power and Frequency to Speed and Acceleration. *J Neurosci*. 2022;42(21):4326-4341. doi:10.1523/JNEUROSCI.0987-21.2022

306. Landfield PW, McGaugh JL, Tusa RJ. Theta Rhythm: A Temporal Correlate of Memory Storage Processes in the Rat. *Science*. 1972;175(4017):87-89. doi:10.1126/science.175.4017.87

307. Greenstein YJ, Pavlides C, Winson J. Lonf-term potentiation in the dentate gyrus is preferentially induced at theta rhythm periodicity. *Brain Research*. 1988;438(1):331-334. doi:10.1016/0006-8993(88)91358-3

308. Drieu C, Zugaro M. Hippocampal Sequences During Exploration: Mechanisms and Functions. *Front Cell Neurosci*. 2019;13:232. doi:10.3389/fncel.2019.00232

309. Gupta AS, van der Meer MAA, Touretzky DS, Redish AD. Segmentation of spatial experience by hippocampal theta sequences. *Nat Neurosci*. 2012;15(7):1032-1039. doi:10.1038/nn.3138

310. Brandon MP, Koenig J, Leutgeb JK, Leutgeb S. New and Distinct Hippocampal Place Codes Are Generated in a New Environment during Septal Inactivation. *Neuron*. 2014;82(4):789-796. doi:10.1016/j.neuron.2014.04.013

311. Reddy L, Self MW, Zoefel B, et al. Theta-phase dependent neuronal coding during sequence learning in human single neurons. *Nat Commun*. 2021;12(1):4839. doi:10.1038/s41467-021-25150-0

312. Wang Y, Romani S, Lustig B, Leonardo A, Pastalkova E. Theta sequences are essential for internally generated hippocampal firing fields. *Nat Neurosci*. 2015;18(2):282-288. doi:10.1038/nn.3904

313. Zielinski MC, Tang W, Jadhav SP. The role of replay and theta sequences in mediating hippocampal-prefrontal interactions for memory and cognition. *Hippocampus*. 2020;30(1):60-72. doi:10.1002/hipo.22821

314. Rex CS, Colgin LL, Jia Y, et al. Origins of an Intrinsic Hippocampal EEG Pattern. Dickson CT, ed. *PLoS ONE*. 2009;4(11):e7761. doi:10.1371/journal.pone.0007761

315. Schlingloff D, Káli S, Freund TF, Hájos N, Gulyás AI. Mechanisms of Sharp Wave Initiation and Ripple Generation. *J Neurosci*. 2014;34(34):11385-11398. doi:10.1523/JNEUROSCI.0867-14.2014

316. Malerba P, Krishnan GP, Fellous JM, Bazhenov M. Hippocampal CA1 Ripples as Inhibitory Transients. *PLoS Comput Biol*. 2016;12(4):e1004880. doi:10.1371/journal.pcbi.1004880

317. Csicsvari tJozsef, Hirase H, Czurkó A, Mamiya A, Buzsáki G. tFast Network Oscillations in the Hippocampal CA1 Region of the Behaving Rat. *J Neurosci*. 1999;19(16):RC20-RC20. doi:10.1523/JNEUROSCI.19-16-j0001.1999

318. Giri B, Miyawaki H, Mizuseki K, Cheng S, Diba K. Hippocampal Reactivation Extends for Several Hours Following Novel Experience. *J Neurosci*. 2019;39(5):866-875. doi:10.1523/JNEUROSCI.1950-18.2018

319. Ma W, Bl M. Reactivation of hippocampal ensemble memories during sleep. *Science (New York, NY)*. 1994;265(5172). doi:10.1126/science.8036517

320. Ji D, Wilson MA. Coordinated memory replay in the visual cortex and hippocampus during sleep. *Nat Neurosci*. 2007;10(1):100-107. doi:10.1038/nn1825

321. Funane T, Jun H, Sutoko S, Saido TC, Kandori A, Igarashi KM. Impaired sharp-wave ripple coordination between the medial entorhinal cortex and hippocampal CA1 of knock-in model of Alzheimer's disease. *Front Syst Neurosci*. 2022;16:955178. doi:10.3389/fnsys.2022.955178

322. Middleton SJ, Kneller EM, Chen S, et al. Altered hippocampal replay is associated with memory impairment in mice heterozygous for the Scn2a gene. *Nat Neurosci*. 2018;21(7):996-1003. doi:10.1038/s41593-018-0163-8

323. Girardeau G, Benchenane K, Wiener SI, Buzsáki G, Zugaro MB. Selective suppression of hippocampal ripples impairs spatial memory. *Nat Neurosci*. 2009;12(10):1222-1223. doi:10.1038/nn.2384

324. Tang W, Jadhav SP. Sharp-wave ripples as a signature of hippocampal-prefrontal reactivation for memory during sleep and waking states. *Neurobiol Learn Mem*. 2019;160:11-20. doi:10.1016/j.nlm.2018.01.002

325. Jadhav SP, Kemere C, German PW, Frank LM. Awake hippocampal sharp-wave ripples support spatial memory. *Science*. 2012;336(6087):1454-1458. doi:10.1126/science.1217230

326. Papale AE, Zielinski MC, Frank L, Jadhav SP, Redish AD. Interplay between hippocampal sharp wave ripple events and vicarious trial and error behaviors in decision making. *Neuron*. 2016;92(5):975-982. doi:10.1016/j.neuron.2016.10.028

327. Davidson TJ, Kloosterman F, Wilson MA. Hippocampal Replay of Extended Experience. *Neuron*. 2009;63(4):497-507. doi:10.1016/j.neuron.2009.07.027

328. English DF, Peyrache A, Stark E, et al. Excitation and Inhibition Compete to Control Spiking during Hippocampal Ripples: Intracellular Study in Behaving Mice. *J Neurosci*. 2014;34(49):16509-16517. doi:10.1523/JNEUROSCI.2600-14.2014

329. Colgin LL. Rhythms of the hippocampal network. *Nat Rev Neurosci*. 2016;17(4):239-249. doi:10.1038/nrn.2016.21

330. Colgin LL, Moser EI. Gamma oscillations in the hippocampus. *Physiology (Bethesda)*. 2010;25(5):319-329. doi:10.1152/physiol.00021.2010

331. Wulff P, Ponomarenko AA, Bartos M, et al. Hippocampal theta rhythm and its coupling with gamma oscillations require fast inhibition onto parvalbumin-positive interneurons. *Proceedings of the National Academy of Sciences*. 2009;106(9):3561-3566. doi:10.1073/pnas.0813176106

332. Lisman JE, Jensen O. The Theta-Gamma Neural Code. *Neuron*. 2013;77(6):1002-1016. doi:10.1016/j.neuron.2013.03.007

333. Başar E. A review of gamma oscillations in healthy subjects and in cognitive impairment. *International Journal of Psychophysiology*. 2013;90(2):99-117. doi:10.1016/j.ijpsycho.2013.07.005

334. Colgin LL, Denninger T, Fyhn M, et al. Frequency of gamma oscillations routes flow of information in the hippocampus. *Nature*. 2009;462(7271):353-357. doi:10.1038/nature08573

335. Csicsvari J, Jamieson B, Wise KD, Buzsáki G. Mechanisms of gamma oscillations in the hippocampus of the behaving rat. *Neuron*. 2003;37(2):311-322. doi:10.1016/s0896-6273(02)01169-8

336. Yuan M. Effects of sepsis on hippocampal volume and memory function. *World J Emerg Med*. 2020;11(4):223. doi:10.5847/wjem.j.1920-8642.2020.04.004

337. Barichello T, Machado RA, Constantino L, et al. Antioxidant treatment prevented late memory impairment in an animal model of sepsis*: *Critical Care Medicine*. 2007;35(9):2186-2190. doi:10.1097/01.CCM.0000281452.60683.96

338. Laitano O, Pindado J, Valera I, et al. The impact of hindlimb disuse on sepsis-induced myopathy in mice. *Physiol Rep*. 2021;9(14):e14979. doi:10.14814/phy2.14979

339. Comim CM, Pereira JG, Steckert A, et al. RIVASTIGMINE REVERSES HABITUATION MEMORY IMPAIRMENT OBSERVED IN SEPSIS SURVIVOR RATS. *Shock*. 2009;32(3):270. doi:10.1097/SHK.0b013e31819963c4

340. Yang H, Wang H, Andersson U. Targeting Inflammation Driven by HMGB1. *Frontiers in Immunology*. 2020;11. Accessed July 20, 2023. https://www.frontiersin.org/articles/10.3389/fimmu.2020.00484

341. Siegle JH, López AC, Patel YA, Abramov K, Ohayon S, Voigts J. Open Ephys: an open-source, plugin-based platform for multichannel electrophysiology. *J Neural Eng*. 2017;14(4):045003. doi:10.1088/1741-2552/aa5eea

342. Rey HG, Pedreira C, Quian Quiroga R. Past, present and future of spike sorting techniques. *Brain Research Bulletin*. 2015;119:106-117. doi:10.1016/j.brainresbull.2015.04.007

343. Diniz Behn CG, Klerman EB, Mochizuki T, Shih-Chieh L, E. Scammell T. Abnormal Sleep/Wake Dynamics in Orexin Knockout Mice. *Sleep*. 2010;33(3):297-306. doi:10.1093/sleep/33.3.297

344. Gervasoni D, Lin SC, Ribeiro S, Soares ES, Pantoja J, Nicolelis MAL. Global Forebrain Dynamics Predict Rat Behavioral States and Their Transitions. *J Neurosci*. 2004;24(49):11137-11147. doi:10.1523/JNEUROSCI.3524-04.2004

345. Donoghue T, Haller M, Peterson EJ, et al. Parameterizing neural power spectra into periodic and aperiodic components. *Nat Neurosci*. 2020;23(12):1655-1665. doi:10.1038/s41593-020-00744-x

346. Haller M, Donoghue T, Peterson E, et al. Parameterizing neural power spectra. Published online April 11, 2018. doi:10.1101/299859

347. Borniger JC, de Lecea L. Peripheral Lipopolyssacharide Rapidly Silences REM-Active LHGABA Neurons. *Frontiers in Behavioral Neuroscience*. 2021;15. Accessed July 6, 2023. https://www.frontiersin.org/articles/10.3389/fnbeh.2021.649428

348. Long S, Ding R, Wang J, Yu Y, Lu J, Yao D. Sleep Quality and Electroencephalogram Delta Power. *Frontiers in Neuroscience*. 2021;15. Accessed July 6, 2023. https://www.frontiersin.org/articles/10.3389/fnins.2021.803507

349. Ji M, Li S, Zhang L, et al. Sepsis induced cognitive impairments by disrupting hippocampal parvalbumin interneuron-mediated inhibitory network via a D4-receptor mechanism. *Aging (Albany NY)*. 2020;12(3):2471-2484. doi:10.18632/aging.102755

350. Zhang L, Gao YZ, Zhao CJ, Xia JY, Yang JJ, Ji MH. Reduced inhibitory and excitatory input onto parvalbumin interneurons mediated by perineuronal net might contribute to cognitive impairments in a mouse model of sepsis-associated encephalopathy. *Neuropharmacology*. 2023;225:109382. doi:10.1016/j.neuropharm.2022.109382

351. Huerta PT, Robbiati S, Huerta TS, et al. Preclinical Models of Overwhelming Sepsis Implicate the Neural System that Encodes Contextual Fear Memory. *Mol Med*. 2016;22(1):789-799. doi:10.2119/molmed.2015.00201

352. Comim CM, Barichello T, Grandgirard D, Dal-Pizzol F, Quevedo J, Leib SL. Caspase-3 Mediates In Part Hippocampal Apoptosis in Sepsis. *Mol Neurobiol*. 2013;47(1):394-398. doi:10.1007/s12035-012-8354-x

353. Ji MH, Qiu LL, Tang H, et al. Sepsis-induced selective parvalbumin interneuron phenotype loss and cognitive impairments may be mediated by NADPH oxidase 2 activation in mice. *Journal of Neuroinflammation*. 2015;12(1):182. doi:10.1186/s12974-015-0401-x

354. Petersen PC, Vöröslakos M, Buzsáki G. Brain temperature affects quantitative features of hippocampal sharp wave ripples. *Journal of Neurophysiology*. 2022;127(5):1417-1425. doi:10.1152/jn.00047.2022

355. Granger JI, Ratti PL, Datta SC, Raymond RM, Opp MR. Sepsis-induced morbidity in mice: Effects on body temperature, body weight, cage activity, social behavior and cytokines in brain. *Psychoneuroendocrinology*. 2013;38(7):1047-1057. doi:10.1016/j.psyneuen.2012.10.010

356. Barichello T, Giridharan VV, Catalão CHR, Ritter C, Dal-Pizzol F. Neurochemical effects of sepsis on the brain. *Clinical Science*. 2023;137(6):401-414. doi:10.1042/CS20220549

357. Zhang Y, Cao L, Varga V, et al. Cholinergic suppression of hippocampal sharp-wave ripples impairs working memory. *Proceedings of the National Academy of Sciences*. 2021;118(15):e2016432118. doi:10.1073/pnas.2016432118

358. Yin L, Zhang J, Ma H, et al. Selective activation of cholinergic neurotransmission from the medial septal nucleus to hippocampal pyramidal neurones improves sepsis-induced cognitive deficits in mice. *British Journal of Anaesthesia*. 2023;130(5):573-584. doi:10.1016/j.bja.2023.01.019

359. Kudrimoti, H.S., Barnes, C.A. and McNaughton, B.L. (1999) 'Reactivation of hippocampal cell assemblies: Effects of behavioral state, experience, and EEG Dynamics', *The Journal of Neuroscience*, 19(10), pp. 4090–4101. doi:10.1523/jneurosci.19-10-04090.1999.

360. O'Keefe JM, Nadel L, O'Keefe J. *The Hippocampus as a Cognitive Map*. Clarendon Press; 1978.

361. Kala A, Leemburg S, Jezek K. Sepsis-Induced Changes in Spectral Segregation and Kinetics of Hippocampal Oscillatory States in Rats. *eNeuro*. 2023;10(6). doi:10.1523/ENEURO.0002-23.2023

7. LIST OF PUBLICATIONS

1. **Kala A**, Leemburg S, Jezek K. Sepsis-Induced Changes in Spectral Segregation and Kinetics of Hippocampal Oscillatory States in Rats. eNeuro. 2023 Jun 20;10(6):ENEURO.0002-23.2023. doi: 10.1523/ENEURO.0002-23.2023. PMID: 37286344; PMCID: PMC10286852. **IF- 4.36**

2. Kavkova M, Zikmund T, Kala A, Salplachta J, Proskauer Pena SL, Kaiser J, Jezek K. Contrast enhanced X-ray computed tomography imaging of amyloid plaques in Alzheimer disease rat model on lab based micro CT system. Sci Rep. 2021 Mar 16;11(1):5999. doi: 10.1038/s41598-021-84579-x. PMID: 33727592; PMCID: PMC7966753. **IF- 4.6**

3. Jedlička J, Tůma Z, Razak K, Kunc R, **Kala A**, Proskauer Pena S, Lerchner T, Ježek K, Kuncová J. Impact of aging on mitochondrial respiration in various organs. Physiol Res. 2022 Dec 31;71(S2):S227-S236. doi: 10.33549/physiolres.934995. PMID: 36647911; PMCID: PMC9906668. **IF- 2.13**